Hyperspectral analysis of selected fabrics submerged in the Indian Ocean: An innovative way to aid in the estimation of the time human remains have spent in water

Elsie Beales

BSc Hons (Forensic Biology & Toxicology)

2020

Supervisors

Dr. Paola A. Magni

Dr. Almantas Pivrikas

This thesis is presented for the degree of

Bachelor of Science Honours in Forensic Biology and Toxicology

College of Science, Health, Engineering and Education

Murdoch University

I declare that this thesis is my own account of my research and contains as its main content work which has not previously been submitted for a degree at any tertiary education institution.

Elsie Beales

Acknowledgements

There were many hurdles which arose over the twelve months it took me to complete this project, and at times I honestly felt I would not be able to finish. With that being said, as this is the acknowledgements section and is usually written last, I must have made it. I would like to take a moment to thank all the people who supported me along the way.

Firstly, to my primary supervisor Dr Paola Magni, whose brilliant mind powered me through this project. Somehow you managed to balance everything in your own life, a global pandemic, and me as an extremely needy honours student. Every day your passion and energy for forensic science has inspired me to pursue a career in science and strive to do the best I can.

To my secondary supervisor, Dr Almantas Pivrikas, for your unwavering optimism throughout the year. Your cheerful approach towards the project helped to keep me grounded when things became overwhelming.

A special thank you goes to Elysia Tingey, for your project, as well as your advice and support over the duration of my honour's year. Without your work, my project would not exist, so I am incredibly thankful for the eighteen months of your honour's year (and a half) that preceded mine.

I would also like to thank Dr David Berryman for granting me access to his equipment in the SABC.

To Jordy and Claire, my honours anonymous support group. I'm so glad I connected with you both during orientation. Your knowledge, patience, and compassion

towards me while completing your own projects was so greatly appreciated. You both have such brilliant minds and will go on to succeed in your fields.

To my family for the chaos I continue to put you through as I complete the different chapters of my life. It seems everything I do comes with an extra obstacle course, and this was no different. Yet you continue to support and encourage me regardless, for which I am incredibly grateful.

Finally, to my wonderful fiancé Keegan. You are truly my biggest supporter who bears the brunt of my burdens. Words cannot express how thankful I am of all the work you put in to encourage me to complete this project. During the times I felt I could not finish this, you pushed me to the end.

Abstract

Estimating the time since death (minimum Post-Mortem Interval, minPMI) is crucial in forensic investigations. In an aquatic environment, this process is particularly challenging because of the complexity of a corpse's decomposition process and the many factors related to the environment. Furthermore, there is a general paucity of research in this field. Recently, the use of the clothing discovered alongside a corpse has come under scrutiny: clothing has a high chance to be present, and their colonisation rate by aquatic organisms could be used to estimate the victim's minimum Post-Mortem Submersion Interval (minPMSI). Besides a biological/zoological-based estimation, no other avenues to age clothing in an underwater context have been tested. This research is the first to focus on the use of Hyperspectral Imaging (HSI) to age fabrics, considering the modification of their optical properties as a result of exposure to a marine environment.

Cotton, neoprene, satin, and velvet were submerged underwater over a period of six months off the coast of Perth, Western Australia. In a pilot study, the fabrics were analysed using two different light scenarios (VIS-NIR and VIS-NIR + VIS-H) to identify which one would provide the best reflectance profiles. Results demonstrated that the additional halogen illumination (VIS-NIR + VIS-H) did not provide any extra information with respect to VIS-NIR. In the main study, the fabric's spectral profiles were therefore captured using only VIS-NIR lighting. Profiles were generated for all submerged samples as well as controls (N=112), and the resulting data were compared within and between fabrics. The most significant differences were observed for the cotton and satin, with a strong negative regression observed between the months spent submerged and the profiles generated. These fabrics showed a

significant change of the colour, texture, and structure, as marine organisms were highly attracted to them. Neoprene and velvet, instead, showed minimal significant changes, with the first few months showing similar profiles to the controls and differences toward the end of the experiment. As opposed to cotton and satin, neoprene and velvet were less affected by the marine organisms. Overall, in a forensic context, when investigated via HSI technology, thin and natural fabrics can provide the most information to the investigators.

This study is the first to provide data to support the estimation of minPMSI based on the use of remote sensing, HSI, on different fabric types placed in Western Australian marine waters, providing the potential for a new tool in estimation of the minPMSI for forensic investigation.

Table of contents

List of tables

List of figures

List of abbreviations

MinPMSI	Minimum Post-Mortem Submersion Interval
MinFI	Minimum Floating Interval
ADD	Accumulated Degree Days
MinPMI	Minimum Post-Mortem Interval
TDS	Total Decomposition Score
ADS	Aquatic Decomposition Score
FADS	Facial Aquatic Decomposition Score
BADS	Body Aquatic Decomposition Score
LADS	Limb Aquatic Decomposition Score
TADS	Total Aquatic Decomposition Score
EPS	Extracellular Polymeric Substance
MSP – VIS	Micro Spectrophotometry Visual
UV	Ultraviolet
FTIR	Fourier Transformed Infrared
EM	Electromagnetic
VIS	Visual
NIR	Near-Infrared
HSI	Hyperspectral Imaging
3D	Three Dimensional
2D	Two Dimensional
IR	Infrared
DFO	1, 8 – Diazafluoren – 9 – One
PTC	Phase Transfer Catalyst
SEM	Scanning Electron Microscopy

Chapter 1: A general review of the literature

1.1 Aquatic forensics

1.1.1 The impact of aquatic deaths

Between July 1st, 2018 and June 30th, 2019, 276 individuals drowned in aquatic locations across Australia, with 32 of these deaths occurring in Western Australia (Royal Life Saving Society, 2019). Globally, there are an estimated 372,000 drowning deaths annually (World Health Organization, 2014). Due to official data categorisation methods, intentional drowning deaths by homicide or suicide, as well as deaths caused by flood disaster and water transport incidents are excluded from this figure. Data gathered from high-income countries suggests that due to this exclusion, there is a significant underrepresentation of the full drowning toll by up to 50% in some countries (World Health Organization, 2014).

1.1.2 Determining cause and manner of death

Diagnosing the cause and establishing the manner of death in submersion cases is considered a significant challenge for forensic pathologists (Papadodima, Athanaselis, Skliros, & Spiliopoulou, 2010). Human remains can be transported great distances in the water, in very little time, and therefore, can be retrieved many kilometres from the point of entry (Giertsen & Morild, 1989). Furthermore, the process of decomposition, as well as the activity of macro-scavengers on the human remains, can further complicate the pathological findings (Heaton, Ladgen, Moffatt, & Simmons, 2010). Not all individuals whose bodies are recovered from the water will have died due to drowning (Piette & Els, 2006). Instead, corpses retrieved from an aquatic environment may have died due to the effects of submersion in water other

than drownings, such as from injury or natural disease occurring before entering the water (Lawler, 1992). Upon initial examination, these cases may show signs of submersion, but this only confirms that they were in the water at some point in the process of their death and did not assist in the differentiation of the mode of death or determining the proper cause of death (Papadodima et al., 2010). In ambiguous cases, laboratory findings (e.g. presence of diatoms in the corpse) and autopsy may not be sufficient in establishing the cause of death, and in these cases, the co-evaluation of other circumstantial factors (such as examination of items retrieved alongside the remains) may be crucial (Lawler, 1992).

1.2 Minimum Post-Mortem Submersion Interval (minPMSI)

The minimum Post-Mortem Submersion Interval (minPMSI) is the estimation of the time elapsed between the death of an individual in an aquatic environment, and the recovery of human remains from the water (van Daalen et al., 2017). Calculation of the minPMSI must consider both the amount of time the corpse spent submerged and the amount of time the corpse spent floating on the water's surface (minimum floating interval, minFI) (hereafter references to the minPMSI is also including the minFI). Knowledge of the minPMSI of discovered human remains is significant in the reconstruction of the events which led up to death (Saukko & Knight, 2015), and a reliable minPMSI can aid in the identification of the deceased individual.

When a corpse is recovered from an aquatic environment, there are both intrinsic and extrinsic factors which must be considered while making an estimation of the minPMSI. A corpse in water will usually sink upon entry but due to the specific gravity of a corpse being very close to that of water, small variations (such as air trapped in clothing) have a considerable effect on the overall buoyancy (Donoghue

& Minnigerode, 1977). To reach the floating stage of aquatic decomposition, a corpse must have been in the water long enough for tissue decomposition from gut bacteria to begin (Donoghue & Minnigerode, 1977). This process forms a gaseous by-product which collects in the body cavities and beneath the skin. This gaseous accumulation within the corpse is what results in its eventual resurfacing due to increased buoyancy (Petrik, Hobischak, & Anderson, 2004). After resurfacing, decomposition continues and as skeletonization advances and body parts begin to detach from the corpse, sinking may reoccur. Intrinsic factors affecting this overall trajectory include; overall body mass, type and amount of clothing or covering (e.g. more buoyant clothing will prevent sinking), exposed surface area, artefacts, and trauma (e.g. an impacted body cavity will halt bacterial progression preventing gaseous accumulation) (Donoghue & Minnigerode, 1977; Petrik, Hobischak, & Anderson, 2004).

Environmental variables and otherwise extrinsic factors such as temperature, tide, salinity, chemical and bacterial composition of the water (Sorg et al., 1997; Heaton et al., 2010; Dickson, Poulter, Maas, Probert, & Keiser, 2011) can complicate measurements leading to erroneous estimations. Furthermore, the actions of aquatic scavengers and tidal flow on the corpse contribute to abrasion of the skin which in turn accelerates the skeletonization process. Consequently, parts of the corpse may be lost (Sorg, et al., 1997) which hinders the correct application of the Aquatic Decomposition Scoring method (Heaton et al., 2010) (further outlined in section 1.2.1). Other methods evaluated for the determination of the minPMSI include decomposition scoring combined with Accumulated Degree Days (ADD), presence of barnacles, algal diversity, diatom diversity, and bacterial growth. These parameters will be explored each in further depth in the following sections.

1.2.1 Decomposition scoring

Traditional methods for the estimation of the terrestrial minimum Post-Mortem Interval (minPMI) of human bodies are based on the observation of the decomposition of the soft tissues (van Daalen et al., 2017). While decomposition in aquatic environments differs greatly from that in terrestrial environments (Heaton et al., 2010), some decomposition phenomena occur in both, such as bloating, hair shedding, epidermolysis, and skeletonization (Saukko & Knight, 2015). Patterns of decomposition in a terrestrial environment are discernible from those in an aquatic environment by the emergence of key visual markers at different time intervals, and progression at different rates (van Daalen et al., 2017). The initial Total Decomposition Score (TDS) was developed for human remains recovered in a terrestrial environment (Megyesi, Nawroki, & Haskell, 2005). This method was then altered for an aquatic environment by Heaton et al. (2010) who developed an Aquatic Decomposition Score (ADS), which has since been the subject of further research. Humphreys et al. (2013) compared the Heaton et al. (2010) ADS to the mass analysis method and concluded that the ADS was less compromising for the samples and more accurate. The Heaton et al. (2010) ADS was also studied by De Donno et al. (2014) who concluded that while this method showed promise, accurate determination of the minPMSI was still extremely challenging due to the wide biological variability of aquatic environments.

Van Daalen et al. (2017) developed an ADS method to estimate the minPMSI for saltwater (the Heaton et al. (2010) method was developed for freshwater), which derived from Megyesi et al. (2005) who studied bodies recovered from a terrestrial environment to create a quantifiable TDS. The TDS was based on decomposition stages of three different areas of the corpse, the face, torso, and limbs. Heaton et al.

(2010) followed this structure in the development of their ADS and termed the 'Facial Aquatic Decomposition Score' (FADS), 'Body Aquatic Decomposition Score' (BADS), 'Limb Aquatic Decomposition Score' (LADS), which were summed to calculate the 'Total Aquatic Decomposition Score' (TADS). The van Daalen et al. (2017) ADS followed this structure and described six specific stages of aquatic decomposition phenomena for the FADS, BADS, and LADS. The van Daalen et al. (2017) methodology differs from the Heaton et al. (2010) methodology, as van Daalen et al. TADS is calculated as a sum of the FADS, BADS, and LADS, while Heaton et al. calculated the TADS as an independent score, and then summed the FADS, BADS, LADS, and TADS.

1.2.2 Decomposition scoring combined with Accumulated Degree Days

The ADD value is calculated as the sum of the average daily temperatures (in Celsius) for the entire minPMSI period. Calculation of the ADD in a terrestrial or aquatic environment allows for an evaluation of whether the cumulative temperature significantly affects the decomposition process within the study sample (Heaton et al., 2010). In recent years, there have been multiple studies investigating the use of ADD and TADS in the calculation and estimation of minPMSI (Reijnen, Gelderman, Grotebevelsborg, Reijnders, & Duijst, 2018). The floatation patterns of corpses in aquatic environments is a particularly relevant aspect to consider when analysing drowning cases (Reisdorf et al., 2012). For significant corpse drift to occur, the buoyancy of the corpse must also exist, and there is a direct relationship between the decomposition rate and the floatation of corpses in drowning cases (Giertsen & Morild, 1989). When a human corpse enters into an aquatic environment, it will initially sink to the bottom of the waterway and will remain submerged until enough putrefaction gas has accumulated for the corpse to attain sufficient floatation force,

undergo vertical displacement, and resurface (Mateus & Vieira, 2014). While submerged along the bottom of a waterway, friction will generally prevent significant drift, however once resurfaced, human remains can be transported vast distances in very little time (Giertsen & Morild, 1989). The decomposition rate of a corpse is a function of temperature, and temperature will vary in time and space, and so due to this, Mateus and Vieira (2014) suggest that studying the ADD can provide relevant clues on the decomposition rate of the corpse.

Unfortunately, accurate information on the minPMSI and ADD are only possible to obtain in cases where the time and place of drowning and recovery of the corpse are known (Mateus, de Pablo, & Vaz, 2013). Furthermore, to use ADD, the mean daily temperature must be known, which can be difficult, if not impossible, in most aquatic environments.

1.2.3 Algal and diatom diversity

Diatoms and other algae have demonstrated use in several criminal investigations (Silver, Lord, & McCarthy, 1994, Casamatta & Verb, 2000; Haefner, Wallace, & Merritt, 2004); however, due to their complex ecology and population dynamics, they have been underutilised in forensic science (Zimmerman & Wallace, 2008). Diatoms (order *Bacillariophyta*) are a unique taxonomic division of algae. They are single-celled and can be characterised by the environment in which they exist, for example, some are exclusive to saltwater, and others to freshwater (Fig. 1.1.) (Allan, 1995). Diatoms are ubiquitous and abundant in naturally occurring waters as well as important primary producers. Traditionally, their usage has been to determine water quality (Cox, 1996) and more recently attention has been paid to them in a criminal

investigation as a tool for determining whether a victim has drowned, and as a method of linking a suspect to a crime scene (Zimmerman & Wallace, 2008).

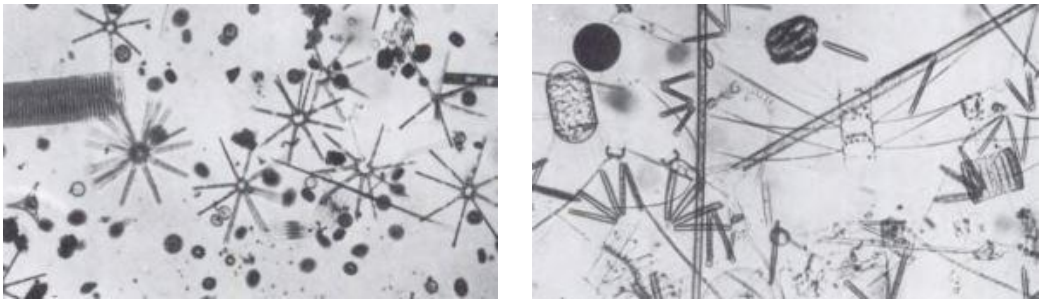

Fig. 1.1. *Examples of the different kinds of diatoms which can occur in different environments, with freshwater planktonic diatoms featured in the left image and marine planktonic diatoms featured in the right image* (Round, Crawford , & Mann , 2007).

Kepier and Casamatta (2001) highlighted three main roles of diatoms in the context of forensic investigation, the first being helping to determine the cause and manner of death of a corpse recovered in an aquatic environment. Diatoms can withstand harsh chemical environments such as that of cadaver digestive tissues and therefore their presence in the lungs, kidneys, brain, and other major organs can positively indicate drowning as the cause of death of an individual.

The second major role of diatoms is to identify the suspected crime scene, which is made possible by the fact that some diatoms have very specific requirements that correlate to their ecological distribution. Issues arise with this technique as determining what constitutes enough similarity between tissue and environmental samples are problematic (Keiper & Casamatta, 2001). Furthermore, determination of similarity is less of an issue when highlighting more general sites (such as marine vs freshwater) (Peabody & Cameron, 1999); however, a definitive habitat may not be identifiable from the information gathered.

The third major role is the use of diatoms for minPMSI estimates. Casamatta and Verb (2000) found in their study of algal diversity on submerged rat carcasses that

rich algal flora developed as the decomposition progressed, with species diversity increasing up until around three weeks submerged, and then stabilising. Furthermore, they quantitively identified early and late-stage algal colonisers and showed that the presence or absence of such species could lead to an estimation of the minPMSI. Zimmerman and Wallace (2008) describe diatoms as the initial colonisers in an aquatic environment and they thereby can be used to estimate the minPMSI as they behave as an underwater time clock with their colonisation rate indicating how long the carcass has been submerged. Haefner et al. (2004) state that for a reliable minPMSI to be made through observation of algal communities, the state of decomposition and the ADD must also be considered in conjunction in order to create a more accurate prediction.

A major limitation in using algal and diatom diversity to predict minPMSI is that many studies have used artificial substrates such as clay pots or tiles to test the colonisation rate of algal communities in an underwater environment (Merritt & Wallace, 2010). The degree of algal growth was demonstrated to be much more significant on mammalian corpses as opposed to artificial substrates, and this observation suggests that it is highly unlikely that artificial substrates can adequately approximate a corpse. Due to this fact, previous studies involving algal growth on artificial substrates may no longer be applicable in the determination of minPMSI on submerged mammalian corpses (Haefner, Wallace, & Merritt, 2004).

1.2.4 Bacterial Growth

Microorganisms have a significant part to play in the natural decomposition process of a corpse, involving both microbial communities endogenous to the corpse as well as the external environment (Dickson et al., 2011). As microbial communities are

ubiquitous within aquatic ecosystems, they have the potential to aid in more accurate estimations of minPMSI on discovered human remains (Benbow, Pechal, Lang, Erb, & Wallace, 2015). Microbes are rarely found in their free-floating form within aquatic environments, and are more predominantly found within biofilms (Costerton, Lewandowski, Caldwell, Korber, & Lappin-Scott, 1995). Biofilms are a matrix made up of microbial communities of both heterotrophs and autotrophs, and are photogenically diverse containing bacterial, algal, protozoan, and fungal species. The microorganisms are encased in an Extracellular Polymeric Substance (EPS) which is attached to the external surfaces in aqueous environments (Costerton et al.,1995). As biofilm development commonly follows a successional pattern, Benbow et al. (2015) suggested that this succession could potentially be used to approximate the amount of time carcasses have spent in an aqueous habitat. The findings from their study which used pig carcasses supported this prediction, and they reported significant changes in the bacterial communities over time, which reflected the time since the submersion. Bacterial growth succession should be used in conjunction with seasonal succession patterns (if available) as like many other methods of estimating minPMSI, factors such as temperature, nutrient content, and salinity should be considered (Dickson et al. 2011). Furthermore, Dickson et al. (2011) highlighted that although dismembered body parts are frequently discovered from aquatic environments, there were no studies that had examined the decomposition process of partial remains in a natural aquatic environment. Due to this observation, their study into bacterial succession was conducted on complete and partial carrion carcasses, which should be further investigated in future literature.

1.2.5 Insect and arthropod activity

The earliest records of forensic entomology as a practice date back to the 13th century in China, and from then until its more modern usage now across Europe, Asia, America, and Australia, it has been well documented (Morris & Dadour, 2015; Byrd & Tomberlin, 2019). In the published literature, there is an 80-20% difference between studies focusing on terrestrial versus aquatic environments, respectively (Merritt & Wallace, 2010). Unlike in an aquatic environment, there are terrestrial insects which have evolved to feed on carrion, and the presence of necrophagous insects is related to both the availability of a food source and the environmental temperature (Byrd & Tomberlin, 2019). The colonisation on a cadaver by aquatic insects depends on abiotic factors such as depth and strength of water flow, and the chemical and physical properties of the water, as well as the biotic factors such as the flora and fauna by which the cadaver may be used for protection or as a food source (Haskell, McShaffrey, Hawley, Williams, & Pless, 1989).

Barrios and Wolff (2011) conducted a study to observe the ecological succession and trophic roles of aquatic arthropods and how they associated with the different stages of decomposition in a freshwater environment. They established ecological categories by creating two groups of organisms, group 1 being those who feed exclusively on the submerged carcass, and group 2 being those who feed exclusively on the exposed carcass during the floating stages. The scavenging activity recorded from both groups indicated that the carcass becomes a food source when it emerges from the water's surface, whereas when submerged, it represents a structure for anchorage and protection for the strictly aquatic species. Barrios and Wolff (2011) concluded that freshwater arthropods could potentially be used in estimating the minPMSI; however, they did not replicate their study.

Wallace et al. (2008) reviewed a homicide case in which a corpse was recovered from a river in separate plastic bags, and the remains were in such an advanced state of decomposition that the colonisation of caddisfly larvae recovered from the corpse and artefacts provided evidence useful in more accurately estimating the period of submersion. Unfortunately, this was just a single case review, and the authors acknowledged that this was a relatively new and under-researched area of forensic science.

Magni et al. (2013) reviewed two cases where individual corpses were discovered in wells in Italy. In the first case, an entomologist was appropriately consulted upon retrieval of the corpse, which allowed for valuable data to be collected from the insects that had colonised the corpse and aid in minimising the potential window of time the corpse had spent submerged. In the second case, an entomologist was not consulted until 20 months after the recovery of the corpse, in which time the insect evidence collected was most definitely incomplete, and the resulting estimated minPMSI erroneous. Conclusions from the review of these cases were that correct technique of corpse retrieval from an aquatic environment is imperative in preserving valuable entomological data, which can be used to better estimate the minPMSI of a recovered corpse if the appropriate specialists are contacted.

1.2.6 Barnacles

The study of barnacles in forensic setting comes under the discipline of forensic entomology, as despite ‘entomology’ suggesting only insects, it also considers arthropods such as crustaceans and spiders. In a marine environment, modern forensic entomology focuses primarily on the most common arthropods present in the ocean, namely barnacles (Crustacea: Cirripedia) (Newman & Abbott, 1980).

Barnacles have demonstrated the potential to aid in the minPMSI approximation as just the presence of barnacles on recovered remains indicates that they were in an intertidal environment long enough for the barnacle to explore, attach, and begin metamorphosis into adult life (Bytheway & Pustilnik, 2013).

Bytheway and Pustilnik (2013) examined the glycoproteinous adhesion deposits of the *Balanus improvisus* (Darwin) (Crustacea: Cirripedia: Sessilia) as well as their basal diameter to determine an approximate minPMSI of human teeth, mandibles, and exposed knee bone. Sorg et al. (1997) investigated specimens of *Balanus crenatus* Bruguière (Crustacea: Cirripedia: Sessilia) using a combination of the barnacle growth rings with the amount of time required for skeletonisation to occur of a human corpse in order to determine the minPMSI of a skull found at sea in British Columbia. Dennison et al. (2004) also used this combination of methods on specimens of *Notobalanus decorus decorus* (Darwin) (Crustacea: Cirripedia: Sessilia) found on a calvaria on the east coast of New Zealand.

Magni et al. (2014) investigated *Lepas anatifera* L. (Crustacea: Cirripedia: Peduculata) removed from the clothing of a corpse which was found in the Tyrrhenian Sea (Italy), and estimated the minPMSI based on the length of the *capitulum* (shelled body of an adult goose necked barnacle). De Donno et al. (2014) also examined the *L. anatifera* as a method of estimating the minPMSI by considering barnacle size in combination with a TADS for an individual corpse pulled from the Adriatic Sea (Italy).

In Australia, Tingey (2019) set up an experiment in the Indian Ocean (Western Australia) which investigated the barnacle colonisation on four different types of fabric (cotton, neoprene, satin, and velvet), and used barnacle growth rings over six

months as a method of estimating the minPMSI of recovered fabrics associated with a corpse. In America, Pirtle et al. (2019) set up an experiment in the Atlantic Ocean (Boston, Massachusetts) which investigated barnacle colonisation on two different types of the shoes (sports shoes, and patented leather shoes). The subsequent species which colonised were examined, and barnacle growth size was considered as a new approach to estimating the minPMSI of recovered clothed human remains.

1.2.7 MinPMSI and fabric

The majority of case studies focusing on examining human remains recovered from aquatic environments report the presence of clothing and shoes together with the remains (Aquila, et al. 2014; Pirtle, Magni, Reinecke, & Dadour, 2019). Therefore, recent developments have focused on the items recovered alongside the human remains to generate more data for completing a more accurate crime scene reconstruction (Tingey, 2019)

There have been two studies which directly considered fabric as a medium of forensic interest with regards to minPMSI calculations. An experiment conducted by Tingey (2019) explored the colonisation rates of barnacles on four different types of fabric, cotton, velvet, satin, and neoprene. Settlement preference was noted on the black neoprene, as opposed to the white cotton, satin, and velvet, and the growth rings of the barnacles were considered as a method of estimating the minPMSI. The second study examined the colonisation of barnacles on different types of shoe, in order to determine whether there was a preference for a particular material, as well as whether barnacles could be utilised as a tool for determining the minPMSI of recovered human remains and their associated artefacts (Pirtle, Magni, Reinecke, & Dadour, 2019). There was a noted settlement preference of the barnacles on the smooth fabric

surface of the patented leather shoe, as opposed to the rough fabric surface of the sport shoe.

Thus far, the fabric has been considered in these studies from a purely biological perspective, focusing on the colonisation of marine flora and fauna. The present study into the potential of fabric analysis from a physical perspective is the first of its kind.

1.3 Fabric

1.3.1 Fabric fibres as trace evidence

Textile fibres have been defined by researchers as a natural or manufactured unit of matter that forms the basic elements of fabrics (Qin, 2015). Textile fibres are one of the most significant forms of trace evidence, given that they have multitudes of classifications and subtypes, have various processing procedures, are chemically and physically differentiable, and are easily transferred. Trace evidence in a forensic setting is broadly defined as "small, often microscopic fragments of various types of material that transfer between people, places and objects, and persists there for a time" (Wiggins & Houck, 2001). Trace evidence can consist of a vast array of materials such as paint, glass, soil, hair, fibres, dust, and pollen, and in the context of criminal investigations, it is inherently associative (Goodpaster & Liszewski, 2009).

1.3.2 Natural and manufactured fibres

Fibres are classified as either natural or manufactured. The natural fibre is "any fiber that exists as a fiber in its natural state" (Houck & Siegel, 2015). A manufactured fibre, on the other hand, is "any fiber derived by a process of manufacture from any substance that, at any point in the manufacturing process, is not a fiber" (Houck & Siegel, 2015).

Natural fibres

Natural fibres constitute over half of the total number of fibres produced annually, and they are commonly derived from plants, animals, or minerals resulting in a variety of compositions, each with distinctive characteristics unique to each class (Houck & Siegel, 2015).

- Plant fibres – plant fibres are derived from three main parts of plants, the stem, leaves, or seeds, and so depending on the qualities desired of the fibre, and the plant structure, fibres are extracted from different parts. Plant fibres exist in two principle forms; individual cells, such as in fabrics or paper, or as technical fibres, used in sacks, mats, or cordage. The most common plant fibre encountered is cotton, which makes up about half of the annual production of plant fibres. Other common plant fibres are jute, ramie, flax, hemp, abaca, sisal, kapok, and coir (Houck & Siegel, 2015).
- Animal fibres – animal fibres come from certain invertebrates, such as the silkworm, or mammals in the form of hairs. In textiles, wool-bearing animals such as sheep and goats, or hair-bearing animals such as mink, fox, and rabbits, are the most common sources of fibres.

Natural fibres are often sought after for their biodegradability, but therefore are subject to unwanted degradation. A process known as ‘finishing’ is utilised to prolong the life of a fibre, increase the versatility of the finished fabric, and sometimes alter the physical properties of the fibre altogether (Srivastava, 2012). A finish will be applied to the fibre either before or after the weaving or knitting in order to change the appearance, performance, and hand (what you feel). Processes such as singeing, carbonising, bleaching, and coating are all examples of finishing,

and these treatments can ultimately result in the narrowing of spaces between the fibres in the finished textile, endowing the fabric with increased functionality such as water repellence, degradation protection, flame retardance, and anti-static (Srivastava, 2012).

Manufactured fibres

Manufactured fibres or human-made fibres are those which are produced from fibre forming substances, such as glass, modified or transformed natural polymers, or synthesised polymers. Human-made fibres can be divided into organic and inorganic types depending on the composition of the fibres. Organic human-made fibres can then be further divided into regenerated or synthetic fibres (Fig. 1.2) (Deopura & Padaki, 2015). Synthetic fibres are synthesised from chemical compounds, like nylon, or polyester. Therefore, all synthetic fibres are manufactured, but not all manufactured fibres are synthetic (Houck & Siegel, 2015). Chemically synthesised fibres have enhanced performance when compared to natural fibres, with advantages such as increased strength and durability, crease-free, chemical resistance, fungi and rot resistance, low moisture absorbency, and minimal shrinkage when washed (Deopura & Padaki, 2015)

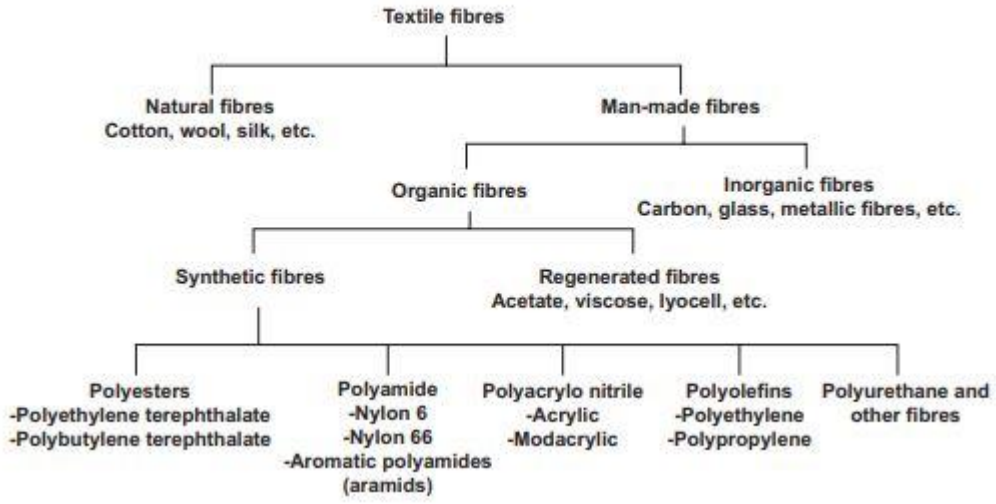

Fig. 1.2. *Classification of man-made fibres (Deopura & Padaki, 2015).*

1.3.3 Forensic examination of textile fibres

The forensic examination of textile fibres involves comparing individual fibres retrieved from a crime scene (*unknown source*), with fibres from samples obtained from suspects or victims (*known source*) to determine their association with the crime (Meleiro & Garcia-Ruiz, 2016). One of the most important differentiable characteristics is colour, which reflects the pigments and dyes used in the manufacture of the fibre and is often one of the only characteristics that can be used reliably in sample discrimination (Goodpaster & Liszewski, 2009). In the process of forensic fibre examination, obtained fibre samples are mounted on glass microscope slides, and are commonly examined firstly with optical microscopy (fluorescence, polarization, and bright-field), followed by Micro Spectrophotometry Visual (MSP-VIS) on the fibres that may correspond. Next, depending on the type of fibre, several methods which can allow for the gathering of more specific information can be used ranging from MSP in the ultraviolet (UV) region, Raman spectroscopy, Fourier

Transformed Infrared (FT-IR), to chromatographic techniques (Lepot, De Wael, Gason, & Gilbert , 2008).

1.3.4 Fabric decomposition in a terrestrial environment

While it is possible to make some generalisations about fabric decomposition and degradation under different soil conditions, the extensive range of fabric types, dyes, fibre mixes, and finishes requires that each set of textiles need to be separately considered in light of specific environmental conditions (Janaway, 2008). Biologically active soils have long been recognised as one of the most aggressive environments for textiles (Lloyd, 1968), and when buried in an oxygenated and moist soil environment most textile materials are subject to rapid decomposition by bacteria and fungi (Janaway, 2008). Natural fabric fibres such as cotton and rayon are much more vulnerable to decay, while synthetic fibres such as polyester and elastin can survive for much longer periods of time under the same conditions (*see Table 1.1*).

Table 1.1.
Textile fabrics classified by vulnerability to decomposition after burial for 3-6 months in a biologically active soil. Table reproduced from (Janaway, 2008).

Vulnerability to Decomposition	Fabrics
Most Vulnerable	Undyed cotton, some light dyed cotton fabrics
	Rayon
Highly Vulnerable	Dyed cotton, including denim
Vulnerable to Decay	Wool
	Silk
	Cotton – polyester (depending on mix)
Resistant to Decay	Nylon
	Acrylic
	Polyester
	Elastin

The durability of metal zippers and buttons on denim fabric was tested in a study conducted by Tigg (2005). Common kinds of metal fasteners such as brass and aluminium zippers, rivets, and buttons were sewn with polyester thread to blue-dyed

indigo denim fabric squares and exposed to three contrasting depositional environments for fifteen weeks. Location one was an agricultural small holding with yellow clay at 40cm depth (fabric was buried at 30cm and 60cm), location two was well tilled garden soil (fabric was buried at 30cm), and location 3 was on the soil surface under a large coniferous hedge (fabric was left on the surface). Fabrics buried in locations one and two, which were in wet soil, ranged from degraded to total fabric loss, while those from location three which was sheltered from precipitation and dry had negligible decay (Tigg, 2005). This study demonstrated that while the denim fabric may undergo varying levels of degradation, the metal fastenings can be much more durable as in all three locations they were all recovered with minimal corrosion (Tigg, 2005; Janaway, 2008).

During the active decay of buried cadavers, decomposition by-products will modify the grave environment in terms of redox and pH, which will in turn affect the rate of decay of the most vulnerable fabrics (Janaway, 2008). A series of experiments conducted by Wilson et al. (2007) were set up in West Yorkshire, U.K., to test the relationships among the decomposition of pig cadavers, hair, metal, and textiles. Three experimental sites were used: pasture, woodland, and moorland, and cadaver and control graves were dug and exhumed after six, twelve, and twenty-four months. All three sites had fluctuating water tables which resulted in the bases of the graves (60cm depth) being below the water table for at least some part of the study.

In a pilot study at the pasture site, replicate fabric samples of undyed cotton, undyed wool, dyed polyester, and synthetic indigo dyed denim were places above (30cm depth) and below (60cm depth) pig cadavers, and at 30cm and 60cm in control graves (Wilson et al., 2007). The findings from these graves were consistent with a number of principles. During the active decomposition of the pig carcass, the burial

environment was modified in such a way that preserved vulnerable textiles from decomposition. Furthermore, during the active decomposition time, synthetic polyester was almost entirely resistant to decay resulting in no major loss of the fabric. The undyed cotton was the most vulnerable to decay, however a small amount of the fabric survived under the pig in the reducing conditions created due to the decomposition. The blue denim fabric and the wool demonstrated good preservation under the pig, and some preservation over the pig. In the control grave however, a total loss of all fabrics was recorded (Wilson et al., 2007).

A similar experiment was repeated at the moorland and woodland sites using undyed cotton, undyed wool, and blue dyed denim which yielded similar results (Wilson et al., 2007). The acidic and semi-waterlogged soils of the moorland site resulted in a slower turnover of fabrics in comparison to the more biologically active and better drained soils at the woodland site. Both sites demonstrated the same trend of best preservation of fabric under the pig cadaver, some preservation on top of the pig cadaver, and equivalent control graves showing more prominent degradation (Wilson et al., 2007).

A study conducted by Daza (2014) in Canberra (Australia) examined the effects of surface soil, decomposition fluid, and the climatic environment on cotton, viscose, and polyester fabric. Red and black fabrics from each type were placed on five pig carcasses and left to decompose for one – eight weeks in the Australian summer (Daza, 2014). The pig carcasses were divided into fourteen sections in which the different fabric samples were distributed to determine whether the location of the fabric on the cadaver would impact the degree of colour loss and exposure. During the experiment, as a result of the decomposition process, the bloat of one pig carcass caused it to roll into a modified position which subjected some of the fabric samples

to increased amounts of decomposition fluid and soil. This excess of decomposition fluid and soil was expected to act as a barrier to the degree of environmental exposure; causing their rate of colour loss to be low (Daza, 2014). Upon collection, the samples were dried, and fibres were pried from the textiles for analysis. All three fabrics exhibited comparable degrees of colour loss over the course of the experiment, and a direct association was made between the degree of colour loss, the type of fabric, and the location on the pig carcass. The samples collected from the rolled pig carcass displayed similarly high levels of colour loss to the samples from the other carcasses, indicating that the excessive contact with decomposition fluids and soil did not impact their environmental exposure. These observations were quantified using hyperspectral imaging (HSI) analysis which compared reference points from the control spectral profile with the environmentally exposed spectral profile to determine that significant colour loss had occurred (Daza, 2014). The major impacting factor on the colours of the fabrics was determined to be the climatic conditions of the location to which the fabrics were exposed. Results from this research show that it is possible to quantify the aging of fabrics through observed colour changes as a result of environmental exposure. This research focused on terrestrial fabric decomposition, and the observed colour loss of the fabric samples was only one of several factors which were being studied (Daza, 2014).

1.4 Hyperspectral imaging

Spectroscopy is a technique which measures the interaction of light with an object of interest to determine physical and chemical properties of the object along the electromagnetic (EM) spectrum within the visible (VIS) wavelength range (340 – 740nm) (Cen & He, 2007). Spectroscopy characterises an objects interaction with the VIS range into opaque, translucent, or transparent. Opaque objects have a high rate

of reflection and absorption of light, transparent objects have little to none, and translucent objects fall somewhere between the two (Amigo, Babamoradi, & Elcoroaristizabal, 2015). Recently, studies have begun focusing on using the near-infrared (NIR) region of the EM (750 – 2500nm) and have found promising results with regards to determining physical and chemical characteristics of objects (Ravn, Skibsted, & Bro, 2008; Oliveira & Franca, 2011).

Hyperspectral imaging (HSI) integrates spectroscopy with conventional imaging to obtain both spectral and spatial information from a specimen. The technique allows investigators to simultaneously analyse the chemical composition of a specimen while also visualising their spectral distribution (Edelman, Gaston, Van Leeuwen, Cullen, & Aalders, 2012). It was first used in the classification and identification of minerals such as iron oxides in remote sensing (Cloutis, 1996). Other applications have included pharmaceuticals, planetary mapping, agriculture, and vegetation mapping. HSI has the ability obtain spectral data for each pixel in an image of a sample or scene, the purpose being to highlight objects, detect processes, identify materials, and estimate the age (Edelman, Gaston, Van Leeuwen, Cullen, & Aalders, 2012).

1.4.1 Hyperspectral equipment

The main components of a HSI setup include a computer with image acquisition software, a light source, a spectrograph, a charge couple device camera, and a translation stage (Fig. 1.3).

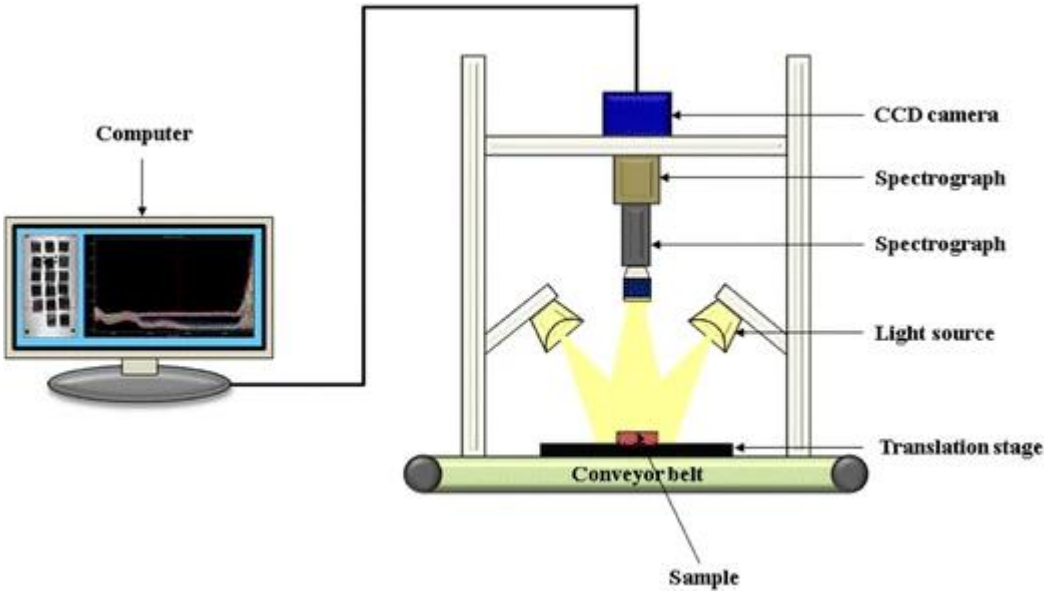

Fig. 1.3. *Schematic of a typical HSI setup. Adapted from (He & Sun, 2015).*

1.4.2 Hyperspectral data acquisition

A hyperspectral cube (also known as a spectral cube, hypercube, or data-cube), is a three dimensional (3D) block of data, composed of a two dimensional (2D) image (x, y) of the object, with spectral information on the third dimension, denoted as lambda (λ). The cube is formed by obtaining a 2D image from each wavelength one at a time, and then stacking them together to compile the 3D form (Fig. 1.4 compares a 2D image with a 3D hyperspectral cube).

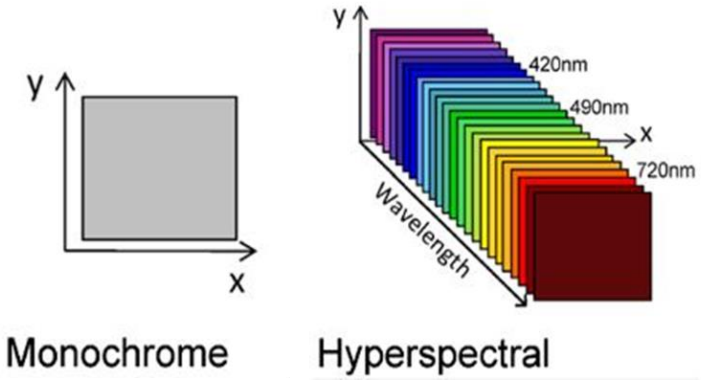

Fig. 1.4. *The comparison of a 2D image with the stacked spectral images along each wavelength of the EM to form a 3D hypercube. Figure reproduced from (Li et al., 2013).*

As HSI measures the interaction between light and a specimen, the type of lighting used is important as different lights will illuminate different areas along the EM spectrum. Various lights are used depending on the application and desired results such as heat lights, halogen lamps, light-emitting diodes, and lasers (Wu & Sun, 2013). Commonly, the first interaction between the specimen and the light source would be on the object surface, where part of the light will be reflected (Fig. 1.5 a). This interaction contains little to no information from within the medium but is governed by the index of refraction difference between the media. Upon entering the material, the light can be scattered (Fig. 1.5 b-c) or absorbed (Fig. 1.5 d-e). The process of scattering occurs when light interacts with the structures within a specimen, and as a result causes a change in the propagation and direction of travel, depending on factors such as particle size, index of refraction, and the wavelength. The absorption properties of chemical compounds are wavelength dependent. While absorbance in the NIR and infrared (IR) is determined by the vibrational modes, absorbance in the visual range correspond to the electronic states of the molecule. Upon relaxation, or return to the ground state, energy will be released from the molecules in the form of photoluminescence or heat, or by transfer to another molecule. Both the spectral absorbance and the induced photoluminescence (if present) can be measured in order to identify the chemical contents of a specimen using HSI (Edelman, Gaston, Van Leeuwen, Cullen, & Aalders, 2012).

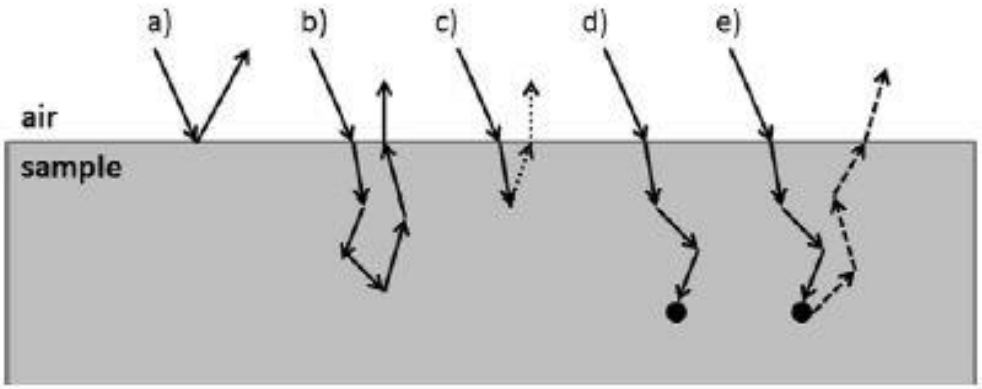

Fig. 1.5. *The interaction of light with a sample which may lead to a) specular reflection, b) elastic scattering followed by diffuse reflection, c) inelastic scattering followed by emissions of Raman shifted light (dotted lines), d) absorption and e) absorption followed by photoluminescence (dashed lines). Reproduced from (Edelman, Gaston, Van Leeuwen, Cullen, & Aalders, 2012).*

1.4.3 Forensic applications of HSI

Estimation of the age of forensic evidence and traces, such as fabric fibres, is imperative in providing investigators with valuable information for constructing an accurate timeline of events, as well as crime scenes. One of the biggest concerns with forensic analysis of specimens is contamination, alteration, and destruction of evidence (Borgwardt & Wells, 2017). HSI is suitable for non-contact analysis of evidence, thus minimising these risks. Further advantages include reduction of human error, high speed of data acquisition, minimal specimen preparation, ability to illustrate results. Furthermore, the increasingly portable nature of HSI systems allow them to be brought directly to crime scenes to photograph evidence before any interference from crime scene personelle (Edelman, Gaston, Van Leeuwen, Cullen, & Aalders, 2012). Although HSI has been primarily used for the analysis of finger-marks in forensic science, there have also been studies which examine blood, bruising, hair, adhesive, inks, and firearm propellants.

1.4.3.1 Finger-marks

Latent (= not visible to the naked eye) finger-marks are a complex mixture of eccrine deposits from the finger and sebaceous deposits which result from touching other body parts with the finger, such as the face (Ng, Walker, Tahtouh, & Reedy, 2009). Detection methods of finger-marks aim to highlight the contrast between the ridge pattern of the latent finger-mark, and the surface on which it was deposited (Edelman, Gaston, Van Leeuwen, Cullen, & Aalders, 2012).

- *Treated finger-marks*

Conventionally, finger-marks are chemically treated to increase contrast with the background and their sensitivity. Exline et al. (2003), and Payne et al. (2005a) compared traditional methods of detecting latent finger-marks with the newer method of HSI investigating the potential to produce results with increased visual quality and contrast. They used HSI in the VIS region to examine finger-marks treated with DFO (1,8-Diazafluoren-9-one), fluorescent dyes, cyanoacrylate, and ninhydrin. In comparison to the traditional method, HSI showed significantly increased enhancement, which was mainly due to the ability of HSI to visualise minute details of the finger-marks by suppressing backgrounds which were highly fluorescent, as well as isolate developed latent impressions (Exline et al., 2003; Payne et al., 2005a). The information provided by HSI could occasionally be sufficient for exclusion purposes, while the traditional methods would lead to inconclusive results. Furthermore, Miskelly and Wagner (2005) demonstrated that background correction is a key step in the successful visualisation of finger-marks on difficult backgrounds such as aluminium.

- *Untreated finger-marks*

Exline (2003) also demonstrated that visible reflectance and photoluminescence; HSI was able to detect untreated latent finger-marks on paper and plastic surfaces. The ability to produce imaging with enhanced contrast on paper surfaces was shown.

While not using HSI, it is worth noting that significant research into underwater evidence recovery has also been conducted on the preservation of submerged finger marks. A study conducted by Castello, Frances, and Verdu (2013) evaluated the possibility of retrieving finger marks from glass and plastic surfaces submerged in tap water for fifteen days. Although their study was preliminary, they deduced that it was possible to recover finger marks from these conditions by using various reagents with Black Powder being the most effective. Trapecar (2012) evaluated submerged fingerprint recovery on glass and metal surfaces which had been exposed and submerged in tap water. Their study concluded that the preservation of finger marks after submersion was directly related to the amount of time spent submerged, with longer submersion times producing a decreased quality of results. Another study conducted by Jasuja, Kumar, and Singh (2015) while evaluating the efficacy of a new fingermark recovery reagent phase transfer catalyst (PTC), submerged finger marks on adhesive tapes in distilled water from two to one hundred hours. They determined that through the use of PTC finger marks could be effectively recovered after submersion.

1.4.3.2 Blood and bruises

Blood is one of the most commonly encountered kinds of biological evidence at the scenes of violent crime (Finnis, Lewis, & Davidson, 2013). Traditionally, bloodstain detection methods focused on blood typing or the usage of alternative light sources

such as high-intensity light sources, or UV. Issues arise in that the former are destructive and require significant sample preparation, and the latter relies on minimal background interference. The UV light also has the potential to degrade the DNA evidence in biological samples (Wawryk & Odell, 2005). Cadd et al. (2016) conducted a novel study investigating the use of VIS wavelength reflectance HSI for the non-destructive and non-contact detection and identification of bloodstains and bloodstained finger marks on ceramic tiles. They conclusively identified both types of bloodstains demonstrating potential advantage over traditional chemical enhancement methods which are destructive and time-consuming.

Analysing bruising, more specifically, the ageing of bruising can give important evidence in cases involving potential child abuse and domestic violence (Randeberg, Skallerud, Langois, Haugen, & Svaasand, 2010). A bruise is formed after blunt force trauma to an area of the body which results in blood pooling under the skin. In time, the haemoglobin in the blood is degraded into other products, including bilirubin. Both bilirubin and haemoglobin have distinctive spectral features within the VIS region of the EM spectrum (Randeberg et al., 2010). Based on this information, Payne et al. (2007) demonstrated the potential of HSI to differentiate pure blood from blood with bilirubin which allowed for bruise age estimation.

1.4.3.3 Hair, ink, and insects

Hair colour is essentially determined by different ratios of eumelanin and phaeomelanin, which produce a variety of colour. Birngruber et al. (2009) investigated using HSI in the VIS-NIR regions to distinguish hairs from different individuals. Their results showed not only an extreme variability of interpersonal hair samples but an even higher variability in the spectra of intrapersonal samples.

Unfortunately, due to this high intrapersonal variability, the hairs were undistinguishable based on HSI imaging.

To demonstrate the full potential of HSI in forensic investigations, Payne et al. (2005b) compared point measurements generated by traditional spectrometers to HSI. Both VIS and NIR HSI was used to differentiate between a set of inks (Fig. 1.6), a set of tapes and adhesives, and two brands of firearm propellants based on photoluminescence and reflectance properties. They concluded that HSI offers a significant advantage in that many samples can be analysed at once, which makes analysis much easier and reduces processing time (Payne et al., 2005b).

Fig. 1.6. *Third principle component of blue ink set, indistinguishable with the human eye (Payne et al., 2005b).*

A proof of concept study was conducted by Voss et al. (2017) which utilised HSI as a non-destructive method of age estimation of blowfly puparia, as traditional methods require dissection of samples. The analytical approach provided proof of concept as they determined a direct puparial age relationship (days since onset of pupation)

between the internal morphological features and the external reflectance features captured by the HSI (Voss, Magni, Dadour, & Nansen, 2017).

1.4.3.4 Fabric and fabric fibres

The ability to identify and categorise biological stains is dependent on effectively locating and visualising them, which is often a challenge on fabrics, especially if they are darker or patterned. Recent studies have turned the focus to HSI as a potential method of both visualising and categorising evidence.

Preliminary research by Schuler, Kish, and Plese (2012) focused on developing a better understanding of how NIR-HSI could be used to visualise bloodstains on commonly encountered black fabric. The images they acquired showed promise, as they were of sufficient quality to differentiate between stains produced by both transfer and impact mechanisms. Furthermore, they demonstrated the ability to differentiate between stains where more than one existed in the same place (Schuler, Kish, & Plese, 2012). A study conducted by Kuula et al. (2014) attempted to determine whether two or more individual's blood could be separated by using HSI on bloodstains deposited on cotton. The results of their study suggested that the samples could be distinguished based on the erythrocyte content; however, due to the small sample size of only four, it was deemed not statistically significant.

Silva et al. (2017) used semen (both human and animal), lubricants, and other biological fluids on different coloured cotton, white satin, and a white cotton/polyester blend to determine whether NIR-HSI could be used to detect and differentiate between the stains. They concluded that the type of fabric in which the stain was deposited on had a strong influence on the spectral profiles and suggested that one model per fabric would need to be developed at this point in order for the

technique to work. Zapata, Ortega-Ojeda, and Garcia-Ruiz (2017) studied the ability of NIR-HSI to discriminate between semen and vaginal fluids when deposited on 100% cotton in a mixture. Their study demonstrated that NIR-HSI could achieve results comparable to the currently used method of UV-VIS light sources, but as of this point in time, cannot be considered a confirmatory technique until further study is done (Zapata, Ortega-Ojeda, & García-Ruiz, 2017).

Due to the abundance of fabrics, it has become time-consuming and complicated to identify textile materials (Fras Zemljič, Strnad, Šauperl, & Stana-Kleinschek, 2009) and fast, digital, and objective evaluation methods are required to improve the accuracy of fabric and fibre identification (Houck, 2009). As a potential technique, HSI can be utilised to distinguish mass fibres non-destructively, and rapidly. Furthermore, it can achieve functions that traditional FTIR (Abidi & Hequet, 2007) instruments do not possess such as spatial information in the form at a certain wavelength at any pixel on an image. Despite the fact that HSI can conveniently obtain images without any pre-treatment of samples, it is not popular in the textile industry at present (Li, Meng, Wang, & Xin, 2019).

A study by Li et al. (2019) looked at classifying eight fabrics, four natural (cotton, wool, silk, and linen), and four synthetics (polyester, polyethylene, nylon, and polyvinyl chloride). They used six different recognition models on the obtained HSI data and established a recognition rate of at least 80% for each fabric. This demonstrated that HSI technology could effectively be applied to the identification of single-component fabrics.

Recently, studies have been conducted into aspects of textile damage in relation to projectile analysis, decomposition, blunt force trauma, and gaining an understanding

of the interaction between the fabric and the implement (Williams, 2018). A major drawback into this area of research, however, has been in the framework by which the findings are analysed and evaluated. Criticisms of the discipline have been that current analysis models are highly subjective and that a global standardisation is not currently in place. Furthermore, most findings relating to textile damage are the secondary consideration of the research project and therefore, are not receiving the level of attention required. The lack of robust and relevant databases to back up claims renders much fabric-related evidence inadmissible in court as they cannot be quantified in such a way that would be supportive to a case (Williams, 2018).

As per the current literature, there does not appear to be any studies which consider fabrics as the primary concern of the research, and by using HSI, an attempt to quantify the results in an objective and reliable way is being made.

1.5 Conclusion

The present study is focused on utilising HSI to explore the optical properties of fabrics aging in a marine environment. This research aims to determine whether the four different types of fabric used in this experiment (cotton, neoprene, satin, and velvet) will display different spectral reflectance profiles as a result of different amounts of time submerged in a marine environment.

The data gathered from this research is significant in forensic cases whereby clothed or partially clothed human remains are recovered from marine environments, as it will provide a tool for better estimating the minPMSI of the individual, and therefore potentially accelerate and support the police investigation.

This research is the first of its kind in Australia, and the data will be the first time that the spectral properties of fabrics were used in marine forensic investigation.

This research has three distinct aims

1. Explore the optical properties of the four fabrics using HSI, and how these change as a result of exposure to a marine environment.
2. Attempt to quantify the rate of structural change in the fabrics by comparing their spectral reflectance profiles within and between fabric samples.
3. Determine whether the acquired data is of use from an investigative standpoint by offering a way of supporting the estimation of the minPMSI of recovered human remains from a marine environment.

Chapter 2: Materials and methods

The fabrics used in the present research are the same used for an experiment performed in 2018 – 2019 by Tingey (2019). For the ease of the reader, a summary of the experimental setup conducted by Tingey is outlined in the following sections (2.1 – 2.3). For a complete description of the experiment, please refer to Tingey (2019).

2.1 Experiment site

The original experiment was conducted at Cockburn Sound, which is a natural embayment in the Indian Ocean off the coast of Perth, WA (Tingey, 2019). The sound measures approximately 16km long and 7km wide (112km^2). The embayment is open to the North and remains sheltered on the Western seaward side by the Garden and Carnac Islands. The research site was located at 32°15'05" S 115°43'17" E (Fig. 2.1).

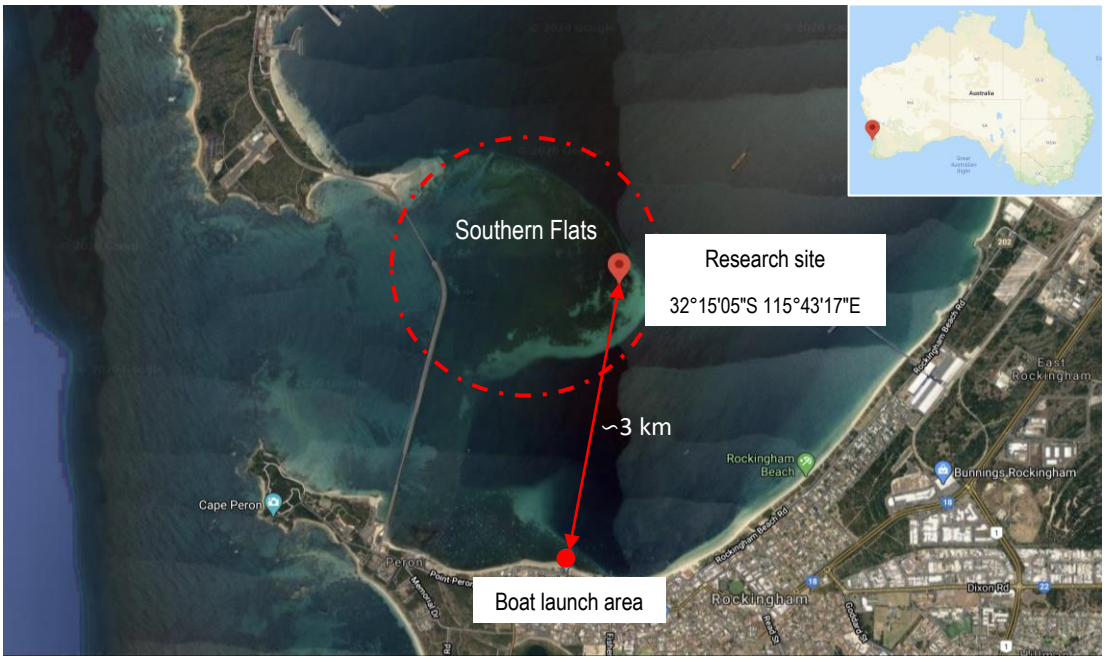

Fig. 2.1. *Location of the research site, Cockburn Sound WA, where the selected fabrics where submerged for six months in Tingey's (2019) experiment. Image indicates where the location is in relation to Australia. (Images sourced from Google Earth).*

2.2 Experimental setup

One hundred twenty (N=120) floats (Rogue Crab Pot Float®) were used for the experiment. The floats were of spherical dimension (150 mm Ø), with a 20mm Ø hole through the centre, white in colour, and made of high-density polystyrene. Of the 120 floats, 96 were covered with four different fabrics: cotton (N=24), satin (N=24), velvet (N=24), and neoprene (N=24), with the remaining floats left uncovered to act as controls (N=24). The dimensions of each of the fabric sheet were 52x32 cm.

The cotton, satin, and velvet were all white fabrics to allow for more straightforward analysis of the colonizing fauna, while the neoprene was black, as it most commonly exists in this shade when worn by divers.

The floats were to spend one to six months submerged in the ocean; therefore, they were attached to weighted crates (60 x 40cm). A total of six crates were prepared and placed in the ocean, with the aim of retrieving a crate every month for six months. The crates were placed with approximately 50cm between each crate. The small number of crates with limited spacing between each crate and selection of a specific research site was done in order to limit the different variable which could potentially impact the results (such as currents and turbulence). A total of 20 floats (16 floats covered by fabrics in replicates of four and 4 uncovered "control" floats) were attached to each crate using polypropylene rope (6mm x 100m). The crates were weighted with railway sleepers to remain submerged. As per requirements of the Department of Transport and the Department of Fisheries, the whole structure needed to remain at least 2m below the ocean surface for the duration of the experiment. Considering the height of the crate (40cm), the length of the cables, the buoyancy of

the floats, and the tides of Cockburn Sound, the crates were placed in a location where the structures remained at 90cm above seabed and a minimum of 2.5m below the surface for the duration of the experiment (Fig. 2.2).

The seawater temperature was measured at hourly intervals for the duration of the experiment with two Odessey® temperature loggers attached to both ends of each crate. Salinity data was also obtained from the Department of Water and Environmental Regulation, Government of Western Australia.

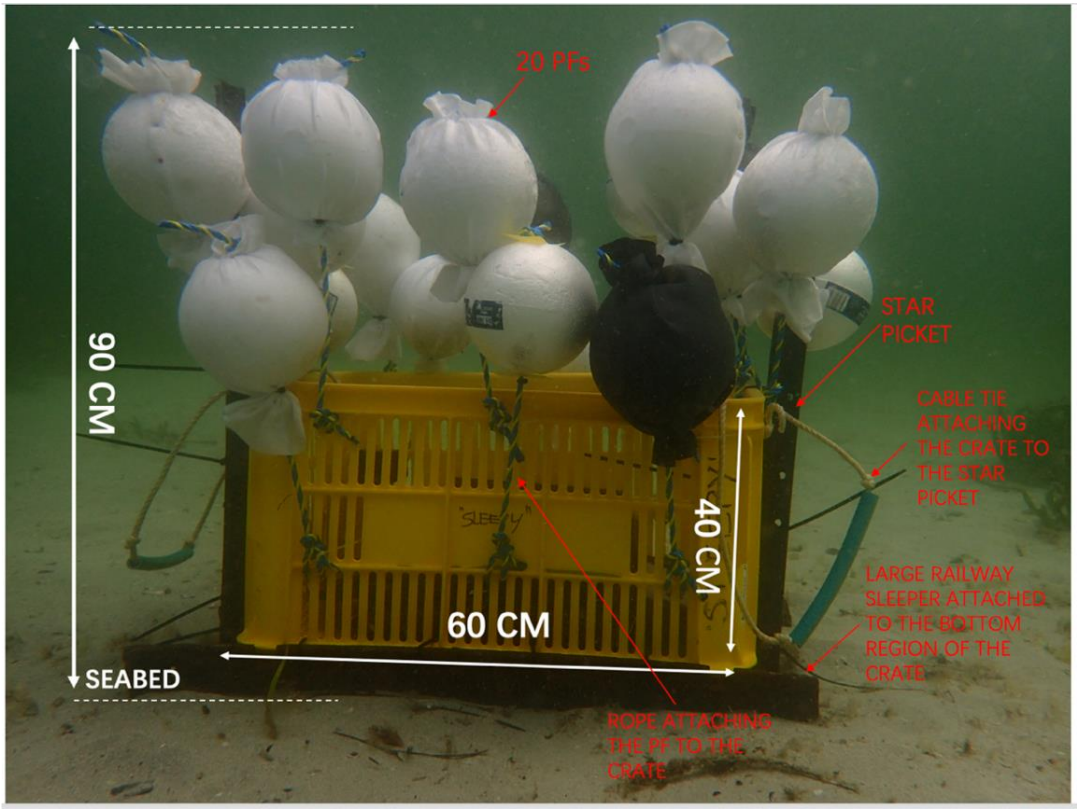

Fig. 2.2. *Image of the experimental setup of Tingey's floats and crates displaying how the fabrics were situated for the one to six-month submersion (Tingey, 2019).*

2.3 Crates removal and analyses of the samples

The crates were removed on a monthly basis, considering the conditions of the ocean to allow the necessary diving activity. Therefore, crates were removed after 28 days

since placement (month 1), 63 days (month 2), 91 days (month 3), 123 days (month 4), 161 days (month 5), and 185 days (month 6).

During the retrieval operations, plastic bags were placed over each float while still submerged to prevent attached marine life from scraping off, and the bags were sealed after surfacing. The samples were stored on ice until they reached the lab where they were kept at -20°C in a freezer (Westinghouse®) before Tingey's (2019) analysis, which involved removing the fabrics from the PFs and the observation of the colonising fauna. Following analyses, the fabrics were folded flat, re-bagged individually in a plastic zip bag, then stored back in the freezer at -20°C until further analysis. The storage time in the freezer was between 248 and 405 days (depending on how long each sample set spent in the ocean). During this period, no electricity outage or freezer issues were detected.

This is where Tingey's experiment is concluded. The subsequent sections detail the follow up investigation conducted by Beales using the fabric samples retrieved in Tingey's experiment.

2.4 Sample preparation

Fabrics were taken out of the freezer one at a time, unfolded, and areas with minimal marine organism interaction were selected. A 5 x 5cm piece of paper was measured out and laminated to ensure that for each fabric, the same amount would be removed for imaging. This laminated paper was then bull-clipped to each fabric and used as a stencil for cutting out the fabric squares. Once the fabric had been selected, clipped, and cut, it was then pinned with 17mm map pins to a cardboard box with a corresponding sample label to dry (the samples were frozen wet from the ocean) (Fig. 2.3). All handling of fabric was done carefully with tweezers a and appropriate PPE

to prevent direct contact between different samples. After 24 hours of drying time, the samples were removed from the box, and the labels were then stapled (26/6 Keji ™) to the fabric squares for easy identification going forward (Fig. 2.4). The dried and labelled samples were then stored flat in PPS™ C5 plain faced white paper envelopes until it was time to image them with HSI. In this experiment the fabrics were not washed or in any way cleaned before the HSI analysis. In the experiment conducted by Tingey the fabrics were also not washed or altered from the state that they were retrieved from the ocean in. The potential impacts of this on the HSI results are discussed further in the discussion section of this thesis. Samples were stored with their repetition sets, for example, the four repetitions of cotton from month 1 were all stored together in the same envelope, but separately from the other fabrics from month 1.

Fig. 2.3. *Pinned wet samples air drying. Murdoch University, building 260, room 2.029.*

Fig. 2.4. *Set of Samples of various fabrics that have undergone extended submersion at Cockburn Sound location. Dried and labelled samples laid out in progressive order from month 0 (left - Control) to month 6 (right) to visually demonstrate the effects of submersion in a seawater environment. Location of Murdoch University, building 260, room 2.029.*

The samples were labelled using a system that included the first letter of the fabric type, the number indicating what month the fabric was removed from the ocean, and a number from 1-4 indicating which sample of the four repetitions it was from the given month. The dried squares were then stored in 229 x 162mm plain white paper envelopes until hyperspectral imaging commenced.

To note, clippings of the same fabrics that were never placed in the ocean were used as control samples. These fabrics were considered as month zero (e.g. C.0.1 = cotton, month zero, repetition 1 of 4).

2.5 Hyperspectral imaging

Samples were removed from the envelopes one repetition set at a time and imaged individually under the camera. The process of placing the sample, checking the software, capturing the image, and then removing the sample took an average of one

minute per sample. Amount of time under the light source was controlled due to the emittance of heat from the light. To further mitigate this, the room was well ventilated with air conditioning set at 23°C. There was not a flow of air applied directly to the fabrics (such as by a fan) as this could interfere with imaging by causing movement on the samples.

Gen ASIs Hyperspectral Imaging Instrument (Applied Science Imaging, Model CCD-1300DS) coupled with Gen ASIs Spectral Imaging 4.0 acquisition software was used to capture and analyse the fabrics reflectance profiles. Prior to capturing the images of the fabrics, white calibration was achieved using a piece of white paper (Keji™, 150 CIE whiteness, 80 gsm). Additionally, a daily average reflectance profile was acquired using a piece of green plastic card as a standard (Voss et al., 2017). Average reflectance from the green plastic card before and after the imaging sessions from each day was used to confirm imaging consistency, with less than 5% variation within and among the two days observed.

A setting of 45 steps and 256 frames ensured the best resolution with 76 wavelengths between 400 – 1020nm resolved in a single acquisition. Images were captured without binning, and with an exposure time of 25 milliseconds (Fig 2.5). Reflectance data were obtained under controlled laboratory conditions using 1 x 100w, 120v digital heat lamp (Exo Terra®) mounted to a metal frame (hereafter referred to as VIS-NIR light, as the light covers the visible and partial near-infrared spectrum), and a KL 1500 HAL halogen cold light source (Schott©) with 2 x 150w, 120v halogen lights (hereafter referred to as VIS-H light) (Fig. 2.6). The position of the mount was marked with tape to ensure consistency of distance of the illuminating source to the sample during the collection process.

The reflectance spectra for each profile were viewed using Gen ASIs SpectraView® 5.0 analysis software. The software allows for the captured hyperspectral image to be considered as a whole, and as the mouse cursor is passed over the image the spectral data for each pixel of the image is displayed in the 'Spectral display window' (Fig. 2.7). From each spectral profile three pixels were chosen from different areas on the image, (from a total of 1264 x 1008 pixels per image), representing three spectral measurements which were then exported as raw text files for further analysis.

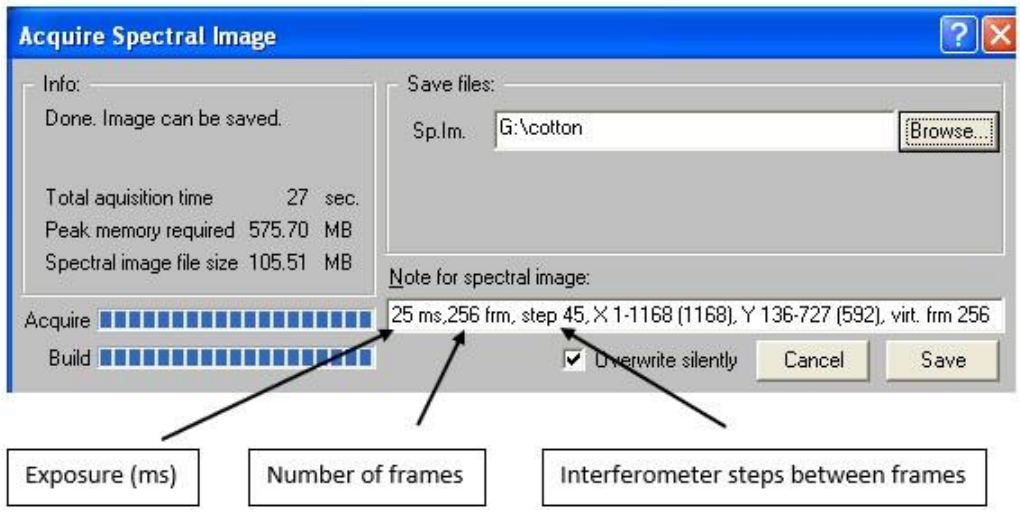

Fig. 2.5. *Instrument parameters for image acquisition. Screenshot from the Acquire Spectral Image window in the Spectra imaging 4.0 software.*

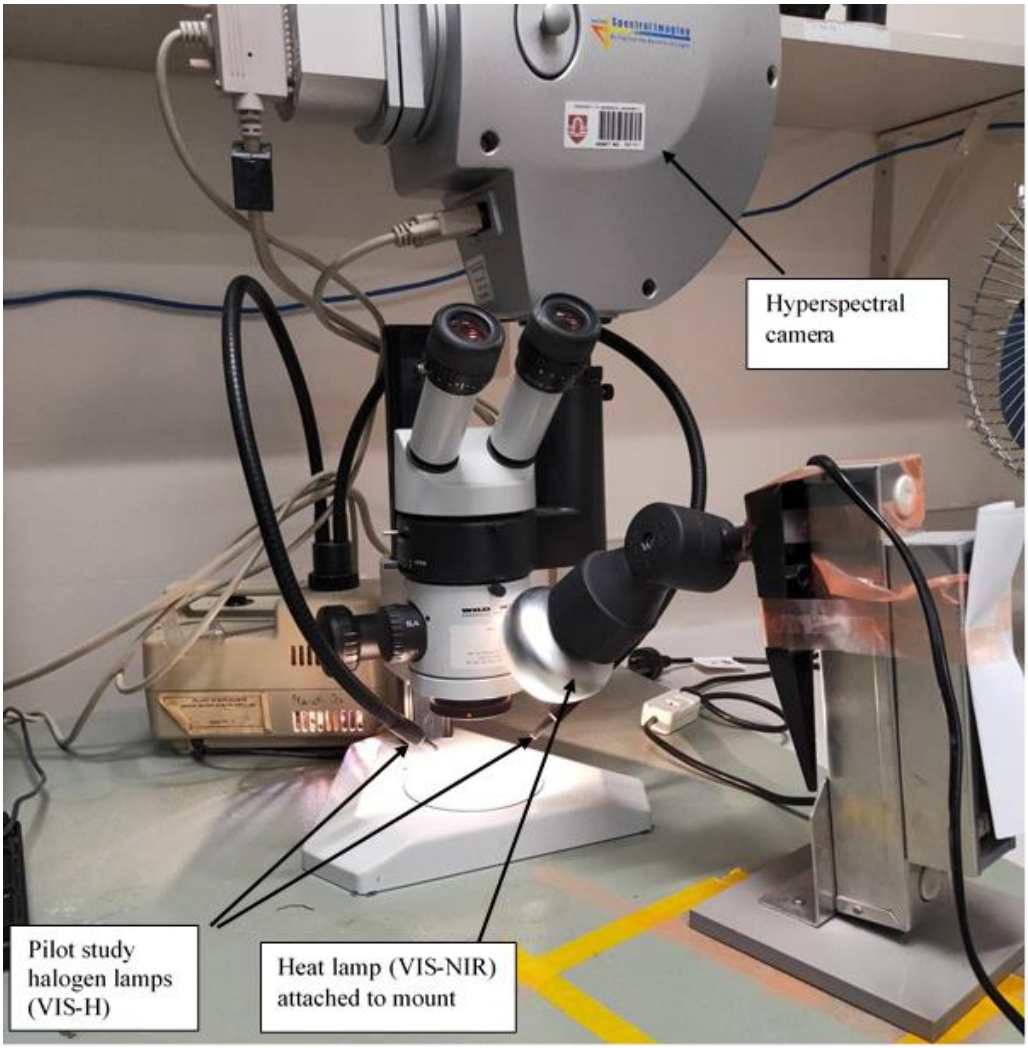

Fig. 2.6. *Camera and light set up. Spectroscopy room in the Western Australia State Agricultural Biotechnology Centre, Murdoch University.*

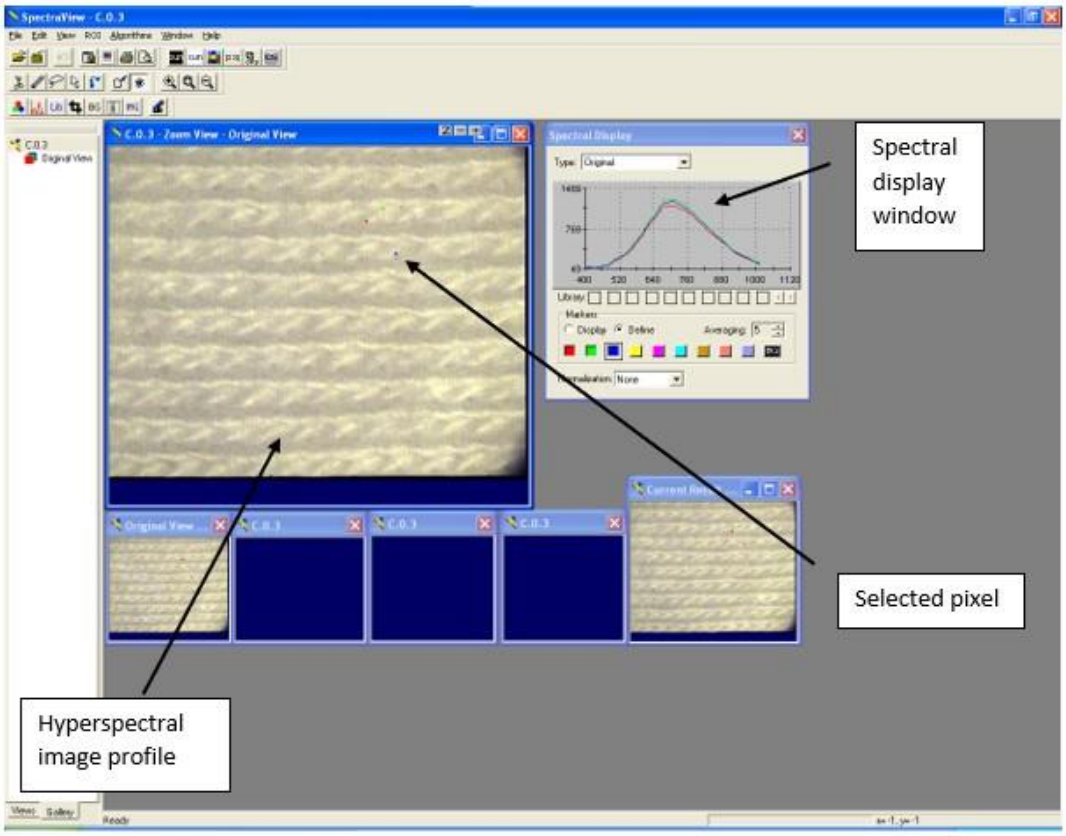

Fig. 2.7. *Screenshot of the SpectraView® 5.0 analysis software display showing the analysis of a Cotton sample, with regular weaving pattern of the fabric being evident. Selected pixels are visible in the "Zoom View" window, with the spectral profiles of selected pixels visible in the "Spectral Display" window.*

2.6 Pilot study

As this is novel research, the best type of lighting to use for capturing the reflectance profiles of the fabrics is not known. To better explore the potential spectral output given by the various available lights, a pilot study was conducted comparing spectra obtained via the VIS-NIR light (highest spectral intensity between 400 – 1000nm) with the spectra obtained via the VIS-NIR coupled with the VIS-H light (highest spectral intensity between 650 – 950nm). We noticed through just using the VIS-NIR lighting that many peaks were occurring around the red part of the electromagnetic spectrum (between 635 – 700nm), and so decided to explore the use of halogen light

to illuminate this area of the spectrum better to determine if more specific differentiation of the peaks was possible. Fig. 2.8 below shows all the relevant spectral ranges compiled together for clarity.

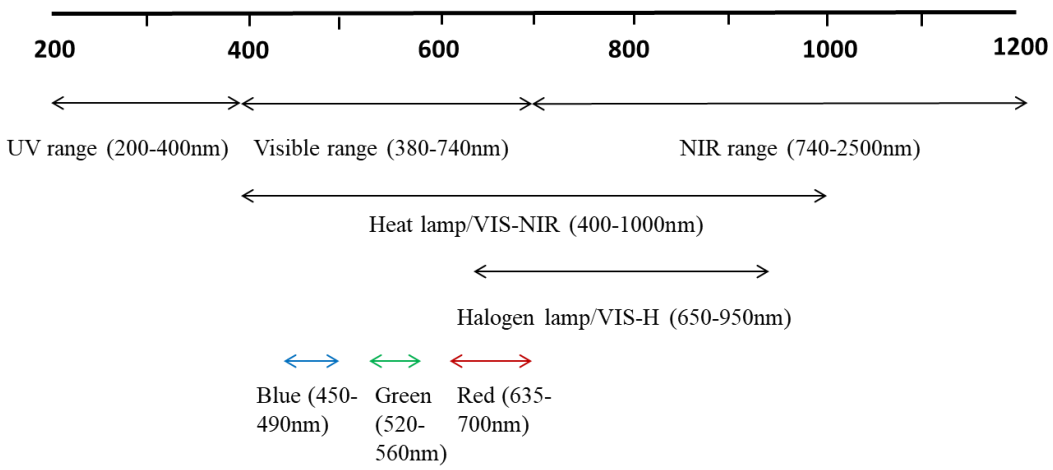

Fig. 2.8. *Relevant spectral ranges of the lighting involved in this experiment compared against UV, visible, NIR, Blue, Green, and Red spectral ranges.*

One control (month 0) and one 6-month sample were selected from each fabric type (8 samples total). A total of 16 reflectance profiles were generated from this pilot study (8 with just VIS-NIR lighting, and 8 with VIS-NIR and VIS-H lighting).

Reflectance profiles were generated in full for the UV (VIS-NIR) lighting, however, due to the developing COVID-19 situation in March 2020; data acquisition was halted so reflectance profiles for VIS-H lighting were not generated outside of this pilot study.

2.7 Primary study

The VIS-NIR light (100w, 120v digital heat lamp, Exo Terra®) (Fig. 2.6) was used to capture a reflectance profile from each fabric sample. There were four repetitions of each fabric for each month, 16 total samples per month from months 0 – 6, giving a total of 112 reflectance profiles. All data were collected within a 48hr time period,

and the laboratory space was reserved to ensure the measurement settings remained consistent for all images.

2.8 Statistical analysis

2.8.1 Pilot study

The raw text files were exported from the SpectraView® 5.0 analysis software program and imported into Excel (Microsoft® Excel® for Office 365) for clean-up and statistical analysis. Each text file contained the information from the three spectral measurements, which represented the relative light intensity between 400 and 1020nm at 76 selected wavelengths. There were two text files corresponding to each fabric sample (VIS-NIR and VIS-H), 16 in total.

The three spectral measurements for each profile were entered into tables as measurement 1, 2 and 3 (M1, M2, and M3 respectively) and a fourth column was generated with the average values for each of the 76 wavelengths (see Fig. 2.9 for an example).

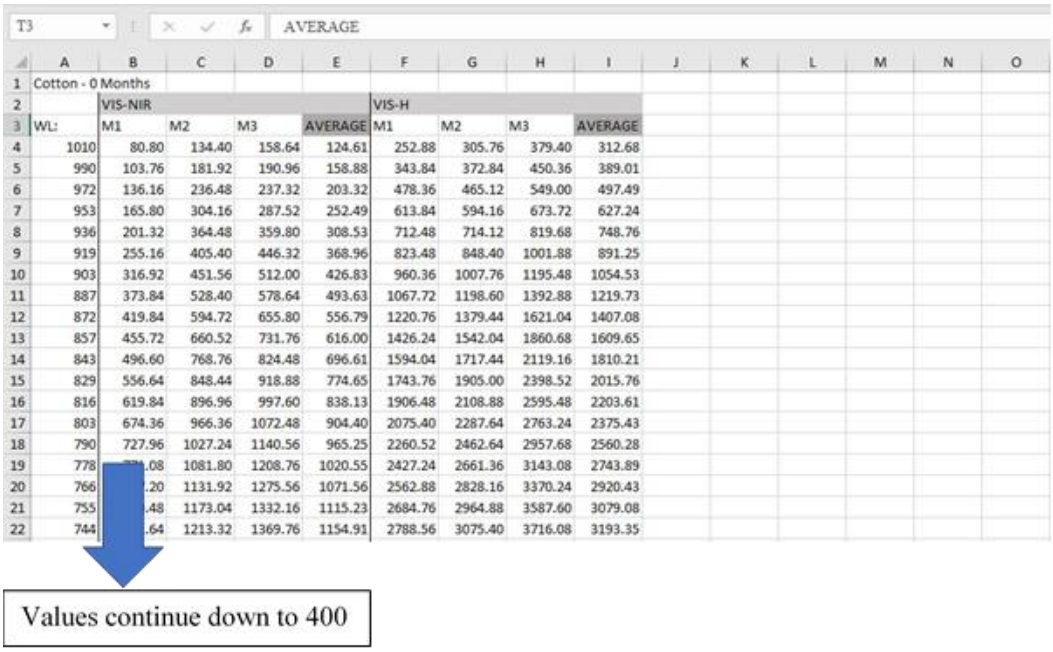

T3 | AVERAGE

	A	B	C	D	E	F	G	H	I
1	Cotton - 0 Months								
2		VIS-NIR				VIS-H			
3	WL:	M1	M2	M3	AVERAGE	M1	M2	M3	AVERAGE
4	1010	80.80	134.40	158.64	124.61	252.88	305.76	379.40	312.68
5	990	103.76	181.92	190.96	158.88	343.84	372.84	450.36	389.01
6	972	136.16	236.48	237.32	203.32	478.36	465.12	549.00	497.49
7	953	165.80	304.16	287.52	252.49	613.84	594.16	673.72	627.24
8	936	201.32	364.48	359.80	308.53	712.48	714.12	819.68	748.76
9	919	255.16	405.40	446.32	368.96	823.48	848.40	1001.88	891.25
10	903	316.92	451.56	512.00	426.83	960.36	1007.76	1195.48	1054.53
11	887	373.84	528.40	578.64	493.63	1067.72	1198.60	1392.88	1219.73
12	872	419.84	594.72	655.80	556.79	1220.76	1379.44	1621.04	1407.08
13	857	455.72	660.52	731.76	616.00	1426.24	1542.04	1860.68	1609.65
14	843	496.60	768.76	824.48	696.61	1594.04	1717.44	2119.16	1810.21
15	829	556.64	848.44	918.88	774.65	1743.76	1905.00	2398.52	2015.76
16	816	619.84	896.96	997.60	838.13	1906.48	2108.88	2595.48	2203.61
17	803	674.36	966.36	1072.48	904.40	2075.40	2287.64	2763.24	2375.43
18	790	727.96	1027.24	1140.56	965.25	2260.52	2462.64	2957.68	2560.28
19	778	[illegible]	1081.80	1208.76	1020.55	2427.24	2661.36	3143.08	2743.89
20	766	[illegible]	1131.92	1275.56	1071.56	2562.88	2828.16	3370.24	2920.43
21	755	[illegible]	1173.04	1332.16	1115.23	2684.76	2964.88	3587.60	3079.08
22	744	[illegible]	1213.32	1369.76	1154.91	2788.56	3075.40	3716.08	3193.35

Values continue down to 400

Fig. 2.9. *Example of how the average values were calculated for the VIS-NIR and VIS-H month 0 cotton samples in the pilot study.*

Statistical analysis was focused on determining whether the addition of the halogen lighting generated different reflectance profiles for each fabric type at the control and 6-month points of the experiment. The profiles were compared using a one-way ANOVA for each fabric type with Tukey post hoc analysis.

As only one repetition from month 0 and month 6 were chosen in the pilot study, the averaged results appear different to those in the primary study even though they include the same samples.

The Real Statistics Resource Pack© software (Zaiontz, 2020) add-in for Excel was used for conducting Tukey post hoc analysis. The significance value for all tests was set to $P < 0.05$.

2.8.2 Primary study

The raw text files were exported from the SpectraView® 5.0 analysis software program and imported into Excel for clean-up and statistical analysis. Each text file contained the information from the three spectral measurements, which represented the relative light intensity between 400 and 1020nm at 76 selected wavelengths. There were 112 text files, one for each fabric sample, in total.

The three spectral measurements for each profile were entered into tables as measurement 1, 2 and 3 (M1, M2, and M3 respectively) and a fourth column was generated with the average values for each of the 76 wavelengths. The four averages for each repetition were then averaged again to generate a 'monthly average' value for each wavelength (see Fig. 2.10 for an example). The monthly average values were then tabulated together for each fabric.

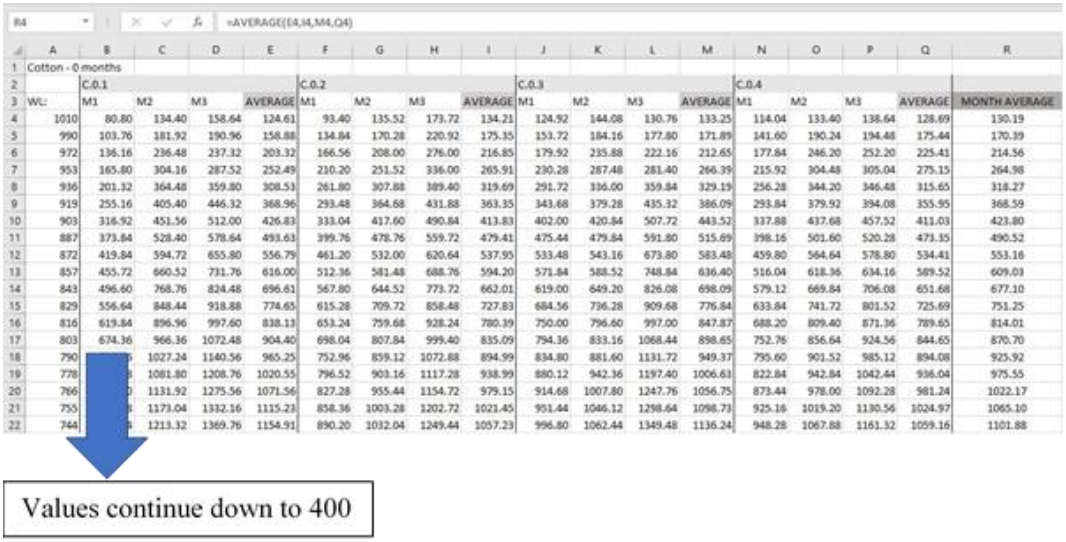

	A	B	C	D	E	F	G	H	I	J	K	L	M	N	O	P	Q	R
1	Cotton - 0 months																	
2		C.0.1				C.0.2				C.0.3				C.0.4				
3	WL:	M1	M2	M3	AVERAGE	M1	M2	M3	AVERAGE	M1	M2	M3	AVERAGE	M1	M2	M3	AVERAGE	MONTH AVERAGE
4	1010	80.80	134.40	158.64	124.61	93.40	135.52	173.72	134.21	124.92	144.08	130.76	133.25	114.04	133.40	138.64	128.69	130.19
5	990	103.76	181.92	190.96	158.88	134.84	170.28	220.92	175.35	153.72	184.16	177.80	171.89	141.60	190.24	194.48	175.44	170.39
6	972	136.16	236.48	237.32	203.32	166.56	208.00	276.00	216.85	179.92	235.88	222.16	212.65	177.84	246.20	252.20	225.41	214.56
7	953	165.80	304.16	287.52	252.49	210.20	251.52	336.00	265.91	230.28	287.48	281.40	266.39	215.92	304.48	305.04	275.15	264.98
8	936	201.32	364.48	359.80	308.53	261.80	307.88	389.40	319.69	291.72	336.00	359.84	329.19	256.28	344.20	346.48	315.65	318.27
9	919	255.16	405.40	446.32	368.96	293.48	364.68	431.88	363.35	343.68	379.28	435.32	386.09	293.84	379.92	394.08	355.95	368.59
10	903	316.92	451.56	512.00	426.83	333.04	417.60	490.84	413.83	402.00	420.84	507.72	443.52	337.88	417.68	457.52	411.03	423.80
11	887	373.84	528.40	578.64	493.63	399.76	478.76	559.72	479.41	475.44	479.84	591.80	515.69	398.16	501.60	520.28	473.35	490.52
12	872	419.84	594.72	655.80	556.79	461.20	532.00	620.64	537.95	533.48	543.16	673.80	583.48	459.80	564.64	578.80	534.41	553.16
13	857	455.72	660.52	731.76	616.00	512.36	581.48	688.76	594.20	571.84	588.52	748.84	636.40	516.04	618.36	634.16	589.52	609.03
14	843	496.60	768.76	824.48	696.61	567.80	644.52	773.72	662.01	619.00	649.20	826.08	698.09	579.12	669.84	706.08	651.68	677.10
15	829	556.64	848.44	918.88	774.65	615.28	709.72	858.48	727.83	684.56	736.28	909.68	776.84	633.84	741.72	801.52	725.69	751.25
16	816	619.84	896.96	997.60	838.13	653.24	759.68	928.24	780.39	750.00	796.60	997.00	847.87	688.20	809.40	871.36	789.65	814.01
17	803	674.36	966.36	1072.48	904.40	698.04	807.84	999.40	835.09	794.36	833.16	1068.44	898.65	752.76	856.64	924.56	844.65	870.70
18	790		1027.24	1140.56	965.25	752.96	859.12	1072.88	894.99	834.80	881.60	1131.72	949.37	795.60	901.52	985.12	894.08	925.92
19	778		1081.80	1208.76	1020.55	796.52	903.16	1117.28	938.99	880.12	942.36	1197.40	1006.63	822.84	942.84	1042.44	936.04	975.55
20	766		1131.92	1275.56	1071.56	827.28	955.44	1154.72	979.15	914.68	1007.80	1247.76	1056.75	873.44	978.00	1092.28	981.24	1022.17
21	755		1173.04	1332.16	1115.23	858.36	1003.28	1202.72	1021.45	951.44	1046.12	1298.64	1098.73	925.16	1019.20	1130.56	1024.97	1065.10
22	744		1213.32	1369.76	1154.91	890.20	1032.04	1249.44	1057.23	996.80	1062.44	1349.48	1136.24	948.28	1067.88	1161.32	1059.16	1101.88

Values continue down to 400

Fig. 2.10. *Example of how the monthly average was calculated for cotton at month 0 through combining the averages from each repetition in the primary study.*

Statistical analysis was focused on determining whether there was a difference in reflectance values between each month of the experiment and between each fabric.

The differences in reflectance values between each month were analysed with four one-way ANOVA tests, one for each fabric, with the independent variable being time, and the dependent variable being reflectance. Tukey post hoc analysis was conducted on each ANOVA to examine significance further.

After this initial analysis, the wavelengths were sorted by variance in reflectance values between months, and the 20 most variable wavelengths for each fabric were selected for further analysis creating what is hereafter known as the 'refined dataset'. The refined dataset was analysed with four one-way ANOVA tests, one for each fabric, with the independent variable being time, and the dependent variable being reflectance. Tukey post hoc analysis was conducted on each ANOVA to examine significance further.

The differences in reflectance values between each month and each fabric were examined using a two-way ANOVA with the independent variables being time and fabric, and the dependent variable being reflectance. Again, a Tukey post hoc analysis was conducted on each ANOVA to examine significance further. Linear regression analysis was also performed on each of the fabrics, again using Excel.

Again, the Real Statistics Resource Pack© software (Zaiontz, 2020) was used for post hoc analysis. The significance value for all tests was set to $p < 0.05$.

Chapter 3: Results

3.1 Pilot study

A total of 16 reflectance profiles were included in this analysis.
The results were collected according to the hypotheses of

- H_0 – the use of halogen lighting in addition to VIS-NIR would not provide significantly different reflectance profiles for each fabric with respect to the use of VIS-NIR light only (VIS-NIR versus VIS-H p>/=0.05); or
- H_1 – the use of halogen lighting in addition to VIS-NIR would produce significantly different reflectance profiles for each fabric with respect to the use of VIS-NIR light only (VIS-NIR versus VIS-H p<0.05).

Before performing statistical analysis, the H_0 is assumed.
Full results of the ANOVA and post hoc analysis are provided in the appendix.

3.1.1 Cotton

When testing for the difference between the reflectance profiles of cotton using VIS-NIR and VIS-H lighting, a significant difference was observed (p<0.001). Although the reflectance profiles were similar with regards to their overall shape for all four profiles with VIS-NIR 0 and VIS-H 0 peaking at 703nm, and VIS-NIR 6 and VIS-H 6 show twin peaks around 690 and 760nm (Fig. 3.1). Post hoc analysis indicated that significant difference (highest value was p<0.021) occurred between all groups except VIS-NIR 0 versus VIS-NIR 6 (p=0.708), and a summary of these results are displayed below in Table 3.1.

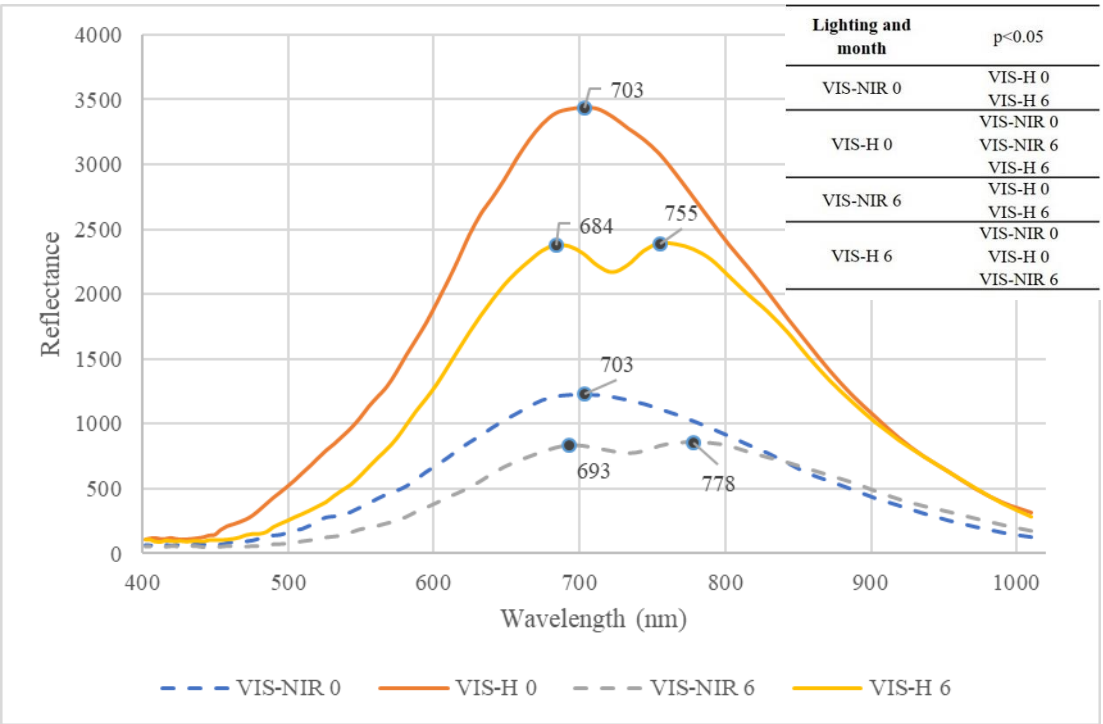

Fig. 3.1. *Spectral reflectance profiles for the cotton samples under the VIS-NIR versus VIS-H lighting. Peak wavelength for each spectral profile is highlighted and labelled on the chart. The table beside the graph indicates the lighting scenarios in which statistical results proved significantly different ($p<0.05$) from the lighting scenario in the corresponding column.*

Table 3.1.
Simplified results of the Tukey post hoc analysis on the cotton data. Bold numbers indicate a significant p-value ($p<0.05$).

Lighting and month	VIS-NIR 0	VIS-H 0	VIS-NIR 6	VIS-H 6
VIS-NIR 0	N/A	**<0.001**	0.708	**0.001**
VIS-H 0	**<0.001**	N/A	**<0.001**	**0.021**
VIS-NIR 6	0.708	**<0.001**	N/A	**<0.001**
VIS-H 6	**0.001**	**0.021**	**<0.001**	N/A

3.1.2 Neoprene

When testing for the difference between the reflectance profiles of neoprene using VIS-NIR and VIS-H lighting no significant difference was observed from the initial ANOVA ($p=0.415$), or in the post hoc analysis ($p>0.468$). The reflectance profiles were similar with regards to their overall shape for all four profiles with VIS-NIR 0,

VIS-H 0, and VIS-H 6 all peaking at 693nm, and VIS-NIR 6 peaking at 713nm (Fig. 3.2).

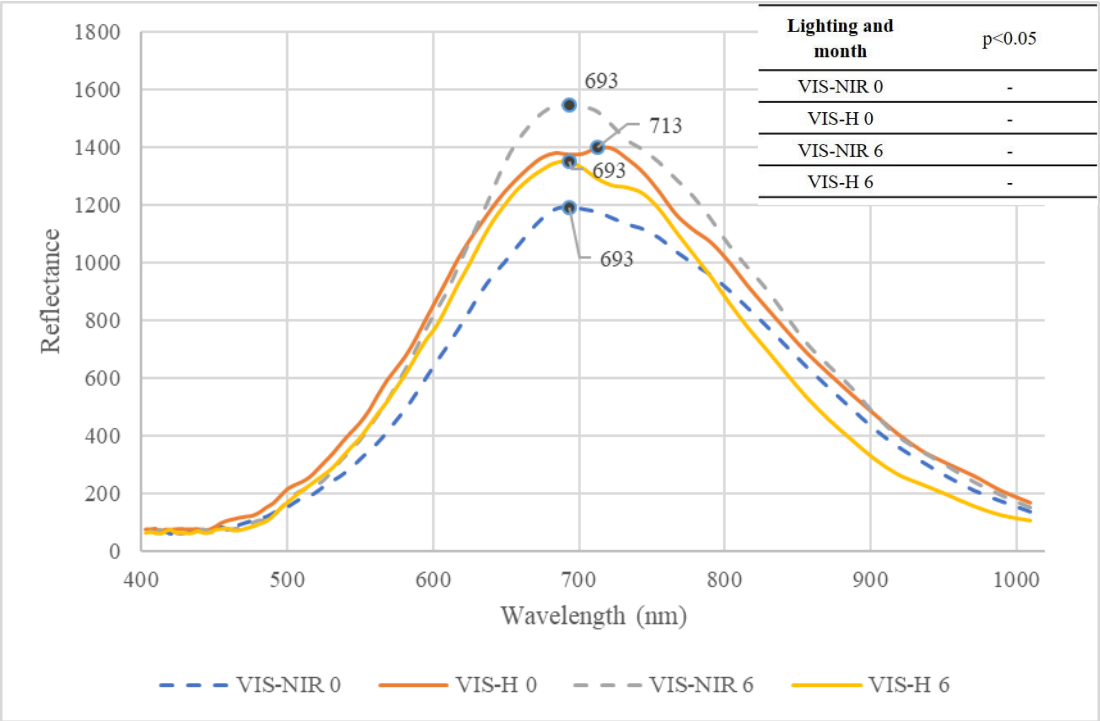

Fig. 3.2. *Spectral reflectance profiles for the neoprene samples under the VIS-NIR versus VIS-H lightings. Peak wavelength for each spectral profile is highlighted and labelled on the chart. The table beside the graph indicates the lighting scenarios in which statistical results proved significantly different ($p<0.05$) from the lighting scenario in the corresponding column. A cell with '-' indicates no significant data for that month.*

3.1.3 Satin

When testing for the difference between the reflectance profiles of satin using VIS-NIR and VIS-H lighting, a significant difference was observed from the ANOVA ($p<0.001$). The reflectance profiles were similar with regards to their overall shape for all four profiles with VIS-NIR 0 and VIS-H 0 peaking at 723 and 703nm respectively, and VIS-NIR 6 and VIS-H 6 peaking at 703 and 693nm respectively (Fig. 3.3). A summary of the post hoc analysis results is displayed below in Table 3.2.

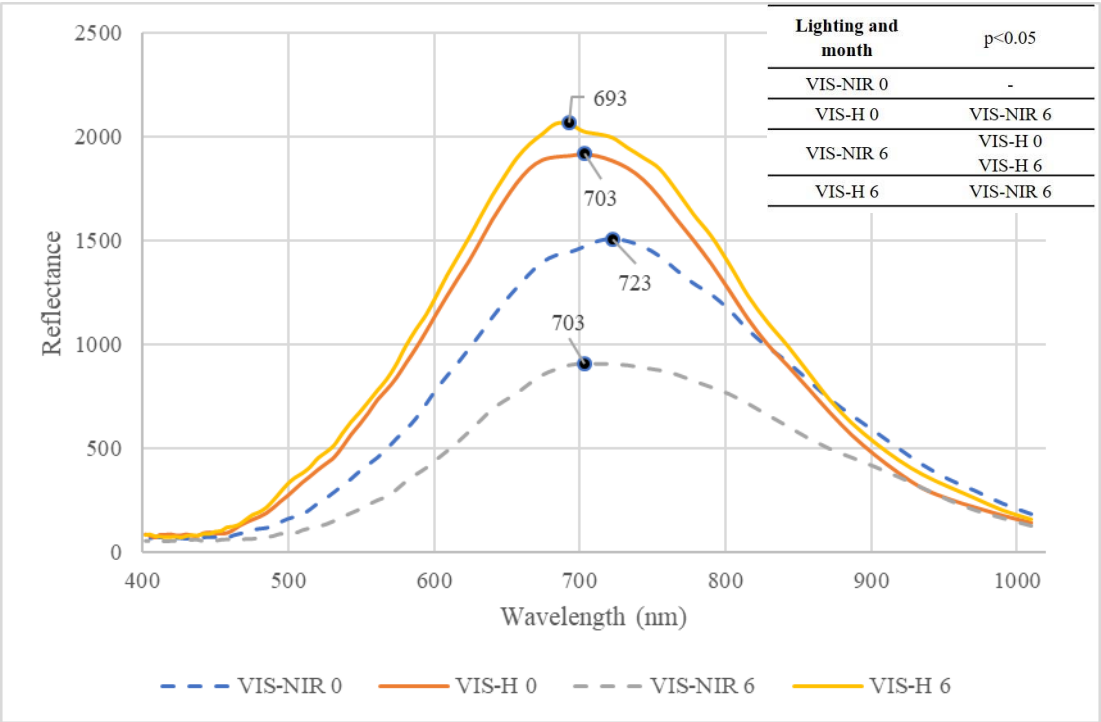

Fig. 3.3. *Spectral reflectance profiles for the satin samples under the VIS-NIR versus VIS-H lightings. Peak wavelength for each spectral profile is highlighted and labelled on the chart. The table beside the graph indicates the lighting scenarios in which statistical results proved significantly different ($p<0.05$) from the lighting scenario in the corresponding column. A cell with '-' indicates no significant data for that month.*

Table 3.2.
Simplified results of the Tukey post hoc analysis on the satin data. Bold numbers indicate a significant p-value ($p<0.05$).

Lighting and month	VIS-NIR 0	VIS-H 0	VIS-NIR 6	VIS-H 6
VIS-NIR 0	N/A	0.301	0.083	0.068
VIS-H 0	0.301	N/A	**<0.001**	0.892
VIS-NIR 6	0.083	**<0.001**	N/A	**<0.001**
VIS-H 6	0.068	0.892	**<0.001**	N/A

3.1.4 Velvet

When testing for the difference between the reflectance profiles of velvet using VIS-NIR and VIS-H lighting no significant difference was observed from the initial ANOVA ($p=0.097$), or in the post hoc analysis ($p>0.094$). The reflectance profiles were similar with regards to their overall shape for all four profiles with VIS-NIR 0

and VIS-H 0 peaking at 713 and 703nm respectively, and VIS-NIR 6 and VIS-H 6 peaking at 703 and 693nm respectively (Fig 3.4).

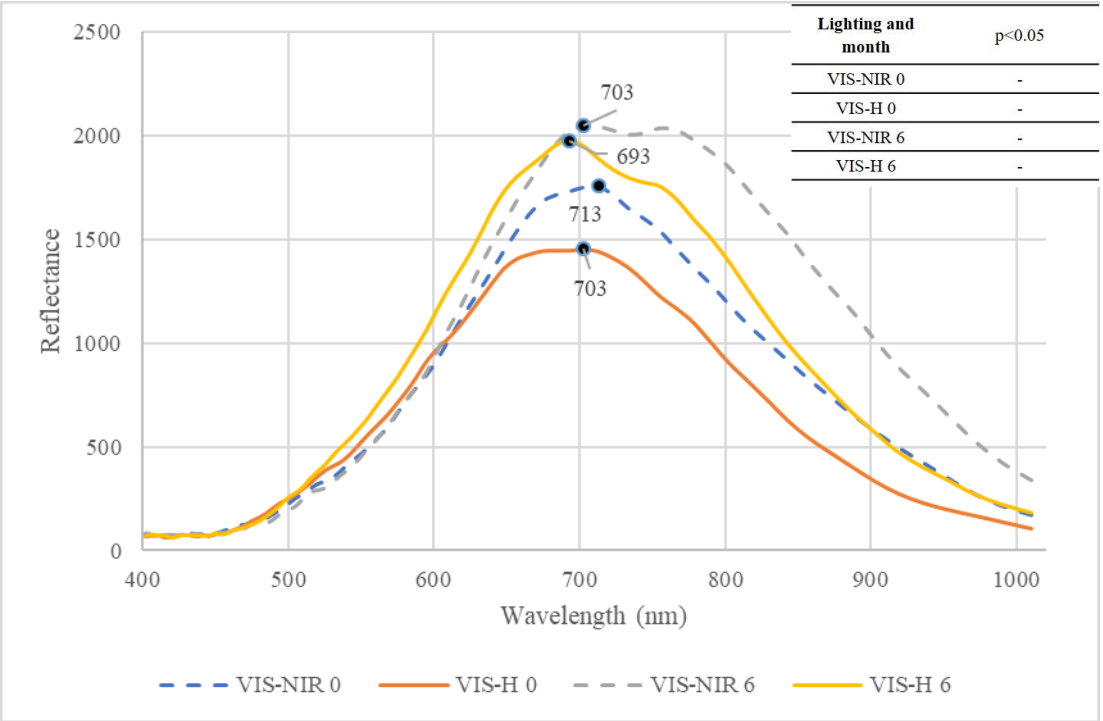

Fig. 3.4. *Spectral reflectance profiles for the velvet samples under the VIS-NIR versus VIS-H lightings. Peak wavelength for each spectral profile is highlighted and labelled on the chart. The table beside the graph indicates the lighting scenarios in which statistical results proved significantly different ($p<0.05$) from the lighting scenario in the corresponding column. A cell with '-' indicates no significant data for that month.*

3.2 Primary study

A total of 112 reflectance profiles were included in this analysis.

The results were collected according to the hypotheses of

- H_0 – there were no significant changes in the reflectance values over time (sample 1 versus samples 2 p>/=0.05);
- H_1 – there were significant changes in the reflectance values over time (sample 1 versus sample 2 p<0.05).

Before performing statistical analysis, the H_0 is assumed.

3.2.1 Evaluation of the differences between the reflectance values for each month for each fabric

The first aim of the analyses was to determine whether significant changes were occurring within the single fabrics over time. Firstly, the full dataset was analysed using an ANOVA on each fabric with Tukey post hoc. The refined datasets were also then tested with an ANOVA for each fabric with Tukey post hoc analysis. The resulting values were then compared with the full dataset to determine whether specificity had an impact on the resulting significance.

3.2.1.1 Cotton

Full dataset – An overall significance was observed when testing for the difference in reflectance values between months for cotton ($p<0.007$), post hoc analysis showed that this significance was between month 0 and 4 ($p<0.030$), and month 0 and 6 ($p<0.001$). This difference is demonstrated visually in Fig 3.5 as months 4, and 6 show the most variance from month 0. Cotton showed the most variance between 590nm and 770nm.

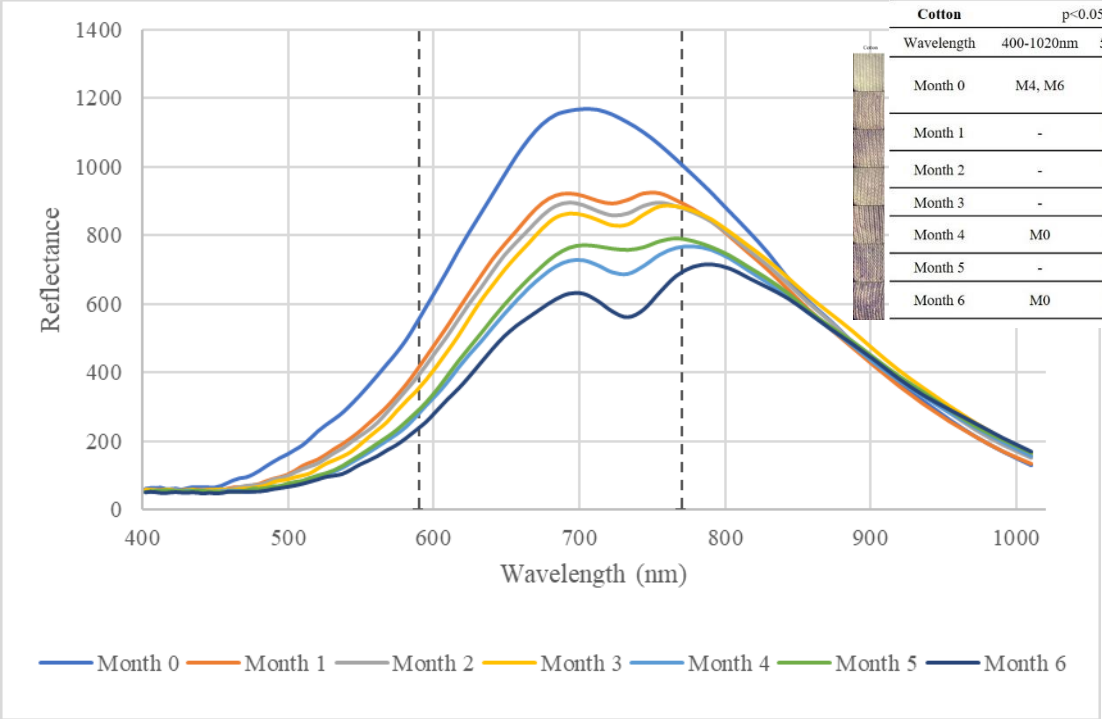

Cotton	p<0.05	
Wavelength	400-1020nm	590-770nm
Month 0	M4, M6	M1, M2, M3, M4, M5, M6
Month 1	-	M0, M4, M5, M6
Month 2	-	M0, M4, M6
Month 3	-	M0, M6
Month 4	M0	M0, M1, M2
Month 5	-	M0, M1
Month 6	M0	M0, M1, M2, M3

Fig. 3.5. *Average monthly spectral data displayed along the full spectrum for cotton. Dotted lines indicate the lower (590nm) and upper (770nm) boundaries between which the 20 most variable measurements lie. The table beside the graph indicates the months in which statistical results proved significantly different ($p<0.05$) from the month in the corresponding column (M1=month 1; M2=month 2; M3=month 3; M4=month 4; M5=month 5; M6=month 6), considering both wavelength ranges studied. A cell with '-' indicates no significant data for that month.*

Refined dataset – An overall significance was observed when testing for the difference in reflectance values between months for the refined cotton dataset ($p<0.001$). A comparison between the two data sets, full and refined, is provided in Tables 3.3 and 3.4, respectively. As shown in the tables, a more considerable significance between the individual months was observable after data refinement, and the analyses focused on the wavelengths with a larger variance in averages.

Table 3.3.
Simplified results of the Tukey post hoc analysis on the full cotton dataset. Bold numbers indicate a significant p-value ($p<0.05$).

Wavelength 400-1020nm	Month 0	Month 1	Month 2	Month 3	Month 4	Month 5	Month 6
Month 0	N/A	0.595	0.485	0.352	**0.028**	0.057	**0.004**
Month 1	0.595	N/A	1.000	1.000	0.785	0.902	0.421
Month 2	0.485	1.000	N/A	1.000	0.867	0.950	0.529
Month 3	0.352	1.000	1.000	N/A	0.940	0.984	0.669
Month 4	**0.028**	0.785	0.867	0.940	N/A	1.000	0.998
Month 5	0.057	0.902	0.950	0.984	1.000	N/A	0.984
Month 6	**0.004**	0.421	0.529	0.669	0.998	0.984	N/A

Table 3.4.
Simplified results of the Tukey post hoc analysis on the refined cotton dataset. Bold numbers indicate a significant p-value ($p<0.05$).

Wavelength 590-770nm	Month 0	Month 1	Month 2	Month 3	Month 4	Month 5	Month 6
Month 0	N/A	**0.003**	**<0.001**	**<0.001**	**<0.001**	**<0.001**	**<0.001**
Month 1	**0.003**	N/A	0.997	0.872	**0.006**	**0.046**	**<0.001**
Month 2	**<0.001**	0.997	N/A	0.994	**0.039**	0.195	**<0.001**
Month 3	**<0.001**	0.872	0.994	N/A	0.199	0.571	**0.002**
Month 4	**<0.001**	**0.006**	**0.039**	0.199	N/A	0.995	0.669
Month 5	**<0.001**	**0.046**	0.195	0.571	0.995	N/A	0.265
Month 6	**<0.001**	**<0.001**	**<0.001**	**0.002**	0.669	0.265	N/A

3.2.1.2 Neoprene

Full dataset - When testing the full dataset, there was no statistical significance shown ($p=0.540$) for neoprene. Neoprene demonstrated the most variance between 615nm and 805nm (Fig 3.6).

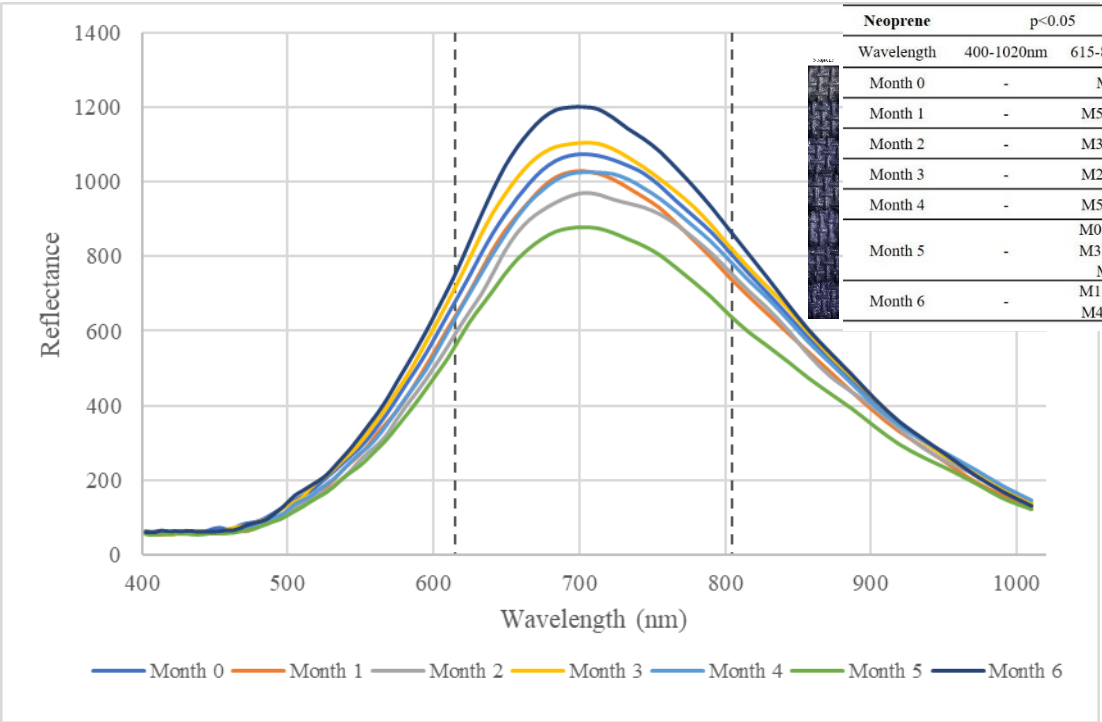

Neoprene	p<0.05	
Wavelength	400-1020nm	615-805nm
Month 0	-	M5
Month 1	-	M5, M6
Month 2	-	M3, M6
Month 3	-	M2, M5
Month 4	-	M5, M6
Month 5	-	M0, M1, M3, M4, M6
Month 6	-	M1, M2, M4, M5

Fig. 3.6. *Average monthly spectral data displayed along the full spectrum for neoprene. Dotted lines indicate the lower (615nm) and upper (805nm) boundaries between which the 20 most variable measurements lie. The table beside the graph indicates the months in which statistical results proved significantly different ($p<0.05$) from the month in the corresponding column (M1=month 1; M2=month 2; M3=month 3; M4=month 4; M5=month 5; M6=month 6), considering both wavelength ranges studied. A cell with '-' indicates no significant data for that month.*

Refined dataset - An overall significance was observed when testing for the difference in reflectance values between months for the refined neoprene dataset ($p<0.001$). A comparison between the two data sets, full and refined, is provided in Tables 3.5 and 3.6, respectively. As shown in the tables, a more considerable significance between the individual months was observable after data refinement, and the analyses focused on the wavelengths with a larger variance in averages.

Table 3.5.
Simplified results of the Tukey post hoc analysis on the full neoprene dataset. There were no significant months recorded for the full neoprene dataset ($p<0.05$).

Wavelength 400-1020nm	Month 0	Month 1	Month 2	Month 3	Month 4	Month 5	Month 6
Month 0	N/A	0.999	0.992	1.000	1.000	0.845	0.995
Month 1	0.999	N/A	1.000	0.992	1.000	0.982	0.916
Month 2	0.992	1.000	N/A	0.965	1.000	0.997	0.819
Month 3	1.000	0.992	0.965	N/A	0.997	0.715	1.000
Month 4	1.000	1.000	1.000	0.997	N/A	0.960	0.955
Month 5	0.845	0.982	0.997	0.715	0.960	N/A	0.436
Month 6	0.995	0.916	0.819	1.000	0.955	0.436	N/A

Table 3.6.
Simplified results of the Tukey post hoc analysis on the refined neoprene dataset. Bold numbers indicate a significant p-value ($p<0.05$).

Wavelength 615-805nm	Month 0	Month 1	Month 2	Month 3	Month 4	Month 5	Month 6
Month 0	N/A	0.791	0.164	0.964	0.909	**<0.001**	0.063
Month 1	0.791	N/A	0.930	0.222	1.000	**0.021**	**0.001**
Month 2	0.164	0.930	N/A	**0.013**	0.826	0.300	**<0.001**
Month 3	0.964	0.222	**0.013**	N/A	0.356	**<0.001**	0.443
Month 4	0.909	1.000	0.826	0.356	N/A	**0.009**	**0.002**
Month 5	**<0.001**	**0.021**	0.300	**<0.001**	**0.009**	N/A	**<0.001**
Month 6	0.063	**0.001**	**<0.001**	0.443	**0.002**	**<0.001**	N/A

3.2.1.3 Satin

Full dataset - An overall significance was observed when testing for the difference in reflectance values for satin ($p=0.029$), and post hoc analysis demonstrated that this significance was between month 0 and 2 ($p=0.010$). This difference is shown visually in Fig. 3.7 as month 0, and 2 record reflectance levels higher and lower, respectively, from the other months. Satin showed the most variance between 600nm and 780nm.

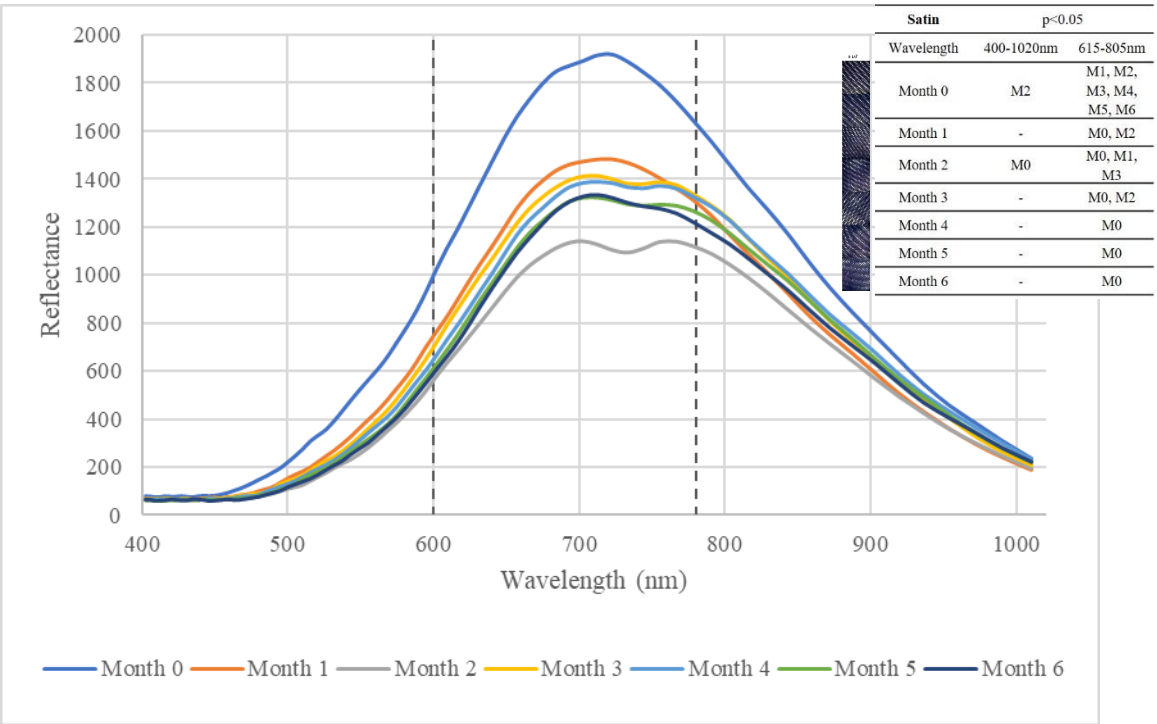

Satin	p<0.05	
Wavelength	400-1020nm	615-805nm
Month 0	M2	M1, M2, M3, M4, M5, M6
Month 1	-	M0, M2
Month 2	M0	M0, M1, M3
Month 3	-	M0, M2
Month 4	-	M0
Month 5	-	M0
Month 6	-	M0

Fig. 3.7. *Average monthly spectral data displayed along the full spectrum for satin. Dotted lines indicate the lower (600nm) and upper (780nm) boundaries between which the 20 most variable measurements lie. The table beside the graph indicates the months in which statistical results proved significantly different ($p<0.05$) from the month in the corresponding column (M1=month 1; M2=month 2; M3=month 3; M4=month 4; M5=month 5; M6=month 6), considering both wavelength ranges studied. A cell with '-' indicates no significant data for that month.*

Refined dataset - An overall significance was observed when testing for the difference in reflectance values between months for the refined satin dataset ($p<0.001$). A comparison between the two data sets, full and refined, is provided in Tables 3.7 and 3.8, respectively. As shown in the tables, a more considerable significance between the individual months was observable after data refinement, and the analyses focused on the wavelengths with a larger variance in averages.

Table 3.7.
Simplified results of the Tukey post hoc analysis on the full satin dataset. Bold numbers indicate a significant p-value ($p<0.05$).

Wavelength 400-1020nm	Month 0	Month 1	Month 2	Month 3	Month 4	Month 5	Month 6
Month 0	N/A	0.353	**0.010**	0.291	0.211	0.101	0.072
Month 1	0.353	N/A	0.824	1.000	1.000	0.997	0.991
Month 2	**0.010**	0.824	N/A	0.875	0.933	0.988	0.996
Month 3	0.291	1.000	0.875	N/A	1.000	0.999	0.996
Month 4	0.211	1.000	0.933	1.000	N/A	1.000	0.999
Month 5	0.101	0.997	0.988	0.999	1.000	N/A	1.000
Month 6	0.072	0.991	0.996	0.996	0.999	1.000	N/A

Table 3.8.
Simplified results of the Tukey post hoc analysis on the refined satin dataset. Bold numbers indicate a significant p-value ($p<0.05$).

Wavelength 600-780nm	Month 0	Month 1	Month 2	Month 3	Month 4	Month 5	Month 6
Month 0	N/A	**<0.001**	**<0.001**	**<0.001**	**<0.001**	**<0.001**	**<0.001**
Month 1	**<0.001**	N/A	**0.006**	0.997	0.912	0.484	0.378
Month 2	**<0.001**	**0.006**	N/A	**0.038**	0.152	0.553	0.665
Month 3	**<0.001**	0.997	**0.038**	N/A	0.998	0.853	0.766
Month 4	**<0.001**	0.912	0.152	0.998	N/A	0.989	0.969
Month 5	**<0.001**	0.484	0.553	0.853	0.989	N/A	1.000
Month 6	**<0.001**	0.378	0.665	0.766	0.969	1.000	N/A

3.2.1.4 Velvet

Full dataset - When testing the full dataset, there was no statistical significance shown ($p=0.921$) for velvet. Velvet demonstrated the most variance between 585nm and 755nm (Fig 3.8).

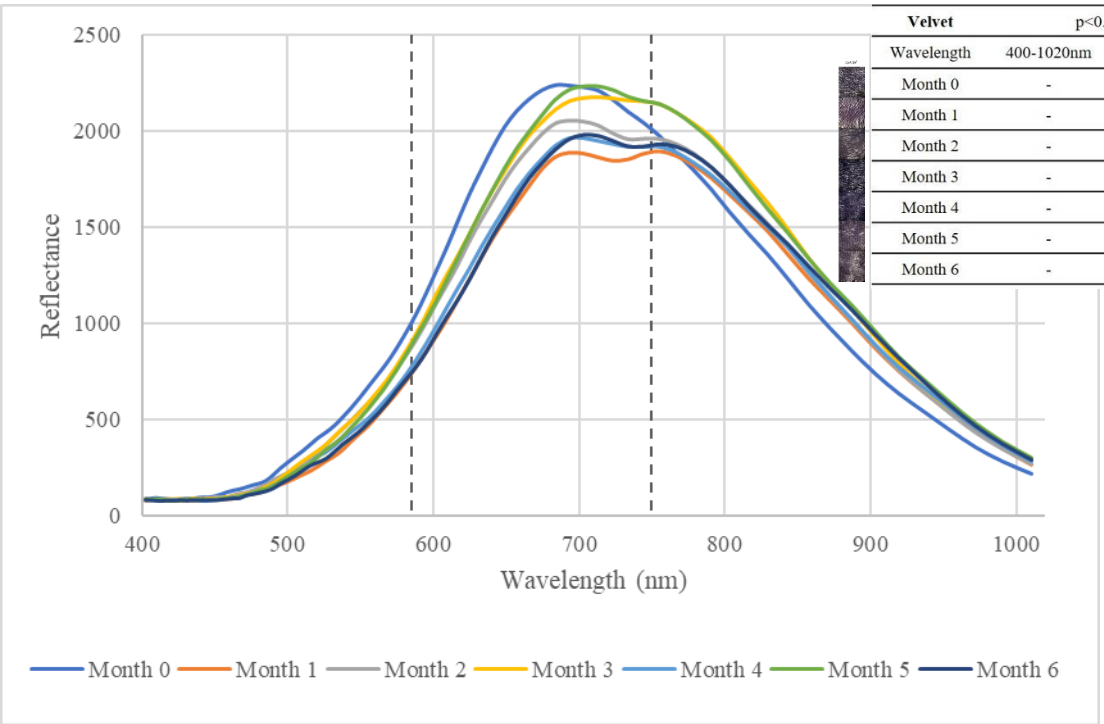

Velvet	p<0.05	
Wavelength	400-1020nm	585-755nm
Month 0	-	-
Month 1	-	-
Month 2	-	-
Month 3	-	-
Month 4	-	-
Month 5	-	-
Month 6	-	-

Fig. 3.8. *Average monthly spectral data displayed along the full spectrum for velvet. Dotted lines indicate the lower (585nm) and upper (755nm) boundaries between which the 20 most variable measurements lie. The table beside the graph indicates the months in which statistical results proved significantly different ($p<0.05$) from the month in the corresponding column (M1=month 1; M2=month 2; M3=month 3; M4=month 4; M5=month 5; M6=month 6), considering both wavelength ranges studied. A cell with '-' indicates no significant data for that month.*

Refined dataset - When testing the refined dataset, there was no statistical significance shown ($p=0.512$) for velvet. While the p-value is approaching 0.05, the reflectance levels in the fabric were still not significantly different from one another.

3.2.2 Evaluation of significant linear correlation within the refined datasets using regression analysis

The second research aim was to determine whether there was any significant trend in the fabric's changes over time. A regression analysis was conducted on the mean reflectance level at each month from the refined dataset. Full resuts of the regression analysis are provided in the appendix.

3.2.2.1 Cotton

The highest levels of variability of reflectance were observed between month 0 and month 6, with mean reflectance levels of 981.27 and 506.88, respectively (SE 36.225 for both). There is a significative negative relationship between the mean reflectance and the time spent in water (r^2=0.90, p=0.00) (Fig. 3.9).

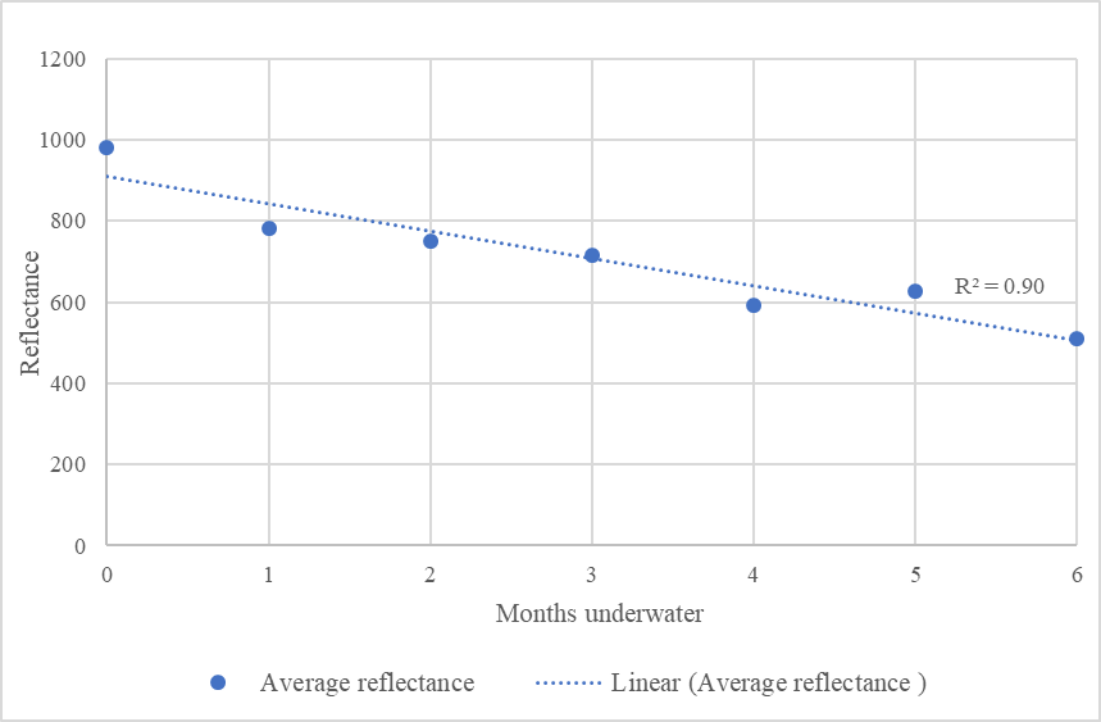

Fig. 3.9. *Linear regression analysis of the mean reflectance levels for cotton at each month of the experiment.*

3.2.2.2 Neoprene

The highest level of variability was demonstrated between month 5 and month 6, with mean reflectance levels of 773.693 and 1051.719, respectively (SE 25.787 for both). There is no significant relationship between the mean reflectance and the time spent in water (r^2=0.01, p=0.81) for the refined neoprene dataset (Fig. 3.10).

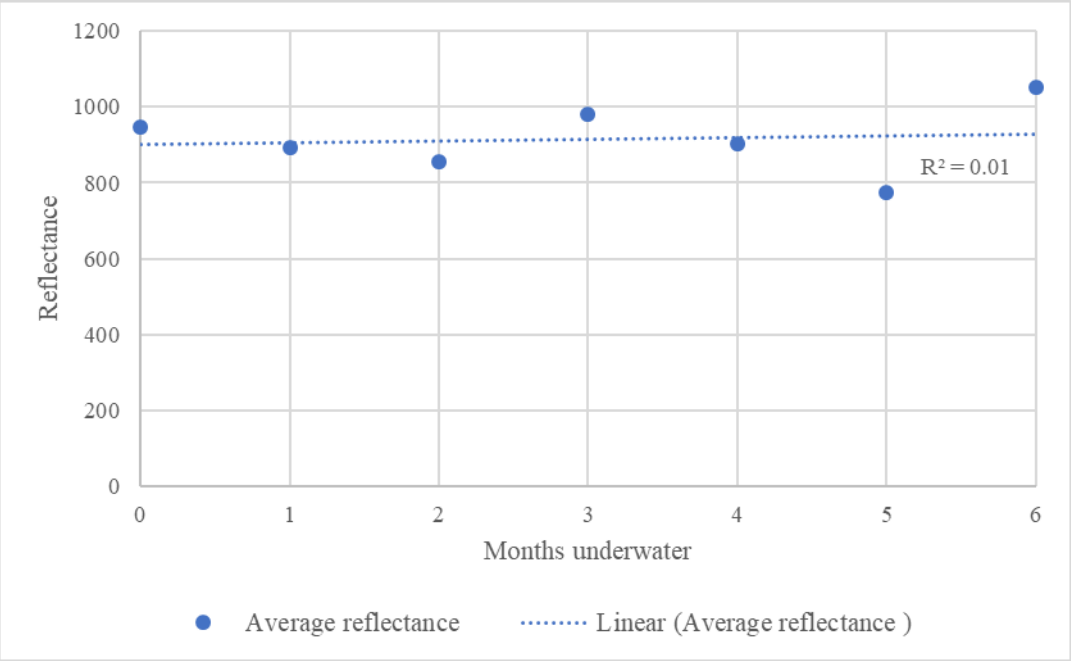

Fig. 3.10. *Linear regression analysis of the mean reflectance levels for neoprene at each month of the experiment.*

3.2.2.3 Satin

The highest level of variability was demonstrated between month 0 and month 2, with mean reflectance levels of 1626.561 and 976.870, respectively (SE 53.547 for both). There is a weak negative relationship between the mean reflectance and the time spent in water (r^2=0.40, p=0.13) (Fig. 3.11), suggesting that a linear relationship is most likely not present in the satin dataset.

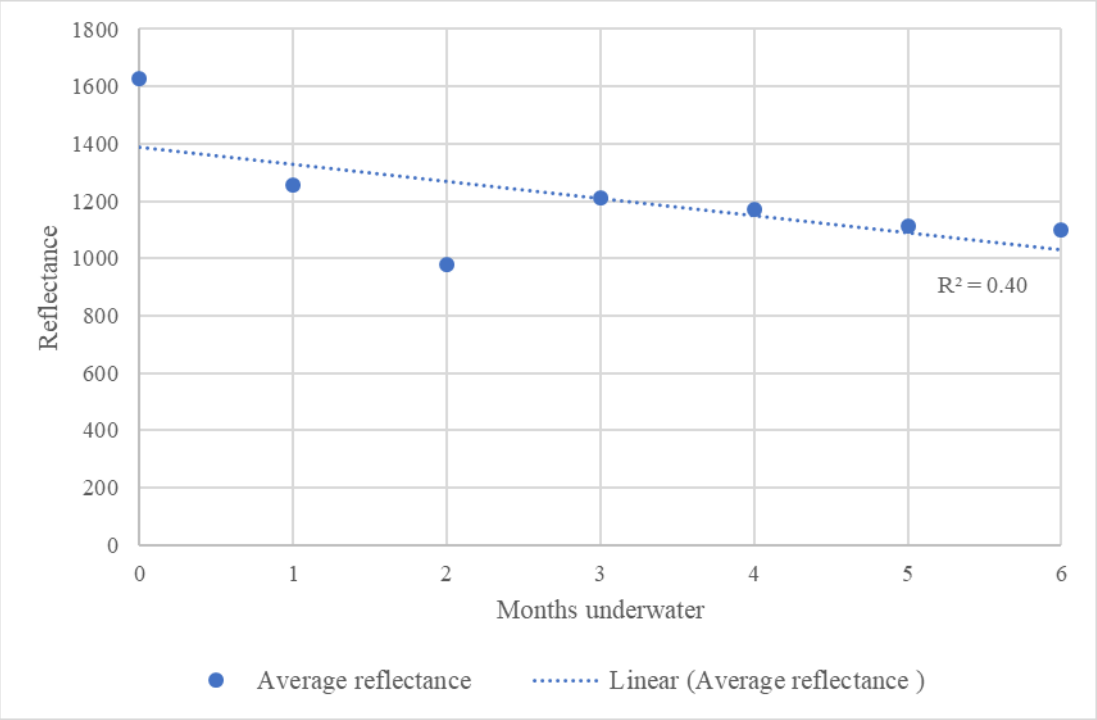

Fig. 3.11. *Linear regression analysis of the mean reflectance levels for satin at each month of the experiment.*

3.2.2.4 Velvet

The highest level of variability was demonstrated between month 0 and month 1, with mean reflectance levels of 1875.038 and 1518.070, respectively (SE 92.376 for both). There is no significant relationship between the mean reflectance and the time spent in water (r^2=0.09, p=0.51) for the refined velvet dataset (Fig. 3.12).

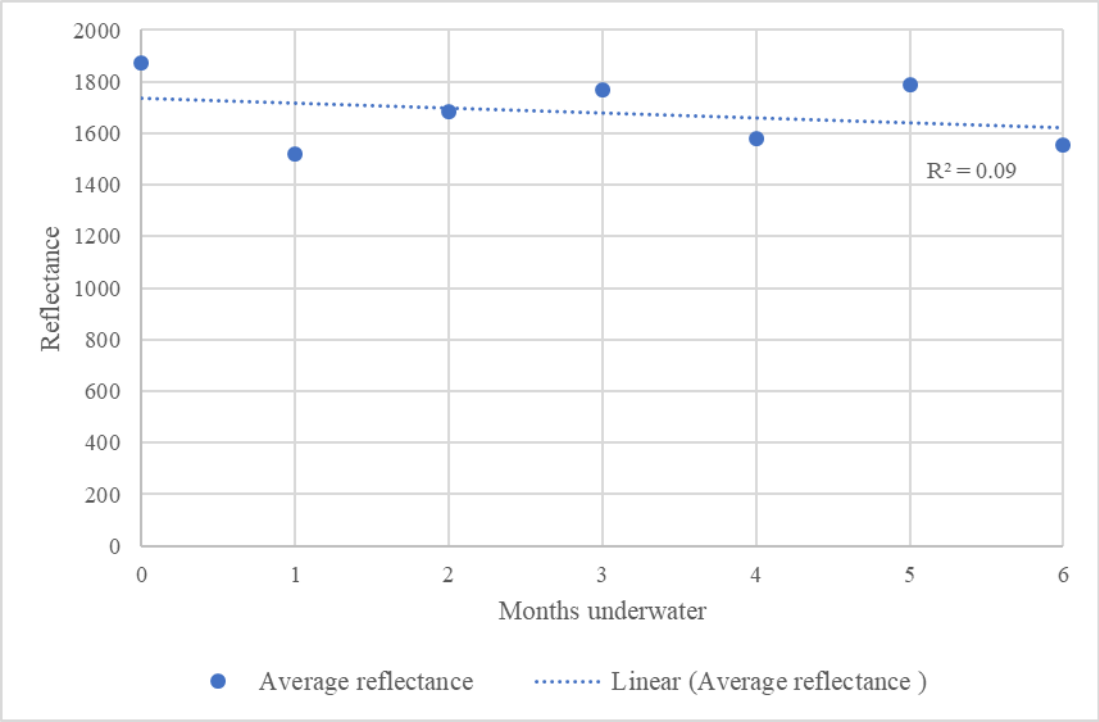

Fig. 3.12. *Linear regression analysis of the mean reflectance levels for velvet at each month of the experiment.*

3.2.3 Evaluation of the differences between the reflectance values for each fabric

The final aim of the research was to determine whether the reflectance data is unique to each fabric. This was tested by conducting a two-way ANOVA (testing time and fabric type against reflectance) on the full and refined datasets.

For the full dataset, overall significance was observed both between months (p=0.039) and between fabrics (p<0.001). Post hoc analysis showed that cotton and

neoprene were not determined to be statistically different from one another (p=0.268), but all other fabric combinations were significantly different. For the refined dataset, significance was observed both between months (p<0.001) and between fabrics (p<0.001). The results of Tukey the post hoc are simplified in Tables 3.9 and 3.10 below. As shown in the tables, a more considerable significance between the individual months was observable after data refinement, and the analyses focused on the wavelengths with a larger variance in averages.

Table 3.9.
Simplified results of the Tukey post hoc analysis on the full fabrics dataset. Bold numbers indicate a significant p-value (p<0.05).

Fabric type	Cotton	Neoprene	Satin	Velvet
Cotton	N/A	0.268	**<0.001**	**<0.001**
Neoprene	0.268	N/A	**<0.001**	**<0.001**
Satin	**<0.001**	**<0.001**	N/A	**<0.001**
Velvet	**<0.001**	**<0.001**	**<0.001**	N/A

Table 3.10.
Simplified results of the Tukey post hoc analysis on the refined fabrics dataset. Bold numbers indicate a significant p-value (p<0.05).

Fabric type	Cotton	Neoprene	Satin	Velvet
Cotton	N/A	**<0.001**	**<0.001**	**<0.001**
Neoprene	**<0.001**	N/A	**<0.001**	**<0.001**
Satin	**<0.001**	**<0.001**	N/A	**<0.001**
Velvet	**<0.001**	**<0.001**	**<0.001**	N/A

3.2.3.1 Month by month comparison of fabrics

One-way ANOVA testing was conducted on the fabrics month by month to examine significant changes between the fabrics at each month of submergence. To test both the full and refined dataset, a wavelength ranges of 400 – 1020nm, and 588 – 803nm were used. The refined dataset wavelength was slightly different from the previous tests as it needed to encompass the 20 most variable measurements from all four

fabrics, which had different ranges from one another. Results from all ANOVA tests on both the full and refined datasets showed that the fabrics reflectance profiles were significantly different from one another each month of the experiment ($p<0.001$ for all). The Tukey post hoc analyses results are tabulated below in Tables 3.11 – 3.24, and a more considerable significance between the individual fabrics was observable after data refinement, and the analyses focused on the wavelengths with a larger variance in averages.

This space is intentionally blank for better comprehension of the following tables and figures.

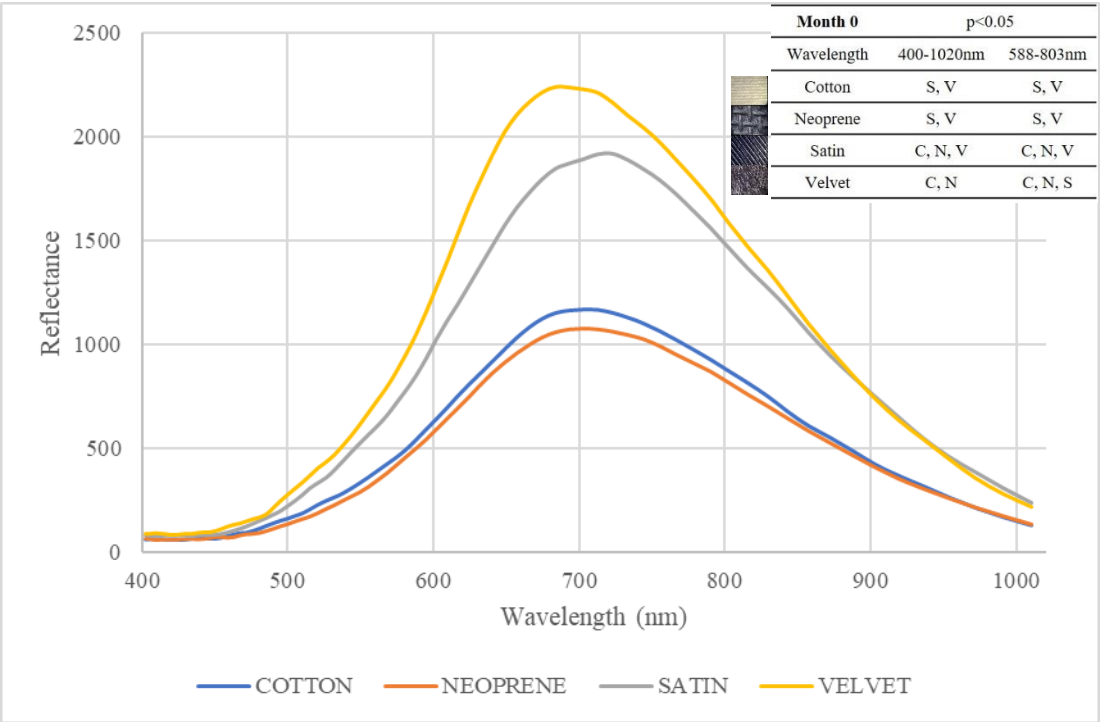

Figure 3.13. *Month 0 spectral comparisons between the four fabrics. The table beside the graph indicates the fabrics in which statistical results proved significantly different (p<0.05) from the fabrics in the corresponding column (C=cotton; N=neoprene; S=satin; V=velvet), considering both wavelength ranges studied.*

Table 3.11.
Simplified results of the Tukey post hoc analysis on the full dataset (400 – 1020nm) of all fabrics for month 0. Bold numbers indicate a significant p-value.

Fabric type (400-1020nm)	Cotton	Neoprene	Satin	Velvet
Cotton	N/A	0.976	**0.013**	**<0.001**
Neoprene	0.976	N/A	**0.003**	**<0.001**
Satin	**0.013**	**0.003**	N/A	0.563
Velvet	**<0.001**	**<0.001**	0.563	N/A

Table 3.12.
Simplified results of the Tukey post hoc analysis on the refined dataset (588 – 803nm) of all fabrics for month 0. Bold numbers indicate a significant p-value.

Fabric type (588-803nm)	Cotton	Neoprene	Satin	Velvet
Cotton	N/A	0.800	**<0.001**	**<0.001**
Neoprene	0.800	N/A	**<0.001**	**<0.001**
Satin	**<0.001**	**<0.001**	N/A	**0.002**
Velvet	**<0.001**	**<0.001**	**0.002**	N/A

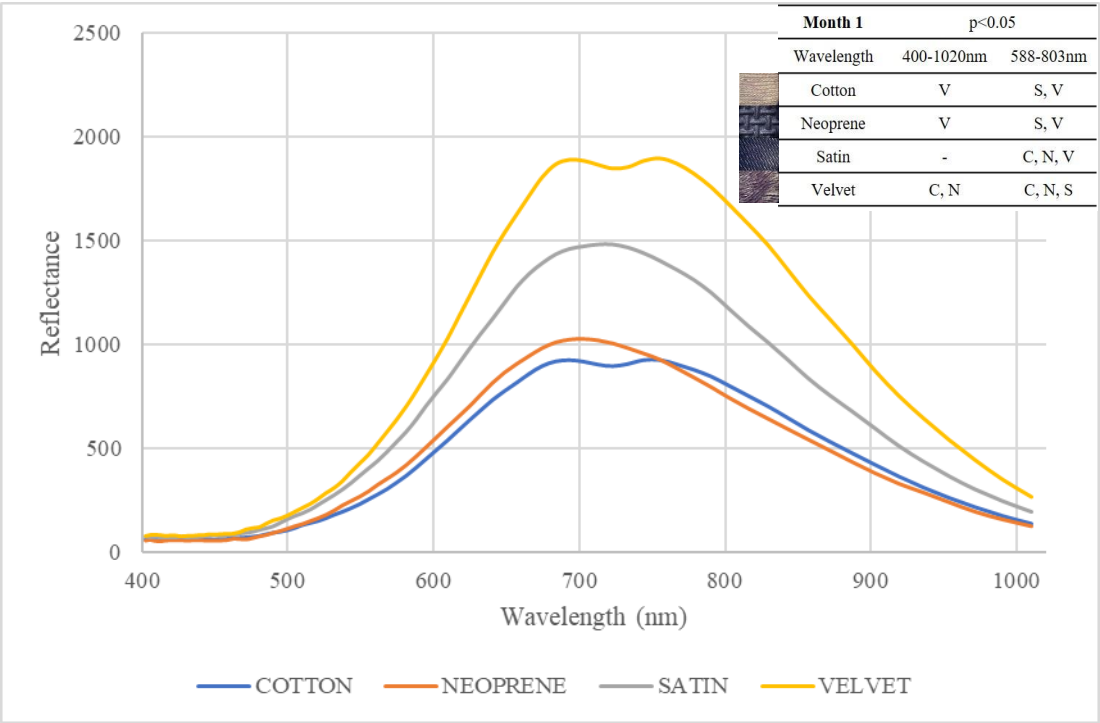

Figure 3.14. *Month 1 spectral comparisons between the four fabrics. The table beside the graph indicates the fabrics in which statistical results proved significantly different ($p<0.05$) from the fabrics in the corresponding column (C=cotton; N=neoprene; S=satin; V=velvet), considering both wavelength ranges studied. A cell with '-' indicates no significant data for that month.*

Table 3.13.
Simplified results of the Tukey post hoc analysis on the full dataset (400 – 1020nm) of all fabrics for month 1. Bold numbers indicate a significant p-value.

Fabric type (400-1020nm)	Cotton	Neoprene	Satin	Velvet
Cotton	N/A	0.994	0.063	**<0.001**
Neoprene	0.994	N/A	0.115	**<0.001**
Satin	0.063	0.115	N/A	0.111
Velvet	**<0.001**	**<0.001**	0.111	N/A

Table 3.14.
Simplified results of the Tukey post hoc analysis on the refined dataset (588 – 803nm) of all fabrics for month 1. Bold numbers indicate a significant p-value.

Fabric type (588-803nm)	Cotton	Neoprene	Satin	Velvet
Cotton	N/A	0.851	**<0.001**	**<0.001**
Neoprene	0.851	N/A	**<0.001**	**<0.001**
Satin	**<0.001**	**<0.001**	N/A	**<0.001**
Velvet	**<0.001**	**<0.001**	**<0.001**	N/A

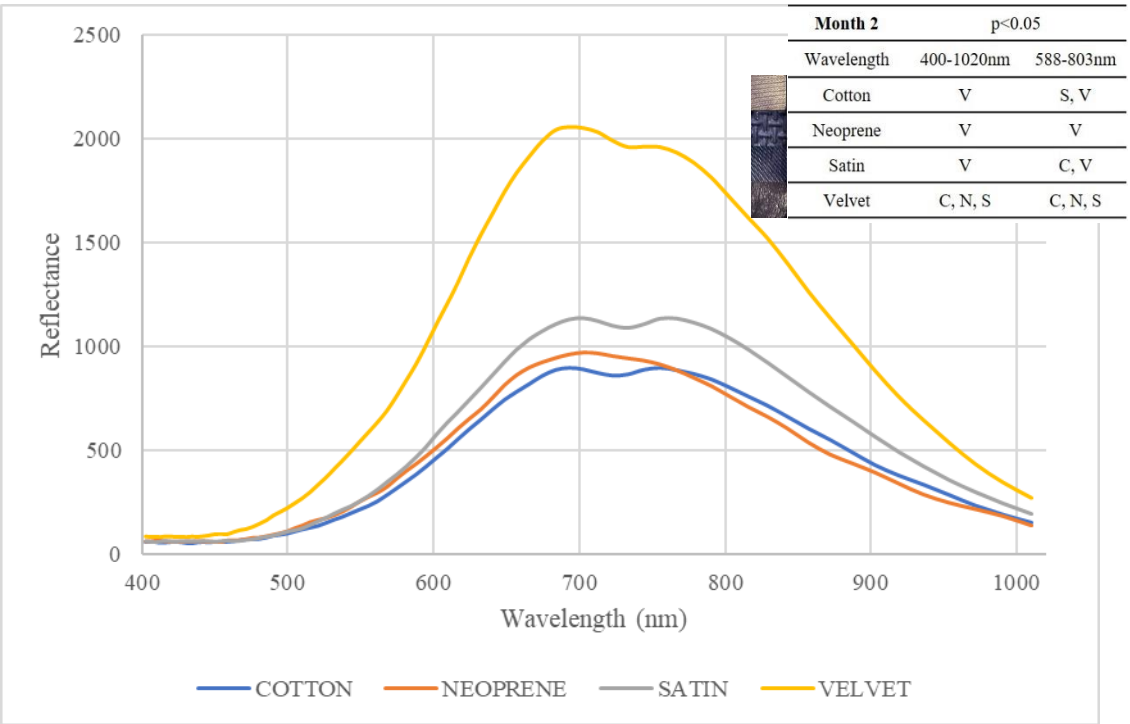

Figure 3.15. *Month 2 spectral comparisons between the four fabrics. The table beside the graph indicates the fabrics in which statistical results proved significantly different (p<0.05) from the fabrics in the corresponding column (C=cotton; N=neoprene; S=satin; V=velvet), considering both wavelength ranges studied. A cell with '-' indicates no significant data for that month.*

Table 3.15.
Simplified results of the Tukey post hoc analysis on the full dataset (400 – 1020nm) of all fabrics for month 2. Bold numbers indicate a significant p-value.

Fabric type (400-1020nm)	Cotton	Neoprene	Satin	Velvet
Cotton	N/A	0.997	0.615	**<0.001**
Neoprene	0.997	N/A	0.734	**<0.001**
Satin	0.615	0.734	N/A	**<0.001**
Velvet	**<0.001**	**<0.001**	**<0.001**	N/A

Table 3.16.
Simplified results of the Tukey post hoc analysis on the refined dataset (588 – 803nm) of all fabrics for month 2. Bold numbers indicate a significant p-value.

Fabric type (588-803nm)	Cotton	Neoprene	Satin	Velvet
Cotton	N/A	0.905	**0.030**	**<0.001**
Neoprene	0.905	N/A	0.151	**<0.001**
Satin	**0.030**	0.151	N/A	**<0.001**
Velvet	**<0.001**	**<0.001**	**<0.001**	N/A

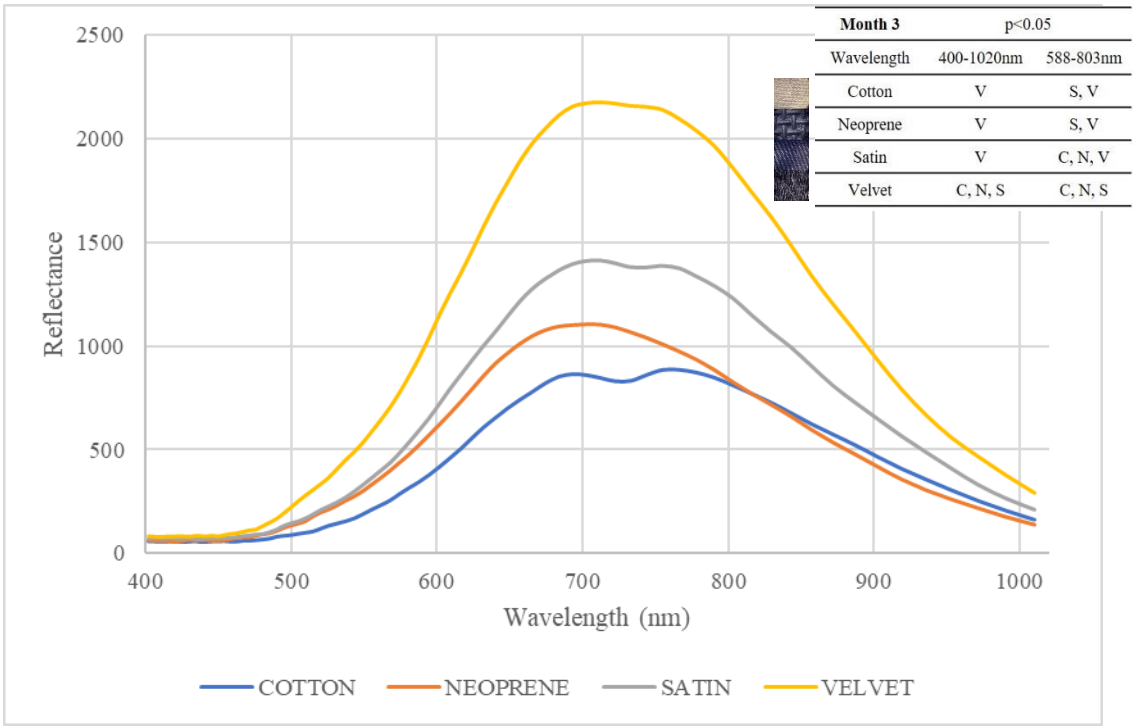

Figure 3.16. *Month 3 spectral comparisons between the four fabrics. The table beside the graph indicates the fabrics in which statistical results proved significantly different (p<0.05) from the fabrics in the corresponding column (C=cotton; N=neoprene; S=satin; V=velvet), considering both wavelength ranges studied.*

Table 3.17.
Simplified results of the Tukey post hoc analysis on the full dataset (400 – 1020nm) of all fabrics for month 3. Bold numbers indicate a significant p-value.

Fabric type (400-1020nm)	Cotton	Neoprene	Satin	Velvet
Cotton	N/A	0.783	0.073	**<0.001**
Neoprene	0.783	N/A	0.443	**<0.001**
Satin	0.073	0.443	N/A	**0.003**
Velvet	**<0.001**	**<0.001**	**0.003**	N/A

Table 3.18.
Simplified results of the Tukey post hoc analysis on the refined dataset (588 – 803nm) of all fabrics for month 3. Bold numbers indicate a significant p-value.

Fabric type (588-803nm)	Cotton	Neoprene	Satin	Velvet
Cotton	N/A	0.062	**<0.001**	**<0.001**
Neoprene	0.062	N/A	**0.011**	**<0.001**
Satin	**<0.001**	**0.011**	N/A	**<0.001**
Velvet	**<0.001**	**<0.001**	**<0.001**	N/A

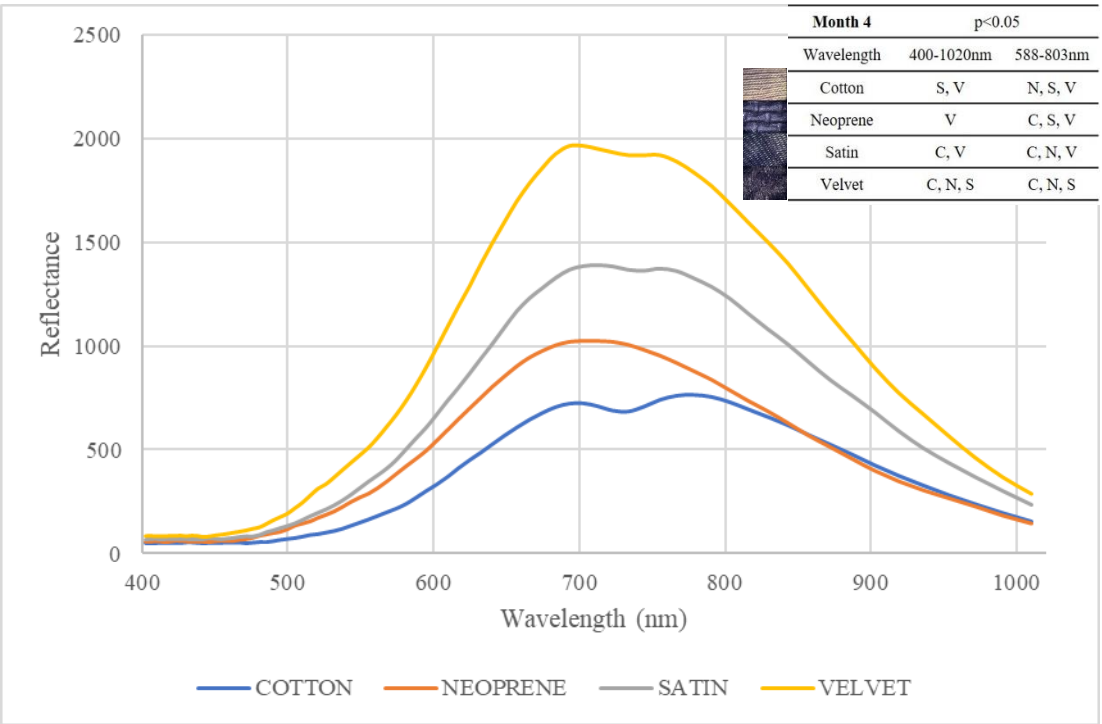

Figure 3.17. *Month 4 spectral comparisons between the four fabrics. The table beside the graph indicates the fabrics in which statistical results proved significantly different ($p<0.05$) from the fabrics in the corresponding column (C=cotton; N=neoprene; S=satin; V=velvet), considering both wavelength ranges studied.*

Table 3.19.
Simplified results of the Tukey post hoc analysis on the full dataset (400 – 1020nm) of all fabrics for month 4. Bold numbers indicate a significant p-value.

Fabric type (400-1020nm)	Cotton	Neoprene	Satin	Velvet
Cotton	N/A	0.576	**0.009**	**<0.001**
Neoprene	0.576	N/A	0.237	**<0.001**
Satin	**0.009**	0.237	N/A	**0.017**
Velvet	**<0.001**	**<0.001**	**0.017**	N/A

Table 3.20.
Simplified results of the Tukey post hoc analysis on the refined dataset (588 – 803nm) of all fabrics for month 4. Bold numbers indicate a significant p-value.

Fabric type (588-803nm)	Cotton	Neoprene	Satin	Velvet
Cotton	N/A	**0.012**	**<0.001**	**<0.001**
Neoprene	**0.012**	N/A	**0.002**	**<0.001**
Satin	**<0.001**	**0.002**	N/A	**<0.001**
Velvet	**<0.001**	**<0.001**	**<0.001**	N/A

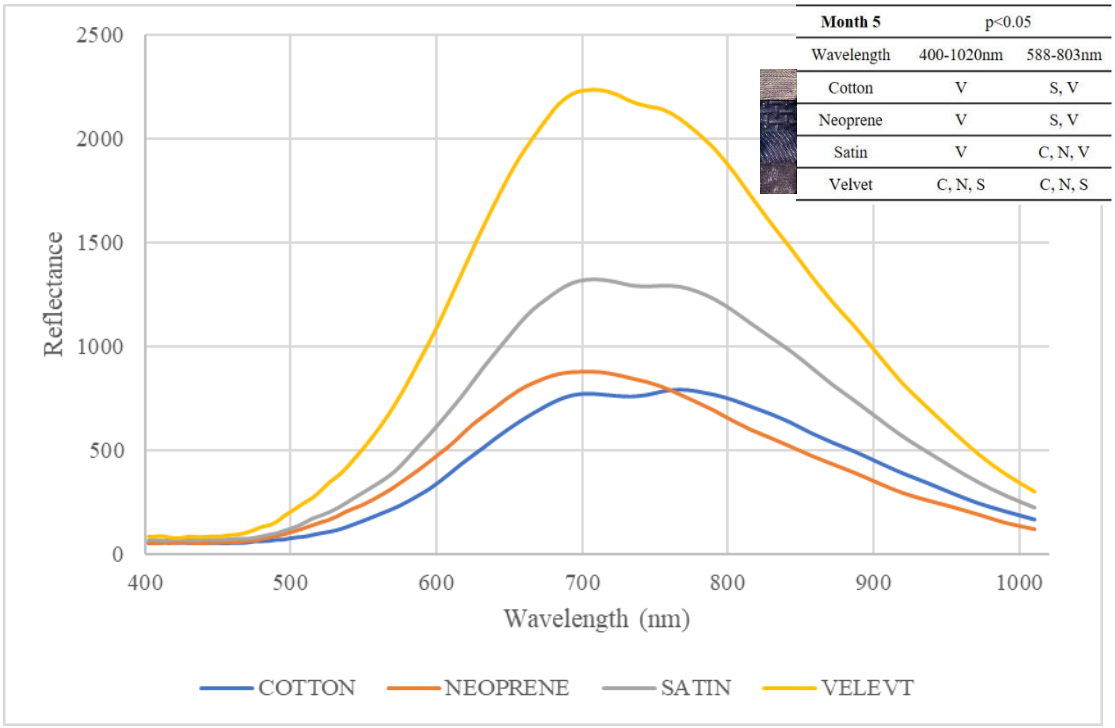

Figure 3.18. *Month 5 spectral comparisons between the four fabrics. The table beside the graph indicates the fabrics in which statistical results proved significantly different ($p<0.05$) from the fabrics in the corresponding column (C=cotton; N=neoprene; S=satin; V=velvet), considering both wavelength ranges studied.*

Table 3.21.
Simplified results of the Tukey post hoc analysis on the full dataset (400 – 1020nm) of all fabrics for month 5. Bold numbers indicate a significant p-value.

Fabric type (400-1020nm)	Cotton	Neoprene	Satin	Velvet
Cotton	N/A	0.981	0.054	**<0.001**
Neoprene	0.981	N/A	0.134	**<0.001**
Satin	0.054	0.134	N/A	**<0.001**
Velvet	**<0.001**	**<0.001**	**<0.001**	N/A

Table 3.22.
Simplified results of the Tukey post hoc analysis on the refined dataset (588 – 803nm) of all fabrics for month 5. Bold numbers indicate a significant p-value.

Fabric type (588-803nm)	Cotton	Neoprene	Satin	Velvet
Cotton	N/A	0.641	**<0.001**	**<0.001**
Neoprene	0.641	N/A	**<0.001**	**<0.001**
Satin	**<0.001**	**<0.001**	N/A	**<0.001**
Velvet	**<0.001**	**<0.001**	**<0.001**	N/A

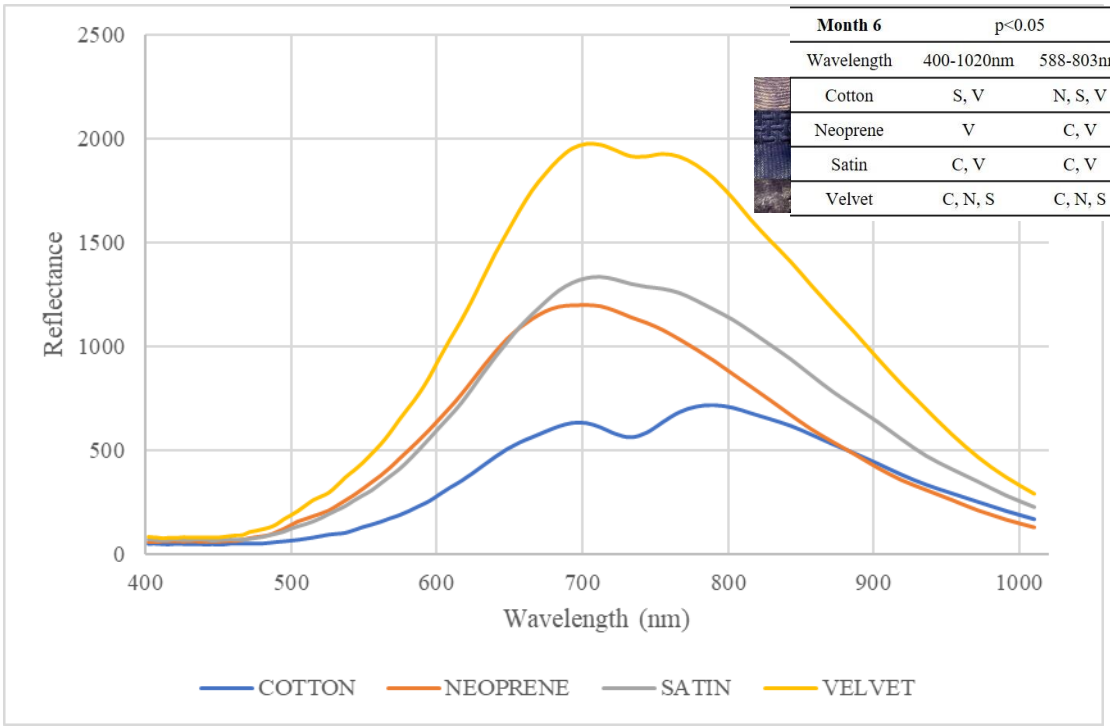

Figure 3.19. *Month 6 spectral comparisons between the four fabrics. The table beside the graph indicates the fabrics in which statistical results proved significantly different (p<0.05) from the fabrics in the corresponding column (C=cotton; N=neoprene; S=satin; V=velvet), considering both wavelength ranges studied.*

Table 3.23.
Simplified results of the Tukey post hoc analysis on the full dataset (400 – 1020nm) of all fabrics for month 6. Bold numbers indicate a significant p-value.

Fabric type (400-1020nm)	Cotton	Neoprene	Satin	Velvet
Cotton	N/A	0.086	**0.014**	**<0.001**
Neoprene	0.086	N/A	0.909	**<0.001**
Satin	**0.014**	0.909	N/A	**0.005**
Velvet	**<0.001**	**<0.001**	**0.005**	N/A

Table 3.24.
Simplified results of the Tukey post hoc analysis on the refined dataset (588 – 803nm) of all fabrics for month 6. Bold numbers indicate a significant p-value.

Fabric type (588-803nm)	Cotton	Neoprene	Satin	Velvet
Cotton	N/A	**<0.001**	**<0.001**	**<0.001**
Neoprene	**<0.001**	N/A	0.773	**<0.001**
Satin	**<0.001**	0.773	N/A	**<0.001**
Velvet	**<0.001**	**<0.001**	**<0.001**	N/A

Chapter 4: Discussion

4.1 Overview

When human remains are discovered under suspicious circumstances, the accurate estimation of the time since death (minPMI) is a crucial aspect of the forensic investigation. Typically, the estimation of the minPMI is performed throughout the analyses of the corpse and/or the insects associated with it (Sorg et al., 1997; Barton, Archer, Quaggiotto, & Wallman, 2019). Use of carrion fauna and interpreting the physical changes of the corpse as methods of estimating the minPMI is more challenging when the remains are recovered from an aquatic environment. In such cases, it becomes necessary to consider factors such as the different type of fauna involved in the decomposition and colonisation of the corpse, and the amount of time the corpse spent submerged (PMSI) and/or floating (FI) (Sorg et al., 1997; Erskine & Armstrong, 2010). Generally, due to the general lack of research in this area, information obtained from the corpse may be insufficient or misleading (Erskine & Armstrong, 2010).

For example, the use of the decomposition scoring method (Heaton et al., 2010) might be limited as there is a wide ecological variability of aquatic environments (De Donno et al., 2014). In damp, moist, or aquatic environments, the corpse might also form adipocere. Adipocere is a fatty, waxy substance which forms on the skin in place of putrefaction in an anaerobic environment. The presence of adipocere compromises decomposition due to its ability to delay the process, harden the skin, and, in some cases, preserve the corpse (Ellingham, Perich, & Tidball-Binz, 2017). Development of adipocere can vary between three days to five years, depending on

the environment, making the estimation of post-mortem timing extremely unsure (Kumar, Monteiro, Bhagavath, & Bakkannavar, 2009).

Another consideration that is unique to an aquatic environment is the potential for human remains in water to be displaced many kilometres in a very short time by tides and waves (Giertsen & Morild, 1989). The decomposition process of the corpse will be affected by both extrinsic factors (e.g., water temperature, turbulence, presence of rocks/debris, and the corpse itself) and intrinsic factors (e.g., differences in size of the corpse, condition, coverings, and associated trauma), which must be taken into consideration (Sorg et al., 1997). Furthermore, especially in marine setups, there is a lack of the typical necrophagous fauna which have a thoroughly mapped and predictable pattern of behaviour, allowing for accurate minPMI in terrestrial environments (Anderson, 2010).

Due to the complex conditions surrounding the investigation which follows the retrieval of a corpse from an aquatic environment, new and innovative avenues of research are being developed to provide more tools for forensic investigators. Considering most human bodies will enter the water partially or fully clothed, current aquatic forensic research is focused on the clothing, shoes, and other items retrieved alongside the corpse. These objects are an attractive surface for the colonisation of several marine organisms, both mobile (e.g., crabs, echinoderms, gastropods) and sessile (e.g., barnacles and bryozoans). The permanent attachment of these organisms to a surface allows them to provide investigators with valuable information useful in developing an estimation of the minPMSI (Newman & Abbott, 1980; Anderson, 2010). Concerning the colonisation of clothing, this area of research falls under the umbrella of forensic textile analysis (Williams, 2018).

In recent times, some research has been focused on different aspects of textile damage analysis concerning blunt force and projectile analysis, terrestrial decomposition, damage staging, and understanding the interaction between the textile and a weapon (Williams, 2018). However, a recent review underlined that there is a fundamental lack of understanding about general wear and tear of fabrics (Williams, 2018) and research in an aquatic environment has yet to receive the level of attention required.

To date, only a single study has been conducted in the area of aquatic forensic textile analysis, which considered the fate of fabrics submerged in the ocean for up to six months (Tingey, 2019). In this study, the fabrics were considered from a biological perspective with the aim being to determine which kinds of aquatic organisms would occupy different fabrics, and to use this information to support the estimation of a minPMSI. As demonstrated by previous research, barnacles and other sessile organisms can provide a great resource of information regarding the amount of time the items connected to the human remains have spent in water (Magni et al., 2014; Pirtle et al., 2019; Tingey, 2019). While these previous studies are valid research, the focus was on the organisms colonising the textiles. Therefore, the results are extremely dependant on the specific environmental conditions and replications are relatively limited by the experimental design and by the fact that the observation was on a single and unique forensic case (Magni et al., 2014).

In accordance with Williams (2018), major limitations and challenges in the forensic textile analysis are the lack of quality, consistency, and robust databases of different datasets which allow for reliable evaluation of hypotheses. A significant criticism of the field of fabric and fibre analysis is that damage analysis is subjective and not standardised. This issue is further highlighted by the fact that expert testimony is only

admissible in court where there are rigorous and relevant databases and research backing the claims.

Hyperspectral Imaging (HSI) is a technique which integrates spectroscopy with conventional imaging to obtain both spatial and spectral information about a specimen (Edelman, Gaston, Van Leeuwen, Cullen, & Aalders, 2012). The use of HSI may solve one of the most important issues within forensic science, that is the preference for fast and non-destructive analyses (Borgwardt & Wells, 2017). Preservation of items recovered from crime scenes is of the uttermost importance in forensic investigations. Some of the biggest concerns with forensic practice are contamination, alteration, and destruction of evidence. HSI analysis is a fast, non-contact, and non-destructive method of investigation, which with technological advancements is becoming increasingly portable (Edelman, Gaston, Van Leeuwen, Cullen, & Aalders, 2012).

HSI analysis has been considered in a forensic setting in the analysis of fabric fibres. However, the majority of the studies have been focused on bruises (Payne, Langlois, Lennard, & Roux, 2007; Randeberg et al., 2010), blood (Cadd et al., 2016), and finger marks (Exline et al., 2003; Payne et al., 2005a). The only other study, to the author's knowledge, which has considered the aging of fabrics in conjunction with HSI analysis is the study conducted by Daza (2014). While Daza's study was only considering the aging of the fabric fibres as one of many different factors being observed, and was a terrestrial study, it demonstrated that it was possible to quantify the aging of fabrics through visible colour change as a result of environmental exposure.

This research is the first attempt at using HSI analysis to explore the modification of the optical properties of four commonly used fabrics, aging in an aquatic environment. This aim was explored by examining the changes in reflectance profiles obtained from each fabric at different time points which spent six months submerged in a marine environment. The use of HSI is an attempt to standardise an investigative approach and produce robust datasets for objective analysis which will allow for the generation of reliable probability values that can be inputted into a case-specific probability model. Statistical comparisons were then made within and between the reflectance profiles. Two different lighting scenarios were also evaluated in a pilot study which examined the reflectance profiles obtained through illuminating different ranges of the electromagnetic (EM) spectrum.

4.2 Pilot study

In the pilot study, HSI reflectance profiles from cotton, neoprene, satin, and velvet were taken at each month of the experiment using VIS-NIR lighting coupled with VIS-H lighting. The VIS-H lighting was added to the VIS-NIR lighting with the aim to increase the level of reflectance variability within the 650 – 950nm range of the electromagnetic spectrum. The increased reflectance allowed us to explore better the red area of the spectrum (635 – 700nm) as this was where many peaks were occurring in the data.

Of the four fabrics used in this experiment, only cotton and satin showed significant differences between the two lighting scenarios, with higher reflectance values occurring under the addition of the VIS-H light. This observation was expected as the cotton and satin samples showed higher levels of physical alteration after six months, while the neoprene and velvet remained relatively unaffected. A statistically

different profile was obtained when comparing the reflectance profile of unaltered control samples (very white, first months) with the highly degraded and discoloured samples (very dark, following months). The effect of the fabrics' colour on the reflectance has been proved previously by Daza (2014), which analysed the impact of the terrestrial decomposition on the colour loss of textile fibres via HSI. In the study by Daza (2014), fabrics which had spent more time exposed to the environment and the carrion fauna lost more colour and produced significantly different spectral profiles. In the two studies, the fabrics modified their colour in opposite directions – in Daza (2014) the fabrics lost colour, while in the present study they gain colour – in both cases such change is reflected in significantly different spectral profiles.

The increase in reflectance generated by the additional lighting gives a higher level of specificity in differentiating between the control and six-month samples. The increase could be useful as it can allow for a more accurate analysis of results in situations where a high number of samples are included a once. However, despite the significance, there was no new information gained other than increased peaks in reflectance at the same wavelengths as just the VIS-NIR lighting.

Neoprene and velvet did not show significant differences in their reflectance profile between the two lighting scenarios. Neoprene remained relatively structurally unchanged after six months of submersion, which is expected as thick synthetic fibre. Neoprene is also the only fabric of the four, which is black, as opposed to white, and black pigment absorbs light more readily than white pigment. During the six months of submergence, neoprene was colonised by "dark" flora and fauna; however, as it was black in colour in the first place, the reflectance profile was not affected. The velvet was less affected than the cotton and satin but still showed some discolouration and fibre loss as a result of exposure. Velvet was also the fabric least affected by flora

and fauna, which did not favour the hairy texture for their settlement (Tingey, 2019) and the minimum change of colour was reflected in its similar reflectance profiles. The lack of differentiation for neoprene and velvet suggests that different lighting (outside of the spectra tested in this research) may be required to facilitate the identification of the reflectance changes occurring within these fabrics over time.

In future studies, the use of two different lights would not be recommended as it may add unnecessary variability. Furthermore, this pilot study demonstrated that no new information was gained through the inclusion of the VIS-H light as the peak values occurred at the same wavelength in both lighting scenarios.

4.3 Primary study

In this study, HSI reflectance profiles from cotton, neoprene, satin, and velvet were taken at each month of the experiment using exclusively VIS-NIR lighting. The resulting profiles were then analysed as a ‘full dataset’ and a ‘refined dataset’ to examine the specificity of the results.

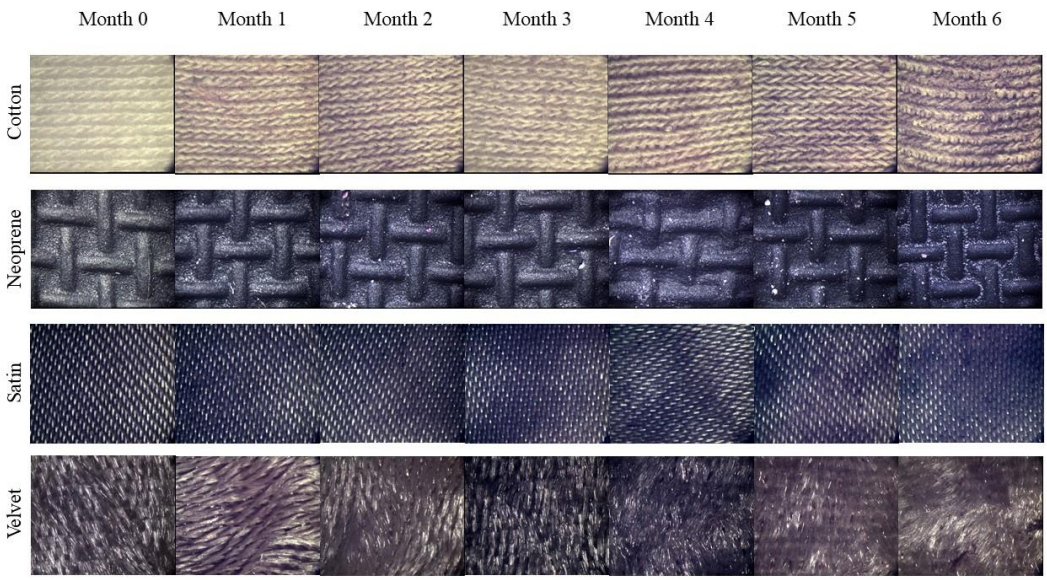

Fig. 4.1. *Raw images captured by the HS camera of the fabrics used in the experiment, aging from Month 0 (control, never placed underwater) to Month 6 (6 months underwater). These are images of the 5x5 cm samples obtained from the original 52x30 cm fabrics. Images were exported from Spectraview® 5.0 analysis software.*

4.3.1 Cotton

Cotton fibres are a natural, plant-derived seed fibre used extensively in the manufacturing industry. Cotton is the most common natural fibre utilised on a global scale (Shahbandeh, 2018) and therefore from an investigative standpoint, it is important to study it, as there would be a higher chance of the recovered human remains being clothed in items made from it. The cotton used in this research was white, naturally woven, soft, stretched easily, and had interlocking fibres, making it suitable for a lightweight t-shirt, if it was a garment.

Before submersion, the fabric was soft and pliable; however, by month 1 of submersion, it was stiff, with a rough texture. The effect of the saltwater and the development of an algal film made the interlocking structure appear firmer (Fig. 4.1). Furthermore, by month 4, the interlocking structure was beginning to break down,

and the fabric could be torn easily. By month 6 the fabric was tattered and in strips with little to no structural integrity maintained. Most of the surface area was occupied by algae, making the finding of a relatively unaffected area for HSI analysis very challenging.

In recent times, several studies have considered the analyses of cotton via HSI. However these studies have been focused on separating contaminants from cotton lint[1] (Jiang & Li, 2015; Zhang, Li, Zhang, & Rogers, 2016), or on the identification, classification and or aging of foreign stains on a cotton textile, such as blood (Kuula, Puupponen, Rinta, & Pölönen, 2014; Cao et al., 2015; Tan, 2016), semen (Zapata, Ortega-Ojeda, & García-Ruiz, 2017), or other fluids (Silva, Pimentel, Amigo, Honorato, & Pasquini, 2017). To the knowledge of the author, only a single study so far has attempted to analyse the aging of the cotton itself, and this was performed in a terrestrial environment with cotton sheets wrapped around decomposing organic material (pigs) (Daza, 2014).

In an aquatic environment, degradation of the cotton's physical structure was matched by a decline in the reflectance profile along the included wavelengths. Significant differences in the reflectance profiles were observed in both the full and refined dataset for the cotton, and a strong negative regression was observed between the months spent submerged and the reflectance profiles. In accordance with the study conducted by Daza (2014) in a terrestrial environment, the modification of the reflectance profile is a direct effect of the modification of the fabrics' colour. However, while in Daza's study, the fabrics lost colours, in the present research fabrics gained colours.

[1] Lint = cotton ball prior to formation of a textile

4.3.2 Neoprene

Neoprene, or polychloroprene, is a synthetic petrochemical substance. Polychloroprene is mixed and baked to form a chloroprene 'loaf' which is then sliced into various thicknesses and shipped off to apparel manufacturers. The neoprene slices can then have patterns and designs printed on to them before the sheets are combined to make up garments. Neoprene is both waterproof and insulative, making it ideal for a divers' wetsuits (Hodakel, 2020a). The neoprene used in this research was black, stretchy, with a crosshatch pattern pressed into the 'external' side of the fabric. The external side was the one which was the focus of this research as it would be the side exposed to the water if a person wore it. The neoprene was also the thickest fabric included in this experiment, at around 4mm.

As stated in section 4.2, the neoprene was the least structurally altered by the effects of the marine environment, which is expected given that it is thicker, synthetic, and waterproof. The fabrics structural integrity remained intact after month 6 in the ocean, but the fabric did become progressively stiffer and less stretchy with time. Figure 4.1 reflects this lack of change as the fabric appears structurally unchanged over the six months of imaging.

The neoprene showed more significant changes in reflectance profiles in the later months of the study, indicating that this fabric can maintain its structural integrity for a longer submersion time compared to other fabrics. These later changes in the reflectance profiles also coincide with the findings in the research conducted by Tingey (2019). In such research, neoprene was found to be preferred medium of the settlement of marine organisms, especially barnacles, and from month 2, the colonization was more substantial. While initially marine organisms affected the

thick neoprene only on the surface, in the later months as the fabric experienced more wear as a result of exposure the organisms had better chance to penetrate further into the structure, playing a role in the changes occurring in the neoprenes spectral profiles. To note – the areas of the fabric selected for HSI analyses were the ones with the least visual faunal interactions; however, HSI is very sensitive technology and is able to identify changes occurring to the fabrics on a more microscopic level. To confirm such a deduction, further investigation using scanning electron microscopy (SEM) on the fabrics is suggested.

To the best knowledge of the author, this research is the first to consider the changes occurring to neoprene fabric as a result of exposure to an aquatic environment. The results obtained demonstrate the potential of this technology to significantly narrow down the minPMSI estimation by categorising neoprene into less than two months submerged, and more than two months submerged. If a hyperspectral database (*HSI library*) could be constructed containing the most common brands of wetsuits, this information would be of great value to aquatic forensics investigators.

4.3.3 Satin

Satin is woven from long continuous fibres, and while traditionally was made with silk, is more commonly and affordably made with synthetic fibres such as polyester and rayon. Satin fabrics have a soft, shiny side, which is the external or front side, and a dull, rougher internal or backing side (Vv.Aa., 2019). The satin used in this research was white, synthetic, and had less interlaces than the other fabrics included in this research. The external side was the focus of this research as it would be the side exposed to the water if a person wore it. Satin was chosen as a fabric to

investigate in this research as it is commonly used as a material for undergarments and sleepwear.

Before submersion, the external side was shiny and soft, and the material had some stretch, however by month 1 the shine was dulled, there was no stretch in the material, and it was stiff when handled. The white colour was stained green and brown, due to exposure to a marine environment, and this colour deepened as the months progressed. The structural integrity of the material was maintained even after month 6 in the water (Fig. 4.1).

While less than cotton, some studies have considered the analysis of satin via HSI. A study by Silva et al. (2017) explored the use of HSI analysis in the detection of semen and vaginal fluid on satin undergarments. Another study proposed the use of HSI in the screening of fabric before garment manufacturing for defects (Kadkol, Rai, & Kulkarni, 2013). This research is the first to consider the changes occurring to the satin fabric as a result of exposure to an aquatic environment. However, similarly to cotton, neoprene and velvet, no studies have been performed on the use of HSI to age satin submerged in the ocean.

Significant differences in the satins reflectance profiles predominantly occurred between the control and submerged samples. This observation suggests that the immersion in water and the colonisation of the aquatic fauna is able to alter the surface of the fabric in a short time. However, the underlying structure of the fabrics remains consistent over a more extended period. This might be justified by the rougher internal side, providing more structural support, which is missing in other more delicate fabrics such as cotton. Such results suggest that in an investigation of

a minPMSI estimation via HSI analyses of the subject's garments, satin should not be prioritised over other fibres, such as cotton.

4.3.4 Velvet

Velvet, while traditionally was made with silk, is nowadays most commonly made of synthetic fibres such as rayon. Velvet is a woven and tufted fabric with a short, dense pile, giving it a soft feel and shiny appearance. Velvet also has a soft and hairy-like external side and a rougher, more densely woven internal side (Hodakel, 2020b). The velvet used in this research was white, synthetic, soft, and stretchy. The external side was the focus of this research as it is the side usually exposed when worn, and therefore it was also the side exposed to the water during the field part of the experiment.

The velvet became stiff and lost its stretch by month 1 of the experiment. The soft tufts of fabric became matted and dense, and while the fabric was wet, they lay flat but after drying stuck up at different angles. The fibres also shed more easily from the fabric when handled, especially after drying. The structural integrity of the fabric remained intact throughout the experiment; however, by month 5, the fabric was noticeably more fragile and could be torn if not handled with enough care.

There have been few studies which have considered velvet in conjunction with HSI analysis. A study by Lin et al. (2007) investigated the potential of NIR-HSI to visualise diluted bloodstains on black velvet, amongst other fabrics. A recent review of the literature by Zapata et al. (2015) called for a more comprehensive study testing stains of blood, semen, saliva, and other bodily fluids on fabrics of different colours, including velvet. However, this research is the first to consider the changes occurring to velvet fabric as a result of exposure to an aquatic environment.

The velvet demonstrated the least amount differentiation between the reflectance profiles over the six months underwater, with no significant changes recorded. Capturing focused profiles of the velvet samples was the most challenging as the fibrous nature of the surface meant that many pieces would stick up towards the lense, throwing off the focus of the camera. The lack of spectral activity for the velvet samples also coincides with an observation from the experiments conducted by Tingey (2019) as velvet was the least favourable surface for colonisation by marine fauna. In a similar fashion to satin, the results of this research suggest that velvet should not be prioritised for investigative analysis using HSI to determine the minPMSI over other fabrics such as cotton.

4.3.5 Fabric comparison

Significant differences in reflectance profiles were observed between all four fabric samples when compared against one another. This observation coincides with expectations as all four fabrics are made up of different materials, weaves, and thread counts. This observation supports that HSI is a useful tool in distinguishing surface properties of materials and more specifically fabrics from one another (Li, Meng, Wang, & Xin, 2019) even after exposure to a marine environment.

In the case of recovering a clothed corpse from an aquatic environment, two specific scenarios are the most probably

1) The recovery of a corpse clothed in a mixture of fabrics, wearing ‘normal’ everyday clothing;
2) The recovery of a corpse clothed in a neoprene wetsuit, where the presence of other clothing is unlikely.

In the case of mixed clothing recovery, cotton fabrics should be the primary focus of HSI analysis as demonstrated by this research. Cotton displayed the most objective pattern of decomposition as a result of exposure as well as changes in colour confirmed both visually, and through HSI. If satin clothing is also present, could offer support to the analysis of the cotton. If satin is present without cotton, it could potentially be used for a tentative minPMSI estimate of up to 3 months; however, for longer periods, a different methodology should be used. Velvet, on the basis of this research, could not provide enough support to an estimation of the minPMSI to be recommended for aquatic investigations.

In the case of a corpse recovered in a neoprene wetsuit, an important consideration is that the fabric begins to show the most significant changes after the period of submergence has exceeded two months. When analysing neoprene that has only been submerged for a few days to about two months with HSI, the results will be able to conclude that the corpse only spent this shorter amount of time in the water. When analysing fabrics which have spent more than two months underwater, the reflectance profile will begin to show significant changes that could indicate that the corpse has been in the aquatic environment for at least three months. Essentially, the fabric can be grouped through use of HSI analysis into shorter submergence time of fewer than two months, or longer submergence time of more than two months. While other fabrics exist in a variety of forms, wetsuits are a limited market, and it would be of great importance for forensic purposes to have a reflectance profile library of them.

An additional point to consider for both scenarios when selecting fabrics from different regions of the corpse for HSI analysis is the various processes which the corpse has undergone, and the different things it has been exposed to in the aquatic

environment. It is necessary to obtain the profile of fabric that had the longest exposure to the aquatic environment. In some cases, when human remains are recovered from being fully submerged (Mateus & Vieira, 2014), a flat area of fabric which has not been dragging along the floor is the most ideal to select for analysis. However, if the corpse was instead recovered in the floating stage (Mateus & Vieira, 2014), as corpses will generally float face down, an area of fabric which was located on the front of the corpse should be selected (Sorg et al., 1997). These points should be considered in conjunction with the recommendations outlined below in section 4.4.

4.4 Recommendations for further research in the field

Prior to analysis, the fabric samples were stored in a freezer at -20°C for 248 – 405 days, depending on what month the sample was removed from the water. The fabrics were put straight from the ocean into sealed plastic bags and were frozen wet. In best practice for crime scene investigation fabrics which are considered as evidence are to be dried under natural conditions before storage (Darnell, 2011). However, if the evidence is associated with a corpse, evidence analysis must wait until the coroner releases the corpse. This process can take days to months depending on the case, and during this period the corpse is stored in a fridge (4°C) or freezer (-20°C) (Darnell, 2011). Once the corpse is released, then the fabrics can be removed from the corpse and laid out on plastic sheeting to air dry (Darnell, 2011). Due to these regulations, storing the fabrics wet at -20°C is considered the second-best practice with regards to forensic evidence investigations. Therefore, as a suggestion to future studies, the wet fabrics from the ocean would potentially serve for more accurate analysis if they were to be dried upon removal from the ocean.

Recommendations to improve the experimental design for further research in this field, with regards to the sample preparation process would be as follows:

1) Air-dry the fabric samples immediately upon removal from the aquatic environment. Once dry, individually store the samples in breathable paper bags. This process would align with best practice in a criminal investigation proceeding (Darnell, 2011), and could remove the potential for damage as freezing and defrosting fabrics introduces more potential for mishandling of samples. If the samples must be stored for a time before drying, plastic sheeting should be placed between areas of fabric which will be folded on itself as contact between the fabric allows it to freeze together which can cause damage when defrosted and unfolded. The folded samples can then be sealed in an air-tight plastic bag and frozen at -20°C.
2) If air drying, as described above, is not possible or cannot occur until after a particular time, as part of a correct chain of custody a full record of how long the fabrics were stored in a fridge or freezer, and at what temperatures, should be kept in order to provide the full history of the preservation and storage conditions.
3) When searching for an area of the fabric to image, look for an intact surface of at least 5 x 5cm, with minimal animal interference (e.g. no barnacles attached, minimal algae growth).
4) Try not to choose an area of the fabric where there is a fold or a seam for best continuity practice. Tingey (2019) noted in their study that barnacle settlement was significantly higher in areas of the fabric that were folded as it offered more protection from the environment. Avoiding such areas would align with the above point about minimal animal interference.

5) Use a soft brush to gently dislodge any loosely attached sand, seaweed, and other debris from the samples before imaging as large foreign inclusions impact the resulting spectral profile.

4.5 Future directions

The ocean is a dynamic environment with many factors that can contribute to the alteration and degradation of clothing worn by a victim. To be as experimentally consistent as possible, and due to the sensitive nature of HSI, areas of the fabrics with minimal animal interference were selected to explore the optical properties of the fabric and not those of the marine wildlife. However, since the fabric samples were not washed before analysis, some interference from marine wildlife may have been included in the spectral profiles. For some of the fabrics (cotton) a washing process could have affected the whole integrity of the fabric, as especially after 5-6 months underwater, it was very delicate because of the prolonged exposure to the marine environment. As nothing is known with regards to how the interaction of washing detergents could impact the results of the spectral profiles, this aspect could be considered in future studies.

Environmental limitations also exist within this study, as the submergence period was restricted to only six months, from the end of winter through to the end of summer. It could not, therefore, be determined in this study whether the effects of environmental temperature play a role in the fabric's degradation. Furthermore, the fabrics were pinned to stationary floats, which emulates a very specific situation of an inorganic object displaced in water, that does not move. This was done purposefully to attempt to limit the number of variables, but it is important to note that in a real case a corpse in water will drift with the tide, and may sink and float to

different depths following the aquatic decomposition process (Mateus & Vieira, 2014). Human remains are made of organic matter, and their decomposition process could affect the fabric, with factors such as adipocere formation having the potential to interrupt the degradation of the fabric and the attachment of aquatic fauna (Kumar et al., 2009; Ellingham, Perich, & Tidball-Binz, 2017). A more longitudinal study with fabrics attached to an organic and more mobile substratum could better serve to more accurately emulate the movement of a corpse in an aquatic environment. Additionally, the fabrics were tested after spending time in the ocean, but corpses can also be recovered from rivers and lakes with varying levels of pollution. All of these variables are worth investigating in future studies.

Furthermore, this study focused on a very specific range within the EM spectrum. Further research into broader areas of the NIR and IR region could potentially yield more differentiable results for the fabrics in this study which did not demonstrate significant differences (such as the neoprene, or velvet). Different ranges of the EM spectrum would be interesting to explore in future works as it would allow for better quantification of the optical changes occurring due to submersion within these fabrics. Utility of comparative technical analysis in order to better validate the HSI method would be beneficial in a future study. Using techniques such as Raman, FTIR, and SEM alongside the HSI is something that not only will provide validation but will also allow for the exploration of different areas of the EM in fabric analysis.

A final suggestion is that as this study only considers four fabrics, with each fabric being one colour, a more extensive study including more fabric types, and different fabric colours, would be beneficial in building a more robust database of results.

Chapter 5: Conclusion

HSI and other remote sensing techniques have been proved useful in investigating the nature of fabrics (Daza, 2014) as well as the nature and age of the stains on them (Kuula et al., 2014; Silva et al., 2017; Zapata, Ortega-Ojeda, & García-Ruiz, 2017). However, despite the enormous potential in the forensic field, there is a paucity of research focused on the use of remote sensing technology to determine the age of fabrics in investigative settings (Daza, 2014). To the knowledge of the authors, no research has yet been conducted into the use of HSI to determine the age of fabrics which have spent various times in an aquatic environment.

This research has shown that HSI coupled with VIS-NIR light is able to provide information on the optical changes of the fabrics throughout time, making it possible to quantify the changes occurring within the fabrics as a result of submersion in a marine environment.

Results show that the reflectance profiles obtained via HSI are directly affected by the wear of fabric and by the possibility of marine organisms to nick and penetrate them. When the fabrics have a thicker and more resistant structure (e.g. neoprene and velvet), the variation in the reflectance profile is less significant for the first month underwater. However, given more time, significant changes begin to appear in the profiles as the structure is gradually affected by the aquatic environment and organisms. This research has covered the first six months of changes which occur in the fabric due to submersion, and it is reasonable to infer based off the results that these changes would become more prominent if more extended periods were tested. Natural and thinner fabrics (e.g. cotton and satin) were more favourable for algal colonisation, both at a superficial and deeper level. As a visible result, such fabrics

quickly darkened their colour, producing a more variable HSI profile after a shorter period underwater. From the forensic perspective, therefore, for fabrics like cotton found in a marine environment, analyses via HSI can provide more detailed short-term information, whereas for fabrics like neoprene, are more suitable for long term information.

The potential to quantify the changes occurring within fabrics discovered alongside a corpse that has spent an unknown amount of time submerged in a marine environment can provide criminal investigators with a more accurate method of estimate a minPMSI. This study is the first of its kind and provides the opening of a new chapter in both aquatic forensics and forensic textile analyses using remote sensing technology, while also offering an innovative investigative tool for aquatic forensic analysis in Australian waters.

Chapter 6: References

Abidi, N., & Hequet, E. (2007). Fourier transform infrared analysis of cotton contamination. *Textile Research Journal, 77*(2), 77-84. doi:10.1177/0040517507074624

Allan, J. D. (1995). *Stream ecology: Structure and function of running waters.* London: UK: Chapman & Hall.

Amigo, J. M., Babamoradi, H., & Elcoroaristizabal, S. (2015). Hyperspectral image analysis. A tutorial. *Analytica Chimica Acta, 896*(1), 34-51. doi:10.1016/j.aca.2015.09.030

Anderson, G. S. (2010). Decomposition and invertebrate colonization of cadavers in coastal marine environments. In J. Amendt, M. L. Goff, C. P. Campobasso, & M. Grassberger, *Current Concepts in Forensic Entomology* (pp. 223-272). Dordrecht: Springer.

Aquila, I., Ausania, F., Di Nunzio, C., Serra , A., Boca, S., Capelli, A., . . . Ricci, P. (2014). The role of forensic botany in crime scene investigation: case report and review of literature. *Journal of Forensic Sciences, 59*(3), 820-824. doi:10.1111/1556-4029.12401

Barrios, M., & Wolff, M. (2011). Initial study of arthropods succession and pig carrion decomposition in two freshwater ecosystems in the Colombian Andes. *Forensic Science International, 212*(1-3), 164-172. doi:10.1016/j.forsciint.2011.06.008

Barton, P. S., Archer, M. S., Quaggiotto, M.-M., & Wallman, J. F. (2019). Chapter 6: Inverterate succession in natural terrestrial environments. In J. H. Byrd, & J. K. Tomberlin, *Forensic Entomology: The Utility of Arthropods in Legal Investigations: Third edition* (pp. 2001-2016). Boca Raton, FL: CRC Press.

Benbow, M. E., Pechal, J. L., Lang, J. M., Erb, R., & Wallace, J. R. (2015). The potential of high-throughput metagenomic sequencing of aquatic bacterial communities to estimate the postmortem submersion interval. *Journal of Forensic Sciences, 60*(6), 1500-1510. doi:10.1111/1556-4029.12859

Birngruber, C., Ramsthaler, F., & Verhoff, M. A. (2009). The color(s) of human hair—Forensic hair analysis with SpectraCube. *Forensic Science International, 185*(1-3), 19-23. doi:10.1016/j.forsciint.2008.12.018

Borgwardt, T. C., & Wells, D. P. (2017). What does non-destructive analysis mean? *Cogent Chemistry, 3*(1), 1-6. doi:10.1080/23312009.2017.1405767

Byrd, J. H., & Tomberlin, J. K. (2019). *Forensic Entomology – The utility of arthropods in legal investigation* (3rd ed.). Boca Raton, FL: USA: CRC Press.

Bytheway, J. A., & Pustilnik, S. M. (2013). Determining postmortem interval using glycoproteinous adhesion deposits by B alanus improvisus on human skeletal and dental remains. *Journal of Forensic Sciences, 58*(1), 200-205. doi:10.1111/j.1556-4029.2012.02278.x

Cadd, S., Li, B., Beveridge, P., O'Hare, W. T., Campbell, A., & Islam, M. (2016). The non-contact detection and identification of blood stained fingerprints using visible wavelength reflectance hyperspectral imaging: Part 1. *Science & Justice, 56*(3), 181-190. doi:10.1016/j.scijus.2016.01.004

Cao, Y., Ma, K., Zhao, X., Wang, H., Wang, F., & Sun, B. (2015). Ressearch on the relationship between the age of bloodstains and the bending rigidity of blooded cotton fabric. *5th International Conference on Advanced Design and Manufacturing Engineering*.

Casamatta, D. A., & Verb, R. G. (2000). Algal colonization of submerged carcasses in a mid-order woodland stream. *Journal of Forensic Science, 45*(6), 1280-1285. doi:/10.1520/JFS14880J

Castello, A., Frances , F., & Verdu, F. (2013). Solving underwater crimes: development of latent prints made on submerged objects. *Science & Justice, 53*(3), 328-331. doi:10.1016/j.scijus.2013.04.002

Cen, H., & He, Y. (2007). Theory and application of near infrared reflectance spectroscopy in determination of food quality. *Trends in Food Science & Technology, 18*(2), 72-83. doi:10.1016/j.tifs.2006.09.003

Cloutis, E. A. (1996). Review article hyperspectral geological remote sensing: evaluation of analytical techniques. *International Journal of Remote Sensing, 17*(2), 2215-2242. doi:10.1080/01431169608948770

Costerton, W. J., Lewandowski, Z., Caldwell, D. E., Korber, D. R., & Lappin-Scott, H. M. (1995). Microbial films. *Annual Review of Microbiology, 49*, 711-722. Retrieved from http://sr4lp2wr3c.scholar.serialssolutions.com/?sid=google&auinit=Z&aulast=Lewandowski&atitle=Microbial+biofilms&title=Annual+review+of+microbiology&volume=49&date=1995&spage=711&issn=0066-4227

Cox, E. (1996). *Identification of freshwater diatoms from live material*. London: UK: Chapman & Hall.

Darnell, C. (2011). Evidence. In C. Darnell, *Forensic science in healthcare: caring for patients, preserving the evidence* (pp. 119-123). New York: CRC Press.

Daza, L. F. (2014). The Environmental Impact on Surface Fabrics and Textile Fibres: Australia. Honours thesis in Bachelor of Applied Science: University of Canberra.

De Donno, A., Campobasso, C. P., Santoro, V., Leonardi, S., Tafuri, S., & Introna, F. (2014). Bodies in sequestered and non-sequestered aquatic environments: a comparative taphonomic study using decompositional scoring system. *Science & Justice, 54*(6), 439-446. doi:10.1016/j.scijus.2014.10.003

Dennison, K. J., Kieser, J. A., Buckeridge, J. S., & Bishop, P. J. (2004). Post mortem cohabition - shell growth as a measure of elapsed time: A case report. *Forensic Science International, 139*(2), 249-254. doi:10.1016/j.forsciint.2003.10.015

Deopura, B. L., & Padaki, N. V. (2015). Synthetic textile fibres: Polyamide, polyester and aramid fibres. In R. Sinclair, *Textiles and fashion: Materials, design and technology* (pp. 97-114). Cambridge: Woodhead Publishing Limited.

Dickson, G. C., Poulter, R. T., Maas, E. W., Probert, K. P., & Keiser, J. A. (2011). Marine bacterial succession as a potential indicator of postmortem submersion interval. *Forensic Science International, 209*(1-3), 1-10. doi:10.1016/j.forsciint.2010.10.016

Donoghue, E. R., & Minnigerode, S. C. (1977). Human body buoyancy: a study of 98 men. *Journal of Forensic Science, 22*(3), 573-579. doi:10.1520/JFS10628J

Edelman, G. J., Gaston, E., Van Leeuwen, T. G., Cullen, P. J., & Aalders, M. C. (2012). Hyperspectral imaging for non-contact analysis of forensic traces. *Forensic Science International, 223*(1-3), 28-39. doi:10.1016/j.forsciint.2012.09.012

Ellingham, S. T., Perich, P., & Tidball-Binz, M. (2017). The fate of human remains in a maritime context and feasibility for forensic humanitarian action to assist in their recovery and identification. *Forensic Science International, 279*, 229-234. doi:10.1016/j.forsciint.2017.07.039

Erskine, K. L., & Armstrong, E. J. (2010). *Water Related Death Investigation, Practical Methods and Forensic Applications.* CRC Press.

Exline, D. L., Wallace, C., Roux, C., Lennard, C., Nelson, M. P., & Treado, P. J. (2003). Forensic applications of chemical imaging: latent fingerprint detection using visible absorption and luminescence. *Journal of Forensic Sciences, 48*(5), 1047-1053. doi:10.1520/JFS2002333

Finnis, J., Lewis, J., & Davidson, A. (2013). Comparison of methods for visualizing blood on dark surfaces. *Science & Justice, 53*(2), 178-186. doi:10.1016/j.scijus.2012.09.001

Fras Zemljič, L., Strnad, S., Šauperl, O., & Stana-Kleinschek, K. (2009). Characterization of amino groups for cotton fibers coated with chitosan. *Textile Research Journal, 79*(3), 219-226. doi:10.1177/0040517508093592

Giertsen, C. J., & Morild, I. (1989). Seafaring bodies. *The American Journal of Forensic Medicine and Pathology, 10*(1), 25-7. Retrieved from https://journals.lww.com/amjforensicmedicine/Abstract/1989/03000/Seafaring_Bodies.7.aspx

Goodpaster, J. V., & Liszewski, E. A. (2009). Forensic analysis of dyed textile fibers. *Analytical and Bioanalytical chemistry, 394*(8), 2009-2018. doi:10.1007/s00216-009-2885-7

Haefner, J. N., Wallace, J. R., & Merritt, R. W. (2004). Pig decomposition in lotic aquatic systems: the potential use of algal growth in establishing a postmortem submersion interval (PMSI). *Journal of Forensic Science, 49*(2), 1-7. doi:/10.1520/JFS2003283

Haskell, N. H., McShaffrey, D. G., Hawley, D. A., Williams, R. E., & Pless, J. E. (1989). Use of aquatic insects in determining submersion interval. *Journal of Forensic Science, 34*(3), 622-632. doi:/10.1520/JFS12682J

He, H.-J., & Sun, D.-W. (2015). Selection of informative spectral wavelength for evaluating and visualising Enterobacteriaceae contamination of salmon flesh. *Food Analytical Methods, 8*(10), 2427-2436. doi:10.1007/s12161-015-0122-x

Heaton, V., Ladgen, A., Moffatt, C., & Simmons, T. (2010). Predicting the postmortem submersion interval for human remains recovered from UK waterways. *Journal of Forensic Sciences, 55*(2), 302-307. doi:10.1111/j.1556-4029.2009.01291.x

Hodakel, B. (2020a, May 6). *What is Neoprene Fabric: Properties, How its Made, and Where*. Retrieved from Sewport: https://sewport.com/fabrics-directory/neoprene-fabric

Hodakel, B. (2020b, May 9). *What is Velvet Fabric: Properties, How its Made and Where*. Retrieved from Sewport: https://sewport.com/fabrics-directory/velvet-fabric

Houck, M. M. (2009). Identification and comparison of textile fibers. In M. M. Houck, *Identification of textile fibers* (pp. 8-9). Cambridge : Woodhead Publishing.

Houck, M. M., & Siegel, J. A. (2015). Textile Fibers. In M. M. Houck, & J. A. Siegel, *Fundamentals of Forensic Science* (pp. 384-402). Oxford: Academic Press.

Humphreys, M. K., Panacek, E., Green, W., & Albers, E. (2013). Comparison of protocols for measuring and calculating postmortem submersion intervals for human analogs in fresh water. *Journal of Forensic Sciences, 58*(2), 513-517. doi:10.1111/1556-4029.12033

Janaway, R. C. (2008). The decomposition of materials associated with buried cadavers. In M. Tibbett, & D. O. Carter, *Soil Analysis in Forensic Taphonomy: Chemical and Biological Effects of Buried Human Remains* (pp. 153-202). Boca Raton: FL: CRC Press.

Jasuja , O. P., Kumar, P., & Singh, G. (2015). Development of latent fingermarks on surfaces submerged in water: Optimization studies for phase transfer catalyst (PTC) based reagents. *Science & Justice, 55*(5), 335-342. doi:10.1016/j.scijus.2015.03.001

Jiang, Y., & Li, C. (2015). Detection and discrimination of cotton foreign matter using push-broom based hyperspectral imaging: system design and capability. *PloS one, 10*(3), e0121969. doi:10.1371/journal.pone.0121969

Kadkol, R. J., Rai, H. M., & Kulkarni, A. H. (2013). Textile defect detection for fabric material using texture feature extraction. *International Journal of Latest Trends in Engineering and Technology, 2*(2), 173-176. Retrieved from https://pdfs.semanticscholar.org/ea4b/d1572fa036b52e5e40a63fb3233d1882b885.pdf

Keiper, J. B., & Casamatta, D. A. (2001). Benthic organisms as forensic indicators. *Journal of the North American Benthological Society, 20*(2), 311-324. doi:10.2307/1468325

Kumar, T. M., Monteiro, F. N., Bhagavath, P., & Bakkannavar, S. M. (2009). Early adipocere formation: a case report and review of literature. *Journal of Forensic and Legal Medicine, 16*(8), 475-477. doi:10.1016/j.jflm.2009.07.004

Kuula, J., Puupponen, H. H., Rinta, H., & Pölönen, I. (2014). The challenges of analysing blood stains with hyperspectral imaging. *Sensing Technologies for Global Health, Military Medicine, and Environmental Monitoring IV, 9112*(1), 20-27. doi:10.1117/12.2050180

Lawler, W. (1992). Bodies recovered from water: a personal approach and consideration of difficulties. *Journal of Clinical Pathology, 45*(8), 654. doi:10.1136/jcp.45.8.654

Lepot, L., De Wael, K., Gason, F., & Gilbert , B. (2008). Application of raman spectroscopy to forensic fibre cases. *Science & Justice, 48*(3), 109-117. doi:10.1016/j.scijus.2007.09.013

Li, J., Meng, X., Wang, W., & Xin, B. (2019). A novel hyperspectral imaging and modeling method for the component identification of woven fabrics. *Textile Research Journal, 89*(18), 3752-3767. doi:10.1177/0040517518821907

Li, Q., He , X., Wang, Y., Liu, H., Xu, D., & Gue, F. (2013). Review of spectral imaging technology in biomedical engineering: achievements and challenges. *Journal of Biomedical Optics, 18*(10), 1-28. doi:10.1117/1.JBO.18.10.100901

Lin, A. C., Hsieh, H. M., Tsai, L. C., Linacre, A., & Lee, J. C. (2007). Forensic applications of infrared imaging for the detection and recording of latent evidence. *Journal of forensic sciences, 52*(5), 1148-1150. doi:10.1111/j.1556-4029.2007.00502.x

Lloyd, A. O. (1968). The evaluation of rot resistance of cellulosic textiles. In A. H. Walters, & J. J. Elphick, *Biodeterioration of Materials: Microbial and Allied Aspects* (pp. 170-177). Amsterdam: Elsevier.

Magni, P. A., Borrini, M., & Dadour, I. R. (2013). Human remains found in two wells: A forensic entomology perspective. *Forensic Science, Medicine, and Pathology, 9*(3), 413-417. doi:10.1007/s12024-013-9428-4

Magni, P. A., Venn, C., Aquilla, I., Pepe, F., Ricci, P., Di Nunzio, C., . . . Dadour, I. R. (2014). Evaluation of the floating time of a corpse found in a marine environment using the barnacle Lepas anatifera L.(Crustacea: Cirripedia: Pedunculata). *Forensic Science International, 247*, 6-10. doi:10.1016/j.forsciint.2014.11.016

Mateus, M., & Vieira, V. (2014). Study on the postmortem submersion interval and accumulated degree days for a multiple drowning accident. *Forensic Science International, 238*, 15-19. doi:10.1016/j.forsciint.2014.02.026

Mateus, M., de Pablo, H., & Vaz, N. (2013). An investigation on body displacement after two drowning accidents. *Forensic Science International, 229*(1-3), 6-12. doi:10.1016/j.forsciint.2013.03.010

Megyesi, M. S., Nawroki, S. P., & Haskell, N. H. (2005). Using accumulated degree-days to estimate the postmortem interval from decomposed human remains. *Journal of Forensic Science, 50*(3), 1-9. doi:/10.1520/JFS2004017

Meleiro, P. P., & Garcia-Ruiz, C. (2016). Spectroscopic techniques for the forensic analysis of textile fibers. *Applied Spectroscopy Reviews, 51*(4), 278-301. doi:10.1080/05704928.2015.1132720

Merritt, R. W., & Wallace, J. R. (2010). The role of aquatic insects in forensic investigations. In J. H. Byrd, & J. L. Castner, *Forensic entomology: the utility of arthropods in legal investigations* (pp. 271-319). Boca Raton: Florida: CRC Press.

Miskelly, G. M., & Wagner, J. H. (2005). Using spectral information in forensic imaging. *Forensic Science International, 155*(2-3), 112-118. doi:10.1016/j.forsciint.2004.11.005

Morris, B., & Dadour, I. (2015). Forensic Entomology: The use of insects in legal cases. In I. Freckelton, & H. Selby, *Expert evidence* . Sydney: NSW: The Law Book Company Limited.

Newman, W. A., & Abbott, D. P. (1980). Cirripedia: the barnacles. In R. H. Morris, D. P. Abbott, & H. E. C, *Intertidal Invertebrates of California* (pp. 504-535). Stanford: California: Stanford University Press.

Ng, P. H., Walker, S., Tahtouh, M., & Reedy, B. (2009). Detection of illicit substances in fingerprints by infrared spectral imaging. *Analytical and Bioanalytical Chemistry, 394*(8), 2039-2048. doi:10.1007/s00216-009-2806-9

Oliveira, L. S., & Franca, A. S. (2011). Applications of Near Infrafred Spectroscopy (NIRS) in food quality evaluation. In D. A. Medina, & M. A. Laine, *Food Quality: Control, Analysis and Consumer Concerns* (pp. 131-179). IN: Nova Science Publishers.

Papadodima, S. A., Athanaselis, S. A., Skliros, E., & Spiliopoulou, C. A. (2010). Forensic investigation of submersion deaths. *International Journal of Clinical Practice, 64*(1), 75-83. doi:10.1111/j.1742-1241.2008.01890.x

Payne, G., Langlois, N., Lennard, C., & Roux, C. (2007). Applying visible hyperspectral (chemical) imaging to estimate the age of bruises. *Medicine, Science and the Law, 47*(3), 225-232. doi:10.1258/rsmmsl.47.3.225

Payne, G., Reedy, B., Lennard, C., Comber, B., Exline, D., & Roux, C. (2005). A further study to investigate the detection and enhancement of latent fingerprints using visible absorption and luminescence chemical imaging. *Forensic Science International, 150*(1), 33-51. doi:10.1016/j.forsciint.2004.06.036

Payne, G., Wallace, C., Reedy, B., Lennard, C., Schular, R., Exline, D., & Roux, C. (2005). Visible and near-infrared chemical imaging methods for the analysis of selected forensic samples. *Talanta, 67*(2), 334-344. doi:10.1016/j.talanta.2005.03.042

Peabody, A. J., & Cameron, N. G. (1999). Forensic science and diatoms. In E. F. Stoemer, & J. P. Smol, *The Diatoms: Applications for the Environmental and Earth Sciences* (pp. 389-401). Cambridge: UK: Cambridge University Press.

Petrik, M. S., Hobischak, N. R., & Anderson, G. S. (2004). Examination of Factors Surrounding Human Decomposition in Freshwater: A Review of Body Recoveries and Coroner Cases In British Columbia. *Canadian Society of Forensic Science Journal, 37*(1), 9-17. doi:10.1080/00085030.2004.10757565

Piette, M. H., & Els, A. (2006). Drowning: still a difficult autopsy diagnosis. *Forensic Science International, 163*(1-2), 1-9. doi:10.1016/j.forsciint.2004.10.027

Pirtle, D., Magni, P. A., Reinecke, G. W., & Dadour, I. R. (2019). Barnacle colonization of shoes: Evaluation of a novel approach to estimate the time spent in water of human remains. *Forensic Science International, 294*, 1-9. doi:10.1016/j.forsciint.2018.10.024

Qin, Y. (2015). A brief description of textile fibers. In *Medical Textile Materials* (pp. 23-42). Woodhead Publishing.

Randeberg, L. L., Skallerud, B., Langois, N. E., Haugen, O. A., & Svaasand, L. O. (2010). The Optics of Bruising. In A. Welch, & M. Van Gemert, *Optical-Thermal Response of Laser-Irradiated Tissue* (pp. 825-858). Dordrecht: Springer.

Ravn, C., Skibsted, E., & Bro, R. (2008). Near-infrared chemical imaging (NIR-CI) on pharmaceutical solid dosage forms—comparing common calibration approaches. *Journal of Pharmaceutical and Biomedical Analysis, 48*(3), 554-561. doi:10.1016/j.jpba.2008.07.019

Reijnen, G., Gelderman, H. T., Grotebevelsborg, B. F., Reijnders, U. J., & Duijst, W. L. (2018). The correlation between the Aquatic Decomposition Score (ADS) and the post-mortem submersion interval measured in Accumulated Degree Days (ADD) in bodies recovered from fresh water. *Forensic Science, Medicine and Pathology, 14*(3), 301-306. doi:10.1007/s12024-018-9987-5

Reisdorf, A. G., Bux, R., Wyler, D., Benecke, M., Klug, C., Maische, M. W., . . . Wetzel, A. (2012). Float, explode or sink: postmortem fate of lung-breathing marine vertebrates. *Palaeobiodiversity and Palaeoenvironments, 92*(1), 67-81. doi:10.1007/s12549-011-0067-z

Round, F. E., Crawford , R. M., & Mann , D. G. (2007). *Diatoms: biology and morphology of the genera.* Cambridge University Press.

Royal Life Saving Society. (2019). *Royal Life Saving National Drowning Report: Research and Policy Highlights.* Sydney, Australia: Royal Life Saving Society.

Saukko, P., & Knight, B. (2015). *Knight's forensic pathology fourth edition.* London: CRC Press.

Schuler, R. L., Kish, P. E., & Plese, C. A. (2012). Preliminary Observations on the Ability of Hyperspectral Imaging to Provide Detection and Visualization of Bloodstain Patterns on Black Fabrics. *Journal of Forensic Sciences, 57*(6), 1562-1569. doi:10.1111/j.1556-4029.2012.02171.x

Shahbandeh, M. (2018, June 4). *Cotton - statistics and facts*. Retrieved from Statista: https://www.statista.com/topics/1542/cotton/

Silva, C. S., Pimentel, M. F., Amigo, J. M., Honorato, R. S., & Pasquini, C. (2017). Detecting semen stains on fabrics using near infrared hyperspectral images and multivariate models. *TrAC Trends in Analytical Chemistry, 95*(1), 23-35. doi:10.1016/j.trac.2017.07.026

Silver, P. A., Lord, W. D., & McCarthy, D. J. (1994). Forensic limnology: the use of freshwater algal community ecology to link suspects to an aquatic crime scene in southern New England. *Journal of Forensic Science, 39*(3), 847-853. Retrieved from http://fmp.conncoll.edu/Silicasecchidisk/PDF_Publications/1993-Forensic_limno.PDF

Sorg, M. H., Dearborn, J. H., Monahan, E. I., Ryan, H. F., Sweeny, K. G., & David, E. (1997). Forensic taphonomy in marine contexts. In W. D. Haglund, & M. H. Sorg, *Forensic taphonomy: the postmortem fate of human remains* (pp. 567-604). Boca Ranton: Florida: CRC Press.

Srivastava, S. (2012). Finishing. In S. Srivastava, *Natural and Man-made Fibres* (pp. 131-141). Allahabad: Pushpa Publishing House.

Tan, G. J. (2016). The development of a hyperspectral imaging method for determining the time of deposition of human blood. Honours thesis in Forensic Biology and Toxicology: Murdoch University .

Tigg, A. E. (2005). The corrosion of metals over forensic timescales. Unpublished M.Sc Dissertation, Bradford, UK: University of Bradford.

Tingey, E. (2019). *Colonisation rates of marine organisms on different clothing fabrics: A new tool for forensic investigation in Western Australia* (Honours Thesis ed.). Perth: Western Australia: Murdoch University.

Trapecar, M. (2012). Finger marks on glass and metal surfaces recovered from stagnant water. *Egyptian Journal of Forensic Sciences, 2*(2), 48-53. doi:10.1016/j.ejfs.2012.04.002

van Daalen, M. A., de Kat, D. S., Oude Grotebevelsborg, B. F., De Leeuwe, R., Warnaar, J., Oostra, R. J., & Dujist-Heesters, W. L. (2017). An aquatic decomposition scoring method to potentially predict the postmortem submersion interval of bodies recovered from the North Sea. *Journal of Forensic Sciences, 62*(2), 369-373. doi:10.1111/1556-4029.13258

Voss, S. C., Magni, P. A., Dadour, I., & Nansen, C. (2017). Reflectance-based determination of age and species of blowfly puparia. *International Journal of Legal Medicine, 131*(1), 263-274. doi:10.1007/s00414-016-1458-5

Vv.Aa. (2019, July 2). *What Is Satin Fabric? A Guide to the Types, Characteristics, and Uses for Satin*. Retrieved from Masterclass: https://www.masterclass.com/articles/what-is-satin-fabric-a-guide-to-the-types-characteristics-and-uses-for-satin#what-are-the-different-satin-weaves

Wallace, J. R., Merritt, R. W., Kimbirauskas, R., Benbow, E. M., & McIntosh, M. (2008). Caddisflies assist with homicide case: determining a postmortem submersion interval using aquatic insects. *Journal of Forensic Sciences, 53*(1), 219-222. doi:10.1111/j.1556-4029.2007.00605.x

Wawryk, J., & Odell, M. (2005). Fluorescent identification of biological and other stains on skin by the use of alternative light sources. *Journal of Clinical Forensic Medicine, 12*(6), 296-301. doi:10.1016/j.jcfm.2005.03.005

Wiggins, K. G., & Houck, M. M. (2001). Introduction. In M. M. Houck, *Mute witnesses: trace evidence analysis.* Calif, London: Academic Press, San Diego.

Williams, G. A. (2018). Forensic textile damage analysis: recent advances. *Research and Reports in Forensic Medical Science, 8*, 1-8. doi:10.2147/RRFMS.S166435

Wilson, A. S., Janaway, R. C., Holland, A. D., Dodson, H. I., Barran, E., Pollard, A. M., & Tobin, D. J. (2007). Modelling the buried human body environment in upland climes using three contrasting field sites. *Forensic Science International, 169*(1), 6-18. doi:10.1016/j.forsciint.2006.07.023

World Health Organization. (2014). *Global Report on Drowning: Preventing a leading killer.* Spain: WHO Press.

Wu, D., & Sun, D.-W. (2013). Advanced applications of hyperspectral imaging technology for food quality and safety analysis and assessment: A review—Part I: Fundamentals. *Innovative Food Science & Emerging Technologies, 19*(1), 1-14. doi:10.1016/j.ifset.2013.04.014

Zaiontz, C. (2020, March 28). *Real Statistics Resource Pack*. Retrieved from Real Statistics Using Excel: http://www.real-statistics.com/free-download/real-statistics-resource-pack/

Zapata , F., Gregorio, I., & Garcia-Ruiz, C. (2015). Body fluids and spectroscopic techniques in forensics: a perfect match. *Journal of Forensic Medicine, 1*(1), 1-7. doi:10.4172/2472-1026.1000101

Zapata, F., Ortega-Ojeda, F. E., & García-Ruiz, C. (2017). Revealing the location of semen, vaginal fluid and urine in stained evidence through near infrared chemical imaging. *Talanta, 166*(1), 292-299. doi:10.1016/j.talanta.2017.01.086

Zhang , R., Li , C., Zhang , M., & Rodgers, J. (2016). Shortwave infrared hyperspectral reflectance imaging for cotton foreign matter classification. *Computers and Electronics in Agriculture, 127*, 260-270. doi:10.1016/j.compag.2016.06.023

Zimmerman, K. A., & Wallace, J. R. (2008). The potential to determine a postmortem submersion interval based on algal/diatom diversity on decomposing mammalian carcasses in brackish ponds in Delaware. *Journal of Forensic Sciences, 53*(4), 935-941. doi:10.1111/j.1556-4029.2008.00748.x

The data analysis for this paper was generated using the Real Statistics Resource Pack software (Release 6.8). Copyright (2013 – 2020) Charles Zaiontz. www.real-statistics.com

Chapter 7: Appendix

Pilot study

Appendix Table 1
One-way ANOVA and Tukey post hoc results for cotton VIS-NIR versus VIS-H test.

ANOVA

Sources	*SS*	*df*	*MS*	*F*	*P value*	*F crit*
Between Groups	46082128.045	3.000	15360709.348	26.542	**<0.001**	2.635
Within Groups	173618158.390	300.000	578727.195			
Total	219700286.436	303.000	725083.454			

TUKEY HSD/KRAMER alpha 0.050

group	*mean*	*n*	*ss*	*df*	*q-crit*
VIS-NIR 0	481.667	76.000	12634010.131		
VIS-H 0	1325.139	76.000	99039406.120		
VIS-NIR 6	349.582	76.000	6800958.860		
VIS-H 6	966.833	76.000	55143783.279		
		304.000	173618158.390	300.000	3.654

Q TEST

group 1	*group 2*	*mean*	*std err*	*lower*	*upper*	*p-value*	*mean-crit*
VIS-NIR 0	VIS-H 0	843.473	87.263	524.631	1162.314	**<0.001**	318.842
VIS-NIR 0	VIS-NIR 6	132.085	87.263	-186.757	450.926	0.708	318.842
VIS-NIR 0	VIS-H 6	485.167	87.263	166.325	804.008	0.001	318.842
VIS-H 0	VIS-NIR 6	975.558	87.263	656.716	1294.399	**<0.001**	318.842
VIS-H 0	VIS-H 6	358.306	87.263	39.465	677.148	0.021	318.842
VIS-NIR 6	VIS-H 6	617.252	87.263	298.410	936.093	**<0.001**	318.842

Appendix Table 2
One-way ANOVA and Tukey post hoc results for neoprene VIS-NIR versus VIS-H test.

ANOVA

Sources	*SS*	*df*	*MS*	*F*	*P value*	*F crit*
Between Groups	614926.482	3.000	204975.494	0.954	0.415	2.635
Within Groups	64434774.766	300.000	214782.583			
Total	65049701.248	303.000	214685.483			

TUKEY HSD/KRAMER alpha 0.050

group	*mean*	*n*	*ss*	*df*	*q-crit*
VIS-NIR 0	467.305	76.000	11972433.931		
VIS-H 0	566.728	76.000	16630233.657		
VIS-NIR 6	576.441	76.000	20298319.585		
VIS-H 6	504.279	76.000	15533787.593		
		304.000	64434774.766	300.000	3.654

Q TEST

group 1	*group 2*	*mean*	*std err*	*lower*	*upper*	*p-value*	*mean-crit*
VIS-NIR 0	VIS-H 0	99.424	53.161	-94.816	293.663	0.549	194.239
VIS-NIR 0	VIS-NIR 6	109.136	53.161	-85.103	303.376	0.468	194.239
VIS-NIR 0	VIS-H 6	36.974	53.161	-157.265	231.214	0.961	194.239
VIS-H 0	VIS-NIR 6	9.713	53.161	-184.526	203.952	0.999	194.239
VIS-H 0	VIS-H 6	62.449	53.161	-131.790	256.689	0.840	194.239
VIS-NIR 6	VIS-H 6	72.162	53.161	-122.077	266.402	0.772	194.239

Appendix Table 3
One-way ANOVA and Tukey post hoc results for satin VIS-NIR versus VIS-H test.

ANOVA

Sources	*SS*	*df*	*MS*	*F*	*P value*	*F crit*
Between Groups	8843700.820	3.000	2947900.273	9.304	<**0.001**	2.635
Within Groups	95050386.241	300.000	316834.621			
Total	103894087.061	303.000	342884.776			

TUKEY HSD/KRAMER alpha 0.050

group	*mean*	*n*	*ss*	*df*	*q-crit*
VIS-NIR 0	574.076	76.000	19460614.301		
VIS-H 0	733.729	76.000	31969726.034		
VIS-NIR 6	356.500	76.000	7324140.621		
VIS-H 6	798.775	76.000	36295905.285		
		304.000	95050386.241	300.000	3.654

Q TEST

group 1	*group 2*	*mean*	*std err*	*lower*	*upper*	*p-value*	*mean-crit*
VIS-NIR 0	VIS-H 0	159.654	64.567	-76.261	395.568	0.301	235.914
VIS-NIR 0	VIS-NIR 6	217.576	64.567	-18.339	453.490	0.083	235.914
VIS-NIR 0	VIS-H 6	224.699	64.567	-11.215	460.613	0.068	235.914
VIS-H 0	VIS-NIR 6	377.229	64.567	141.315	613.144	<**0.001**	235.914
VIS-H 0	VIS-H 6	65.045	64.567	-170.869	300.960	0.892	235.914
VIS-NIR 6	VIS-H 6	442.275	64.567	206.360	678.189	<**0.001**	235.914

Appendix Table 4
One-way ANOVA and Tukey post hoc results for velvet VIS-NIR versus VIS-H test.

ANOVA

Sources	*SS*	*df*	*MS*	*F*	*P value*	*F crit*
Between Groups	2463753.838	3.000	821251.279	2.123	0.097	2.635
Within Groups	116023754.837	300.000	386745.849			
Total	118487508.675	303.000	391047.883			

TUKEY HSD/KRAMER alpha 0.050

group	*mean*	*n*	*ss*	*df*	*q-crit*
VIS-NIR 0	656.214	76.000	25082617.022		
VIS-H 0	576.313	76.000	18195688.905		
VIS-NIR 6	811.135	76.000	39623950.766		
VIS-H 6	753.414	76.000	33121498.144		
		304.000	116023754.837	300.000	3.654

Q TEST

group 1	*group 2*	*mean*	*std err*	*lower*	*upper*	*p-value*	*mean-crit*
VIS-NIR 0	VIS-H 0	79.901	71.336	-180.745	340.547	0.858	260.646
VIS-NIR 0	VIS-NIR 6	154.922	71.336	-105.724	415.568	0.417	260.646
VIS-NIR 0	VIS-H 6	97.200	71.336	-163.445	357.846	0.770	260.646
VIS-H 0	VIS-NIR 6	234.823	71.336	-25.823	495.469	0.094	260.646
VIS-H 0	VIS-H 6	177.101	71.336	-83.544	437.747	0.297	260.646
VIS-NIR 6	VIS-H 6	57.721	71.336	-202.924	318.367	0.940	260.646

Primary study

Appendix Table 5

One-way ANOVA and Tukey post hoc results for cotton full dataset reflectance values monthly comparison.

ANOVA

Sources	*SS*	*df*	*MS*	*F*	*P value*	*F crit*
Between Groups	1668998	6	278166.4	2.970273	0.007	2.115836
Within Groups	49166297	525	93650.09			
Total	50835296	531	95735.02			

TUKEY HSD/KRAMER alpha 0.05

group	*mean*	*n*	*ss*	*df*	*q-crit*
MONTH 0	463.28	76	11379056		
MONTH 1	377.34	76	7856340		
MONTH 2	369	76	7453403		
MONTH 3	358.89	76	7209082		
MONTH 4	306.33	76	5262729		
MONTH 5	318.78	76	5757662		
MONTH 6	278.44	76	4248025		
		532	49166297	525	4.17

Q TEST

group 1	*group 2*	*mean*	*std err*	*lower*	*upper*	*p-value*	*mean-crit*
MONTH 0	MONTH 1	85.940	35.103	-60.441	232.320	0.595	146.381
MONTH 0	MONTH 2	94.061	35.103	-52.319	240.442	0.485	146.381
MONTH 0	MONTH 3	104.397	35.103	-41.983	250.778	0.352	146.381
MONTH 0	MONTH 4	156.951	35.103	10.570	303.331	0.028	146.381
MONTH 0	MONTH 5	144.505	35.103	-1.876	290.885	0.057	146.381
MONTH 0	MONTH 6	184.842	35.103	38.461	331.223	0.004	146.381
MONTH 1	MONTH 2	8.121	35.103	-138.259	154.502	1.000	146.381
MONTH 1	MONTH 3	18.457	35.103	-127.923	164.838	1.000	146.381
MONTH 1	MONTH 4	71.011	35.103	-75.370	217.391	0.785	146.381
MONTH 1	MONTH 5	58.565	35.103	-87.816	204.945	0.902	146.381
MONTH 1	MONTH 6	98.902	35.103	-47.478	245.283	0.421	146.381
MONTH 2	MONTH 3	10.336	35.103	-136.045	156.716	1.000	146.381
MONTH 2	MONTH 4	62.889	35.103	-83.491	209.270	0.867	146.381
MONTH 2	MONTH 5	50.443	35.103	-95.937	196.824	0.950	146.381
MONTH 2	MONTH 6	90.781	35.103	-55.600	237.161	0.529	146.381
MONTH 3	MONTH 4	52.554	35.103	-93.827	198.934	0.940	146.381
MONTH 3	MONTH 5	40.108	35.103	-106.273	186.488	0.984	146.381
MONTH 3	MONTH 6	80.445	35.103	-65.936	226.825	0.669	146.381
MONTH 4	MONTH 5	12.446	35.103	-133.935	158.827	1.000	146.381
MONTH 4	MONTH 6	27.891	35.103	-118.489	174.272	0.998	146.381
MONTH 5	MONTH 6	40.337	35.103	-106.043	186.718	0.984	146.381

Appendix Table 6
One-way ANOVA and Tukey post hoc results for neoprene full dataset reflectance values monthly comparison.

ANOVA

Sources	*SS*	*df*	*MS*	*F*	*P value*	*F crit*
Between Groups	627499.851	6.000	104583.309	0.839	0.540	2.116
Within Groups	65421279.404	525.000	124611.961			
Total	66048779.255	531.000	124385.648			

TUKEY HSD/KRAMER alpha 0.050

group	*mean*	*n*	*ss*	*df*	*q-crit*
MONTH 0	425.043	76.000	9841340.549		
MONTH 1	397.300	76.000	8914327.805		
MONTH 2	384.118	76.000	8068930.685		
MONTH 3	438.352	76.000	10636944.488		
MONTH 4	405.400	76.000	9055835.711		
MONTH 5	349.698	76.000	6511990.045		
MONTH 6	462.404	76.000	12391910.121		
		532.000	65421279.404	525.000	4.170

Q TEST

group 1	*group 2*	*mean*	*std err*	*lower*	*upper*	*p-value*	*mean-crit*
MONTH 0	MONTH 1	27.743	40.492	-141.110	196.596	0.999	168.853
MONTH 0	MONTH 2	40.925	40.492	-127.928	209.778	0.992	168.853
MONTH 0	MONTH 3	13.309	40.492	-155.544	182.162	1.000	168.853
MONTH 0	MONTH 4	19.643	40.492	-149.210	188.496	1.000	168.853
MONTH 0	MONTH 5	75.345	40.492	-93.508	244.199	0.845	168.853
MONTH 0	MONTH 6	37.361	40.492	-131.492	206.214	0.995	168.853
MONTH 1	MONTH 2	13.182	40.492	-155.671	182.035	1.000	168.853
MONTH 1	MONTH 3	41.051	40.492	-127.802	209.905	0.992	168.853
MONTH 1	MONTH 4	8.100	40.492	-160.753	176.953	1.000	168.853
MONTH 1	MONTH 5	47.603	40.492	-121.250	216.456	0.982	168.853
MONTH 1	MONTH 6	65.104	40.492	-103.749	233.957	0.916	168.853
MONTH 2	MONTH 3	54.234	40.492	-114.619	223.087	0.965	168.853
MONTH 2	MONTH 4	21.282	40.492	-147.571	190.135	1.000	168.853
MONTH 2	MONTH 5	34.420	40.492	-134.433	203.273	0.997	168.853
MONTH 2	MONTH 6	78.286	40.492	-90.567	247.139	0.819	168.853
MONTH 3	MONTH 4	32.952	40.492	-135.902	201.805	0.997	168.853
MONTH 3	MONTH 5	88.654	40.492	-80.199	257.507	0.715	168.853
MONTH 3	MONTH 6	24.052	40.492	-144.801	192.906	1.000	168.853
MONTH 4	MONTH 5	55.703	40.492	-113.151	224.556	0.960	168.853
MONTH 4	MONTH 6	57.004	40.492	-111.849	225.857	0.955	168.853
MONTH 5	MONTH 6	112.707	40.492	-56.147	281.560	0.436	168.853

Appendix Table 7
One-way ANOVA and Tukey post hoc results for satin full dataset reflectance values monthly comparison.

ANOVA

Sources	*SS*	*df*	*MS*	*F*	*P value*	*F crit*
Between Groups	3571158.544	6.000	595193.091	2.365	0.029	2.116
Within Groups	132145866.789	525.000	251706.413			
Total	135717025.333	531.000	255587.618			

TUKEY HSD/KRAMER alpha 0.050

group	*mean*	*n*	*ss*	*df*	*q-crit*
MONTH 0	744.442	76.000	31671147.711		
MONTH 1	573.346	76.000	19323570.875		
MONTH 2	462.919	76.000	12429272.399		
MONTH 3	564.498	76.000	18604202.257		
MONTH 4	551.107	76.000	17911659.663		
MONTH 5	525.073	76.000	16309859.355		
MONTH 6	514.356	76.000	15896154.529		
		532.000	132145866.789	525.000	4.170

Q TEST

group 1	*group 2*	*mean*	*std err*	*lower*	*upper*	*p-value*	*mean-crit*
MONTH 0	MONTH 1	171.096	57.549	-68.885	411.077	0.353	239.981
MONTH 0	MONTH 2	281.523	57.549	41.542	521.504	0.010	239.981
MONTH 0	MONTH 3	179.945	57.549	-60.036	419.926	0.291	239.981
MONTH 0	MONTH 4	193.335	57.549	-46.646	433.316	0.211	239.981
MONTH 0	MONTH 5	219.369	57.549	-20.612	459.350	0.101	239.981
MONTH 0	MONTH 6	230.086	57.549	-9.895	470.067	0.072	239.981
MONTH 1	MONTH 2	110.427	57.549	-129.554	350.408	0.824	239.981
MONTH 1	MONTH 3	8.849	57.549	-231.132	248.830	1.000	239.981
MONTH 1	MONTH 4	22.239	57.549	-217.742	262.220	1.000	239.981
MONTH 1	MONTH 5	48.273	57.549	-191.708	288.254	0.997	239.981
MONTH 1	MONTH 6	58.990	57.549	-180.991	298.971	0.991	239.981
MONTH 2	MONTH 3	101.578	57.549	-138.402	341.559	0.875	239.981
MONTH 2	MONTH 4	88.188	57.549	-151.793	328.169	0.933	239.981
MONTH 2	MONTH 5	62.154	57.549	-177.827	302.135	0.988	239.981
MONTH 2	MONTH 6	51.437	57.549	-188.544	291.418	0.996	239.981
MONTH 3	MONTH 4	13.390	57.549	-226.591	253.371	1.000	239.981
MONTH 3	MONTH 5	39.424	57.549	-200.556	279.405	0.999	239.981
MONTH 3	MONTH 6	50.141	57.549	-189.839	290.122	0.996	239.981
MONTH 4	MONTH 5	26.034	57.549	-213.947	266.015	1.000	239.981
MONTH 4	MONTH 6	36.751	57.549	-203.230	276.732	0.999	239.981
MONTH 5	MONTH 6	10.717	57.549	-229.264	250.698	1.000	239.981

Appendix Table 8
One-way ANOVA and Tukey post hoc results for velvet full dataset reflectance values monthly comparison.

ANOVA

Sources	*SS*	*df*	*MS*	*F*	*P value*	*F crit*
Between Groups	1060282.681	6.000	176713.780	0.330	0.921	2.116
Within Groups	281148178.370	525.000	535520.340			
Total	282208461.051	531.000	531466.028			

TUKEY HSD/KRAMER			alpha	0.050	
group	*mean*	*n*	*ss*	*df*	*q-crit*
MONTH 0	864.451	76.000	44217229.901		
MONTH 1	750.801	76.000	34417687.788		
MONTH 2	821.711	76.000	39273181.997		
MONTH 3	861.859	76.000	44855076.742		
MONTH 4	781.096	76.000	36022614.348		
MONTH 5	862.404	76.000	45881686.123		
MONTH 6	773.024	76.000	36480701.470		
		532.000	281148178.370	525.000	4.170

Q TEST

group 1	*group 2*	*mean*	*std err*	*lower*	*upper*	*p-value*	*mean-crit*
MONTH 0	MONTH 1	113.650	83.942	-236.389	463.690	0.963	350.040
MONTH 0	MONTH 2	42.739	83.942	-307.300	392.779	1.000	350.040
MONTH 0	MONTH 3	2.592	83.942	-347.448	352.632	1.000	350.040
MONTH 0	MONTH 4	83.354	83.942	-266.685	433.394	0.992	350.040
MONTH 0	MONTH 5	2.047	83.942	-347.993	352.086	1.000	350.040
MONTH 0	MONTH 6	91.427	83.942	-258.612	441.467	0.988	350.040
MONTH 1	MONTH 2	70.911	83.942	-279.129	420.950	0.997	350.040
MONTH 1	MONTH 3	111.058	83.942	-238.981	461.098	0.967	350.040
MONTH 1	MONTH 4	30.296	83.942	-319.744	380.335	1.000	350.040
MONTH 1	MONTH 5	111.604	83.942	-238.436	461.643	0.966	350.040
MONTH 1	MONTH 6	22.223	83.942	-327.817	372.263	1.000	350.040
MONTH 2	MONTH 3	40.148	83.942	-309.892	390.187	1.000	350.040
MONTH 2	MONTH 4	40.615	83.942	-309.425	390.655	1.000	350.040
MONTH 2	MONTH 5	40.693	83.942	-309.347	390.732	1.000	350.040
MONTH 2	MONTH 6	48.688	83.942	-301.352	398.728	1.000	350.040
MONTH 3	MONTH 4	80.763	83.942	-269.277	430.802	0.994	350.040
MONTH 3	MONTH 5	0.545	83.942	-349.494	350.585	1.000	350.040
MONTH 3	MONTH 6	88.835	83.942	-261.204	438.875	0.989	350.040
MONTH 4	MONTH 5	81.308	83.942	-268.732	431.347	0.993	350.040
MONTH 4	MONTH 6	8.073	83.942	-341.967	358.113	1.000	350.040
MONTH 5	MONTH 6	89.381	83.942	-260.659	439.420	0.989	350.040

Appendix Table 9
One-way ANOVA and Tukey post hoc results for cotton refined dataset reflectance values monthly comparison.

ANOVA

Sources	*SS*	*df*	*MS*	*F*	*P value*	*F crit*
Between Groups	2821859.017	6.000	470309.836	17.920	**<0.001**	2.167
Within Groups	3490525.191	133.000	26244.550			
Total	6312384.208	139.000	45412.836			

TUKEY HSD/KRAMER alpha 0.050

group	*mean*	*n*	*ss*	*df*	*q-crit*
MONTH 0	981.273	20.000	687041.915		
MONTH 1	781.086	20.000	506796.951		
MONTH 2	750.721	20.000	500173.044		
MONTH 3	716.903	20.000	552956.386		
MONTH 4	592.924	20.000	426372.872		
MONTH 5	626.285	20.000	502634.195		
MONTH 6	509.883	20.000	314549.829		
		140.000	3490525.191	133.000	4.234

Q TEST

group 1	*group 2*	*mean*	*std err*	*lower*	*upper*	*p-value*	*mean-crit*
MONTH 0	MONTH 1	200.187	36.225	46.813	353.561	0.003	153.374
MONTH 0	MONTH 2	230.552	36.225	77.178	383.926	**<0.001**	153.374
MONTH 0	MONTH 3	264.371	36.225	110.997	417.744	**<0.001**	153.374
MONTH 0	MONTH 4	388.349	36.225	234.975	541.723	**<0.001**	153.374
MONTH 0	MONTH 5	354.988	36.225	201.614	508.362	**<0.001**	153.374
MONTH 0	MONTH 6	471.390	36.225	318.016	624.764	**<0.001**	153.374
MONTH 1	MONTH 2	30.365	36.225	-123.009	183.739	0.997	153.374
MONTH 1	MONTH 3	64.183	36.225	-89.191	217.557	0.872	153.374
MONTH 1	MONTH 4	188.162	36.225	34.788	341.536	0.006	153.374
MONTH 1	MONTH 5	154.801	36.225	1.427	308.175	0.046	153.374
MONTH 1	MONTH 6	271.203	36.225	117.829	424.577	**<0.001**	153.374
MONTH 2	MONTH 3	33.818	36.225	-119.556	187.192	0.994	153.374
MONTH 2	MONTH 4	157.797	36.225	4.423	311.171	0.039	153.374
MONTH 2	MONTH 5	124.436	36.225	-28.938	277.810	0.195	153.374
MONTH 2	MONTH 6	240.838	36.225	87.464	394.212	**<0.001**	153.374
MONTH 3	MONTH 4	123.979	36.225	-29.395	277.353	0.199	153.374
MONTH 3	MONTH 5	90.617	36.225	-62.756	243.991	0.571	153.374
MONTH 3	MONTH 6	207.020	36.225	53.646	360.394	0.002	153.374
MONTH 4	MONTH 5	33.361	36.225	-120.013	186.735	0.995	153.374
MONTH 4	MONTH 6	83.041	36.225	-70.333	236.415	0.669	153.374
MONTH 5	MONTH 6	116.402	36.225	-36.972	269.776	0.265	153.374

Appendix Table 10
One-way ANOVA and Tukey post hoc results for neoprene refined dataset reflectance values monthly comparison.

ANOVA

Sources	*SS*	*df*	*MS*	*F*	*P value*	*F crit*
Between Groups	962596.576	6.000	160432.763	12.063	**<0.001**	2.167
Within Groups	1768829.871	133.000	13299.473			
Total	2731426.447	139.000	19650.550			

TUKEY HSD/KRAMER alpha 0.050

group	*mean*	*n*	*ss*	*df*	*q-crit*
MONTH 0	945.577	20.000	259109.635		
MONTH 1	893.881	20.000	258953.493		
MONTH 2	854.078	20.000	232983.037		
MONTH 3	980.140	20.000	247894.361		
MONTH 4	903.365	20.000	256932.131		
MONTH 5	773.693	20.000	172744.638		
MONTH 6	1051.719	20.000	340212.576		
		140.000	1768829.871	133.000	4.234

Q TEST

group 1	*group 2*	*mean*	*std err*	*lower*	*upper*	*p-value*	*mean-crit*
MONTH 0	MONTH 1	51.696	25.787	-57.486	160.877	0.791	109.182
MONTH 0	MONTH 2	91.499	25.787	-17.682	200.681	0.164	109.182
MONTH 0	MONTH 3	34.563	25.787	-74.619	143.745	0.964	109.182
MONTH 0	MONTH 4	42.212	25.787	-66.970	151.393	0.909	109.182
MONTH 0	MONTH 5	171.884	25.787	62.702	281.065	**<0.001**	109.182
MONTH 0	MONTH 6	106.142	25.787	-3.039	215.324	0.063	109.182
MONTH 1	MONTH 2	39.804	25.787	-69.378	148.985	0.930	109.182
MONTH 1	MONTH 3	86.259	25.787	-22.923	195.440	0.222	109.182
MONTH 1	MONTH 4	9.484	25.787	-99.698	118.665	1.000	109.182
MONTH 1	MONTH 5	120.188	25.787	11.006	229.370	0.021	109.182
MONTH 1	MONTH 6	157.838	25.787	48.656	267.019	0.001	109.182
MONTH 2	MONTH 3	126.062	25.787	16.881	235.244	0.013	109.182
MONTH 2	MONTH 4	49.287	25.787	-59.894	158.469	0.826	109.182
MONTH 2	MONTH 5	80.384	25.787	-28.797	189.566	0.300	109.182
MONTH 2	MONTH 6	197.641	25.787	88.460	306.823	**<0.001**	109.182
MONTH 3	MONTH 4	76.775	25.787	-32.407	185.956	0.356	109.182
MONTH 3	MONTH 5	206.447	25.787	97.265	315.628	**<0.001**	109.182
MONTH 3	MONTH 6	71.579	25.787	-37.602	180.761	0.443	109.182
MONTH 4	MONTH 5	129.672	25.787	20.490	238.853	0.009	109.182
MONTH 4	MONTH 6	148.354	25.787	39.172	257.536	0.002	109.182
MONTH 5	MONTH 6	278.026	25.787	168.844	387.207	**<0.001**	109.182

Appendix Table 11
One-way ANOVA and Tukey post hoc results for satin refined dataset reflectance values monthly comparison.

ANOVA

Sources	*SS*	*df*	*MS*	*F*	*P value*	*F crit*
Between Groups	5063254.425	6.000	843875.737	14.715	**<0.001**	2.167
Within Groups	7627076.772	133.000	57346.442			
Total	12690331.197	139.000	91297.347			

TUKEY HSD/KRAMER alpha 0.050

group	*mean*	*n*	*ss*	*df*	*q-crit*
MONTH 0	1626.561	20.000	1551882.454		
MONTH 1	1256.675	20.000	1048842.497		
MONTH 2	976.870	20.000	682887.478		
MONTH 3	1210.882	20.000	1004406.155		
MONTH 4	1169.698	20.000	1158519.197		
MONTH 5	1112.851	20.000	1045578.248		
MONTH 6	1100.058	20.000	1134960.743		
		140.000	7627076.772	133.000	4.234

Q TEST

group 1	*group 2*	*mean*	*std err*	*lower*	*upper*	*p-value*	*mean-crit*
MONTH 0	MONTH 1	369.886	53.547	143.168	596.603	**<0.001**	226.718
MONTH 0	MONTH 2	649.690	53.547	422.973	876.408	**<0.001**	226.718
MONTH 0	MONTH 3	415.679	53.547	188.961	642.397	**<0.001**	226.718
MONTH 0	MONTH 4	456.863	53.547	230.145	683.580	**<0.001**	226.718
MONTH 0	MONTH 5	513.710	53.547	286.993	740.428	**<0.001**	226.718
MONTH 0	MONTH 6	526.503	53.547	299.785	753.221	**<0.001**	226.718
MONTH 1	MONTH 2	279.805	53.547	53.087	506.522	0.006	226.718
MONTH 1	MONTH 3	45.793	53.547	-180.924	272.511	0.997	226.718
MONTH 1	MONTH 4	86.977	53.547	-139.740	313.695	0.912	226.718
MONTH 1	MONTH 5	143.825	53.547	-82.893	370.542	0.484	226.718
MONTH 1	MONTH 6	156.618	53.547	-70.100	383.335	0.378	226.718
MONTH 2	MONTH 3	234.011	53.547	7.294	460.729	0.038	226.718
MONTH 2	MONTH 4	192.828	53.547	-33.890	419.545	0.152	226.718
MONTH 2	MONTH 5	135.980	53.547	-90.737	362.698	0.553	226.718
MONTH 2	MONTH 6	123.187	53.547	-103.530	349.905	0.665	226.718
MONTH 3	MONTH 4	41.184	53.547	-185.534	267.901	0.998	226.718
MONTH 3	MONTH 5	98.031	53.547	-128.686	324.749	0.853	226.718
MONTH 3	MONTH 6	110.824	53.547	-115.894	337.542	0.766	226.718
MONTH 4	MONTH 5	56.847	53.547	-169.870	283.565	0.989	226.718
MONTH 4	MONTH 6	69.640	53.547	-157.077	296.358	0.969	226.718
MONTH 5	MONTH 6	12.793	53.547	-213.925	239.510	1.000	226.718

Appendix Table 12
One-way ANOVA and Tukey post hoc results for velvet refined dataset reflectance values monthly comparison.

ANOVA

Sources	*SS*	*df*	*MS*	*F*	*P value*	*F crit*
Between Groups	1060282.681	6.000	176713.780	0.330	0.921	2.116
Within Groups	281148178.370	525.000	535520.340			
Total	282208461.051	531.000	531466.028			

TUKEY HSD/KRAMER			alpha	0.050	
group	*mean*	*n*	*ss*	*df*	*q-crit*
MONTH 0	864.451	76.000	44217229.901		
MONTH 1	750.801	76.000	34417687.788		
MONTH 2	821.711	76.000	39273181.997		
MONTH 3	861.859	76.000	44855076.742		
MONTH 4	781.096	76.000	36022614.348		
MONTH 5	862.404	76.000	45881686.123		
MONTH 6	773.024	76.000	36480701.470		
		532.000	281148178.370	525.000	4.170

Q TEST

group 1	*group 2*	*mean*	*std err*	*lower*	*upper*	*p-value*	*mean-crit*
MONTH 0	MONTH 1	113.650	83.942	-236.389	463.690	0.963	350.040
MONTH 0	MONTH 2	42.739	83.942	-307.300	392.779	1.000	350.040
MONTH 0	MONTH 3	2.592	83.942	-347.448	352.632	1.000	350.040
MONTH 0	MONTH 4	83.354	83.942	-266.685	433.394	0.992	350.040
MONTH 0	MONTH 5	2.047	83.942	-347.993	352.086	1.000	350.040
MONTH 0	MONTH 6	91.427	83.942	-258.612	441.467	0.988	350.040
MONTH 1	MONTH 2	70.911	83.942	-279.129	420.950	0.997	350.040
MONTH 1	MONTH 3	111.058	83.942	-238.981	461.098	0.967	350.040
MONTH 1	MONTH 4	30.296	83.942	-319.744	380.335	1.000	350.040
MONTH 1	MONTH 5	111.604	83.942	-238.436	461.643	0.966	350.040
MONTH 1	MONTH 6	22.223	83.942	-327.817	372.263	1.000	350.040
MONTH 2	MONTH 3	40.148	83.942	-309.892	390.187	1.000	350.040
MONTH 2	MONTH 4	40.615	83.942	-309.425	390.655	1.000	350.040
MONTH 2	MONTH 5	40.693	83.942	-309.347	390.732	1.000	350.040
MONTH 2	MONTH 6	48.688	83.942	-301.352	398.728	1.000	350.040
MONTH 3	MONTH 4	80.763	83.942	-269.277	430.802	0.994	350.040
MONTH 3	MONTH 5	0.545	83.942	-349.494	350.585	1.000	350.040
MONTH 3	MONTH 6	88.835	83.942	-261.204	438.875	0.989	350.040
MONTH 4	MONTH 5	81.308	83.942	-268.732	431.347	0.993	350.040
MONTH 4	MONTH 6	8.073	83.942	-341.967	358.113	1.000	350.040
MONTH 5	MONTH 6	89.381	83.942	-260.659	439.420	0.989	350.040

Appendix Table 13
Two-way ANOVA and Tukey post hoc results for fabrics comparison.

ANOVA				Alpha	0.050	
	SS	*df*	*MS*	*F*	*p-value*	*sig*
Rows	74688703.574	3.000	24896234.525	372.199	<**0.001**	yes
Columns	5688315.744	6.000	948052.624	14.173	<**0.001**	yes
Inter	5366754.671	18.000	298153.037	4.457	<**0.001**	yes
Within	35585262.088	532.000	66889.590			
Total	121329036.076	559.000	217046.576			

TUKEY HSD; ROW EFFECT			alpha	0.050
group	*mean*	*size*	*df*	*q-crit*
COTTON	708.439	140.000		
NEOPRENE	914.636	140.000		
SATIN	1207.656	140.000		
VELVET	1680.802	140.000		
		560.000	532.000	3.633

Q TEST

group 1	*group 2*	*mean*	*std err*	*mean-crit*	*lower*	*upper*	*p-value*
COTTON	NEOPRENE	206.197	21.858	79.411	126.786	285.608	<**0.001**
COTTON	SATIN	499.217	21.858	79.411	419.806	578.628	<**0.001**
COTTON	VELVET	972.363	21.858	79.411	892.952	1051.774	<**0.001**
NEOPRENE	SATIN	293.020	21.858	79.411	213.609	372.431	<**0.001**
NEOPRENE	VELVET	766.166	21.858	79.411	686.755	845.577	<**0.001**
SATIN	VELVET	473.146	21.858	79.411	393.735	552.557	<**0.001**

Appendix Table 14

One-way ANOVA and Tukey post hoc results for fabrics month 0 comparison full dataset.

ANOVA

Sources	*SS*	*df*	*MS*	*F*	*P value*	*F crit*
Between Groups	10467956.015	3	3489319	10.780	**<0.001**	2.635
Within Groups	97108774.624	300	323696			
Total	107576730.639	303	355039			

TUKEY HSD/KRAMER alpha 0.050

group	*mean*	*n*	*ss*	*df*	*q-crit*
COTTON	463.284	76.000	11379056.463		
NEOPRENE	425.043	76.000	9841340.549		
SATIN	744.442	76.000	31671147.711		
VELVET	864.451	76.000	44217229.901		
		304.000	97108774.624	300.000	3.654

Q TEST

group 1	*group 2*	*mean*	*std err*	*lower*	*upper*	*p-value*	*mean-crit*
COTTON	NEOPRENE	38.240	65.262	-200.215	276.696	0.976	238.455
COTTON	SATIN	281.159	65.262	42.704	519.614	0.013	238.455
COTTON	VELVET	401.167	65.262	162.712	639.622	**<0.001**	238.455
NEOPRENE	SATIN	319.399	65.262	80.944	557.854	0.003	238.455
NEOPRENE	VELVET	439.408	65.262	200.953	677.863	**<0.001**	238.455
SATIN	VELVET	120.008	65.262	-118.447	358.464	0.563	238.455

Appendix Table 15
One-way ANOVA and Tukey post hoc results for fabrics month 0 comparison refined dataset.

ANOVA

Sources	*SS*	*df*	*MS*	*F*	*P value*	*F crit*
Between Groups	15902732.531	3.000	5300910.844	67.662	**<0.001**	2.704
Within Groups	7207613.474	92.000	78343.625			
Total	23110346.005	95.000	243266.800			

TUKEY HSD/KRAMER			alpha	0.050	
group	*mean*	*n*	*ss*	*df*	*q-crit*
COTTON	955.817	24.000	879802.437		
NEOPRENE	882.426	24.000	749263.576		
SATIN	1555.086	24.000	2554553.717		
VELVET	1852.485	24.000	3023993.743		
		96.000	7207613.474	92.000	3.701

Q TEST

group 1	*group 2*	*mean*	*std err*	*lower*	*upper*	*p-value*	*mean-crit*
COTTON	NEOPRENE	73.391	57.134	-138.053	284.834	0.800	211.444
COTTON	SATIN	599.269	57.134	387.825	810.713	**<0.001**	211.444
COTTON	VELVET	896.668	57.134	685.225	1108.112	**<0.001**	211.444
NEOPRENE	SATIN	672.660	57.134	461.216	884.103	**<0.001**	211.444
NEOPRENE	VELVET	970.059	57.134	758.615	1181.503	**<0.001**	211.444
SATIN	VELVET	297.399	57.134	85.955	508.843	0.002	211.444

Appendix Table 16

One-way ANOVA and Tukey post hoc results for fabrics month 1 comparison full dataset.

ANOVA

Sources	*SS*	*df*	*MS*	*F*	*P value*	*F crit*
Between Groups	6948874.217	3.000	2316291.406	9.855	**<0.001**	2.635
Within Groups	70511926.043	300.000	235039.753			
Total	77460800.260	303.000	255646.205			

TUKEY HSD/KRAMER alpha 0.050

group	*mean*	*n*	*ss*	*df*	*q-crit*
COTTON	377.344	76.000	7856339.575		
NEOPRENE	397.300	76.000	8914327.805		
SATIN	573.346	76.000	19323570.875		
VELVET	750.801	76.000	34417687.788		
		304.000	70511926.043	300.000	3.654

Q TEST

group 1	*group 2*	*mean*	*std err*	*lower*	*upper*	*p-value*	*mean-crit*
COTTON	NEOPRENE	19.957	55.611	-183.236	223.150	0.994	203.193
COTTON	SATIN	196.003	55.611	-7.190	399.196	0.063	203.193
COTTON	VELVET	373.457	55.611	170.264	576.650	**<0.001**	203.193
NEOPRENE	SATIN	176.046	55.611	-27.147	379.239	0.115	203.193
NEOPRENE	VELVET	353.500	55.611	150.307	556.693	**<0.001**	203.193
SATIN	VELVET	177.454	55.611	-25.739	380.647	0.111	203.193

Appendix Table 17

One-way ANOVA and Tukey post hoc results for fabrics month 1 comparison refined dataset.

ANOVA

Sources	*SS*	*df*	*MS*	*F*	*P value*	*F crit*
Between Groups	9643481.794	3.000	3214493.931	46.924	**<0.001**	2.704
Within Groups	6302396.993	92.000	68504.315			
Total	15945878.787	95.000	167851.356			

TUKEY HSD/KRAMER alpha 0.050

group	*mean*	*n*	*ss*	*df*	*q-crit*
COTTON	772.484	24.000	661151.811		
NEOPRENE	833.449	24.000	708419.841		
SATIN	1203.470	24.000	1684237.621		
VELVET	1561.520	24.000	3248587.720		
		96.000	6302396.993	92.000	3.701

Q TEST

group 1	*group 2*	*mean*	*std err*	*lower*	*upper*	*p-value*	*mean-crit*
COTTON	NEOPRENE	60.965	53.426	-136.756	258.686	0.851	197.721
COTTON	SATIN	430.986	53.426	233.265	628.707	**<0.001**	197.721
COTTON	VELVET	789.036	53.426	591.316	986.757	**<0.001**	197.721
NEOPRENE	SATIN	370.021	53.426	172.300	567.742	**<0.001**	197.721
NEOPRENE	VELVET	728.071	53.426	530.351	925.792	**<0.001**	197.721
SATIN	VELVET	358.050	53.426	160.330	555.771	**<0.001**	197.721

Appendix Table 18

One-way ANOVA and Tukey post hoc results for fabrics month 2 comparison full dataset.

ANOVA

Sources	*SS*	*df*	*MS*	*F*	*P value*	*F crit*
Between Groups	10263360.550	3.000	3421120.183	15.267	**<0.001**	2.635
Within Groups	67224787.883	300.000	224082.626			
Total	77488148.433	303.000	255736.463			

TUKEY HSD/KRAMER

					alpha	0.050
group	*mean*	*n*	*ss*	*df*	*q-crit*	
COTTON	369.222	76.000	7453402.802			
NEOPRENE	384.118	76.000	8068930.685			
SATIN	462.919	76.000	12429272.399			
VELVET	821.711	76.000	39273181.997			
		304.000	67224787.883	300.000	3.654	

Q TEST

group 1	*group 2*	*mean*	*std err*	*lower*	*upper*	*p-value*	*mean-crit*
COTTON	NEOPRENE	14.896	54.300	-183.505	213.296	0.997	198.400
COTTON	SATIN	93.697	54.300	-104.703	292.097	0.615	198.400
COTTON	VELVET	452.489	54.300	254.089	650.889	**<0.001**	198.400
NEOPRENE	SATIN	78.801	54.300	-119.599	277.201	0.734	198.400
NEOPRENE	VELVET	437.593	54.300	239.193	635.994	**<0.001**	198.400
SATIN	VELVET	358.792	54.300	160.392	557.192	**<0.001**	198.400

Appendix Table 19

One-way ANOVA and Tukey post hoc results for fabrics month 2 comparison refined dataset.

ANOVA

Sources	*SS*	*df*	*MS*	*F*	*P value*	*F crit*
Between Groups	14527223.886	3.000	4842407.962	81.592	**<0.001**	2.704
Within Groups	5460099.057	92.000	59348.903			
Total	19987322.943	95.000	210392.873			

TUKEY HSD/KRAMER alpha 0.050

group	*mean*	*n*	*ss*	*df*	*q-crit*
COTTON	746.064	24.000	659983.657		
NEOPRENE	793.844	24.000	676808.854		
SATIN	943.797	24.000	1143926.606		
VELVET	1710.332	24.000	2979379.939		
		96.000	5460099.057	92.000	3.701

Q TEST

group 1	*group 2*	*mean*	*std err*	*lower*	*upper*	*p-value*	*mean-crit*
COTTON	NEOPRENE	47.780	49.728	-136.254	231.815	0.905	184.035
COTTON	SATIN	197.733	49.728	13.698	381.767	0.030	184.035
COTTON	VELVET	964.268	49.728	780.233	1148.302	**<0.001**	184.035
NEOPRENE	SATIN	149.953	49.728	-34.082	333.987	0.151	184.035
NEOPRENE	VELVET	916.488	49.728	732.453	1100.522	**<0.001**	184.035
SATIN	VELVET	766.535	49.728	582.500	950.569	**<0.001**	184.035

Appendix Table 20

One-way ANOVA and Tukey post hoc results for fabrics month 3 comparison full dataset.

ANOVA

Sources	*SS*	*df*	*MS*	*F*	*P value*	*F crit*
Between Groups	11120069.075	3.000	3706689.692	13.677	**<0.001**	2.635
Within Groups	81305305.640	300.000	271017.685			
Total	92425374.715	303.000	305034.240			

TUKEY HSD/KRAMER alpha 0.050

group	*mean*	*n*	*ss*	*df*	*q-crit*
COTTON	358.886	76.000	7209082.153		
NEOPRENE	438.352	76.000	10636944.488		
SATIN	564.498	76.000	18604202.257		
VELVET	861.859	76.000	44855076.742		
		304.000	81305305.640	300.000	3.654

Q TEST

group 1	*group 2*	*mean*	*std err*	*lower*	*upper*	*p-value*	*mean-crit*
COTTON	NEOPRENE	79.465	59.716	-138.726	297.656	0.783	218.191
COTTON	SATIN	205.611	59.716	-12.580	423.802	0.073	218.191
COTTON	VELVET	502.972	59.716	284.781	721.163	**<0.001**	218.191
NEOPRENE	SATIN	126.146	59.716	-92.045	344.337	0.443	218.191
NEOPRENE	VELVET	423.507	59.716	205.316	641.698	**<0.001**	218.191
SATIN	VELVET	297.361	59.716	79.170	515.552	0.003	218.191

Appendix Table 21

One-way ANOVA and Tukey post hoc results for fabrics month 3 comparison refined dataset.

ANOVA

Sources	*SS*	*df*	*MS*	*F*	*P value*	*F crit*
Between Groups	16185950.531	3.000	5395316.844	72.591	**<0.001**	2.704
Within Groups	6837875.622	92.000	74324.735			
Total	23023826.153	95.000	242356.065			

TUKEY HSD/KRAMER alpha 0.050

group	*mean*	*n*	*ss*	*df*	*q-crit*
COTTON	717.235	24.000	741913.829		
NEOPRENE	916.162	24.000	752222.349		
SATIN	1166.236	24.000	1655880.085		
VELVET	1807.417	24.000	3687859.359		
		96.000	6837875.622	92.000	3.701

Q TEST

group 1	*group 2*	*mean*	*std err*	*lower*	*upper*	*p-value*	*mean-crit*
COTTON	NEOPRENE	198.928	55.649	-7.021	404.877	0.062	205.949
COTTON	SATIN	449.002	55.649	243.053	654.951	**<0.001**	205.949
COTTON	VELVET	1090.183	55.649	884.234	1296.132	**<0.001**	205.949
NEOPRENE	SATIN	250.074	55.649	44.125	456.023	0.011	205.949
NEOPRENE	VELVET	891.255	55.649	685.306	1097.204	**<0.001**	205.949
SATIN	VELVET	641.181	55.649	435.232	847.130	**<0.001**	205.949

Appendix Table 22

One-way ANOVA and Tukey post hoc results for fabrics month 4 comparison full dataset.

ANOVA

Sources	*SS*	*df*	*MS*	*F*	*P value*	*F crit*
Between Groups	9697644.872	3.000	3232548.291	14.208	**<0.001**	2.635
Within Groups	68252838.833	300.000	227509.463			
Total	77950483.705	303.000	257262.322			

TUKEY HSD/KRAMER

			alpha	0.050	
group	*mean*	*n*	*ss*	*df*	*q-crit*
COTTON	306.333	76.000	5262729.110		
NEOPRENE	405.400	76.000	9055835.711		
SATIN	551.107	76.000	17911659.663		
VELVET	781.096	76.000	36022614.348		
		304.000	68252838.833	300.000	3.654

Q TEST

group 1	*group 2*	*mean*	*std err*	*lower*	*upper*	*p-value*	*mean-crit*
COTTON	NEOPRENE	99.067	54.713	-100.844	298.979	0.576	199.911
COTTON	SATIN	244.774	54.713	44.863	444.686	0.009	199.911
COTTON	VELVET	474.763	54.713	274.852	674.675	**<0.001**	199.911
NEOPRENE	SATIN	145.707	54.713	-54.204	345.619	0.237	199.911
NEOPRENE	VELVET	375.696	54.713	175.785	575.608	**<0.001**	199.911
SATIN	VELVET	229.989	54.713	30.078	429.900	0.017	199.911

Appendix Table 23

One-way ANOVA and Tukey post hoc results for fabrics month 4 comparison refined dataset.

ANOVA

Sources	*SS*	*df*	*MS*	*F*	*P value*	*F crit*
Between Groups	13710558.374	3.000	4570186.125	65.182	**<0.001**	2.704
Within Groups	6450469.360	92.000	70113.797			
Total	20161027.734	95.000	212221.345			

TUKEY HSD/KRAMER			alpha	0.050	
group	*mean*	*n*	*ss*	*df*	*q-crit*
COTTON	599.398	24.000	606135.459		
NEOPRENE	839.995	24.000	749465.289		
SATIN	1127.680	24.000	1831956.691		
VELVET	1614.078	24.000	3262911.921		
		96.000	6450469.360	92.000	3.701

Q TEST

group 1	*group 2*	*mean*	*std err*	*lower*	*upper*	*p-value*	*mean-crit*
COTTON	NEOPRENE	240.597	54.050	40.567	440.627	0.012	200.030
COTTON	SATIN	528.282	54.050	328.252	728.312	**<0.001**	200.030
COTTON	VELVET	1014.680	54.050	814.650	1214.710	**<0.001**	200.030
NEOPRENE	SATIN	287.685	54.050	87.655	487.715	0.002	200.030
NEOPRENE	VELVET	774.083	54.050	574.053	974.113	**<0.001**	200.030
SATIN	VELVET	486.398	54.050	286.368	686.428	**<0.001**	200.030

Appendix Table 24

One-way ANOVA and Tukey post hoc results for fabrics month 5 comparison full dataset.

ANOVA

Sources	*SS*	*df*	*MS*	*F*	*P value*	*F crit*
Between Groups	14182713.495	3.000	4727571.165	19.047	**<0.001**	2.635
Within Groups	74461197.896	300.000	248203.993			
Total	88643911.391	303.000	292554.163			

TUKEY HSD/KRAMER alpha 0.050

group	*mean*	*n*	*ss*	*df*	*q-crit*
COTTON	318.779	76.000	5757662.372		
NEOPRENE	349.698	76.000	6511990.045		
SATIN	525.073	76.000	16309859.355		
VELEVT	862.404	76.000	45881686.123		
		304.000	74461197.896	300.000	3.654

Q TEST

group 1	*group 2*	*mean*	*std err*	*lower*	*upper*	*p-value*	*mean-crit*
COTTON	NEOPRENE	30.919	57.148	-177.887	239.724	0.981	208.806
COTTON	SATIN	206.294	57.148	-2.511	415.100	0.054	208.806
COTTON	VELEVT	543.625	57.148	334.820	752.431	**<0.001**	208.806
NEOPRENE	SATIN	175.376	57.148	-33.430	384.181	0.134	208.806
NEOPRENE	VELEVT	512.707	57.148	303.901	721.512	**<0.001**	208.806
SATIN	VELEVT	337.331	57.148	128.525	546.137	**<0.001**	208.806

Appendix Table 25

One-way ANOVA and Tukey post hoc results for fabrics month 5 comparison refined dataset.

ANOVA

Sources	*SS*	*df*	*MS*	*F*	*P value*	*F crit*
Between Groups	21009785.154	3.000	7003261.718	93.260	**<0.001**	2.704
Within Groups	6908628.400	92.000	75093.787			
Total	27918413.555	95.000	293878.037			

TUKEY HSD/KRAMER alpha 0.05

group	*mean*	*n*	*ss*	*df*	*q-crit*
COTTON	628.975	24.000	677635.643		
NEOPRENE	722.332	24.000	496953.144		
SATIN	1072.791	24.000	1668337.716		
VELVET	1818.580	24.000	4065701.896		
		96.000	6908628.400	92.000	3.701

Q TEST

group 1	*group 2*	*mean*	*std err*	*lower*	*upper*	*p-value*	*mean-crit*
COTTON	NEOPRENE	93.357	55.937	-113.655	300.369	0.641	207.012
COTTON	SATIN	443.816	55.937	236.804	650.827	**<0.001**	207.012
COTTON	VELVET	1189.605	55.937	982.593	1396.617	**<0.001**	207.012
NEOPRENE	SATIN	350.458	55.937	143.447	557.470	**<0.001**	207.012
NEOPRENE	VELVET	1096.248	55.937	889.236	1303.260	**<0.001**	207.012
SATIN	VELVET	745.789	55.937	538.778	952.801	**<0.001**	207.012

Appendix Table 26

One-way ANOVA and Tukey post hoc results for fabrics month 6 comparison full dataset.

ANOVA

Sources	*SS*	*df*	*MS*	*F*	*P value*	*F crit*
Between Groups	9503828.080	3.000	3167942.693	13.770	**<0.001**	2.635
Within Groups	69016790.884	300.000	230055.970			
Total	78520618.965	303.000	259143.957			

TUKEY HSD/KRAMER alpha 0.050

group	*mean*	*n*	*ss*	*df*	*q-crit*
COTTON	278.442	76.000	4248024.765		
NEOPRENE	462.404	76.000	12391910.121		
SATIN	514.356	76.000	15896154.529		
VELVET	773.024	76.000	36480701.470		
		304.000	69016790.884	300.000	3.654

Q TEST

group 1	*group 2*	*mean*	*std err*	*lower*	*upper*	*p-value*	*mean-crit*
COTTON	NEOPRENE	183.963	55.019	-17.065	384.990	0.086	201.027
COTTON	SATIN	235.915	55.019	34.888	436.942	0.014	201.027
COTTON	VELVET	494.582	55.019	293.555	695.609	**<0.001**	201.027
NEOPRENE	SATIN	51.952	55.019	-149.075	252.979	0.909	201.027
NEOPRENE	VELVET	310.619	55.019	109.592	511.646	**<0.001**	201.027
SATIN	VELVET	258.667	55.019	57.640	459.694	0.005	201.027

Appendix Table 27
One-way ANOVA and Tukey post hoc results for fabrics month 6 comparison refined dataset.

ANOVA

Sources	*SS*	*df*	*MS*	*F*	*P value*	*F crit*
Between Groups	14003876.412	3.000	4667958.804	61.994	**<0.001**	2.704
Within Groups	6927335.576	92.000	75297.126			
Total	20931211.988	95.000	220328.547			

TUKEY HSD/KRAMER alpha 0.050

group	*mean*	*n*	*ss*	*df*	*q-crit*
COTTON	523.086	24.000	506500.142		
NEOPRENE	980.801	24.000	957796.884		
SATIN	1056.697	24.000	1754994.885		
VELVET	1599.027	24.000	3708043.665		
		96.000	6927335.576	92.000	3.701

Q TEST

group 1	*group 2*	*mean*	*std err*	*lower*	*upper*	*p-value*	*mean-crit*
COTTON	NEOPRENE	457.715	56.012	250.423	665.007	**<0.001**	207.292
COTTON	SATIN	533.611	56.012	326.319	740.903	**<0.001**	207.292
COTTON	VELVET	1075.941	56.012	868.649	1283.233	**<0.001**	207.292
NEOPRENE	SATIN	75.896	56.012	-131.396	283.188	0.773	207.292
NEOPRENE	VELVET	618.227	56.012	410.935	825.518	**<0.001**	207.292
SATIN	VELVET	542.330	56.012	335.039	749.622	**<0.001**	207.292

Appendix Table 28
Raw dataset, refined dataset bolded.

WAVELENGTH	MONTH 0	MONTH 1	MONTH 2	MONTH 3	MONTH 4	MONTH 5	MONTH 6
COTTON							
1010.012	130.193	132.707	150.097	161.357	155.590	164.527	168.807
990.415	170.390	169.293	188.440	205.417	196.240	202.543	208.730
971.555	214.560	211.950	232.347	252.477	239.150	242.390	251.230
953.392	264.983	257.783	283.880	302.953	283.050	291.503	292.407
935.888	318.267	307.217	333.170	354.840	329.517	342.243	333.523
919.006	368.587	360.667	377.080	406.820	376.027	388.550	381.560
902.716	423.800	416.903	427.237	464.140	426.170	440.030	434.607
886.985	490.520	473.130	489.283	522.030	479.277	490.767	483.420
871.787	553.157	527.783	549.280	573.360	527.723	533.950	527.930
857.093	609.030	583.830	603.070	623.503	573.820	579.670	573.583
842.880	677.100	642.747	659.610	677.090	620.533	630.663	615.777
829.125	751.253	699.700	713.030	727.720	660.730	672.283	647.223
815.804	814.010	749.223	757.810	770.670	697.190	707.307	675.623
802.900	870.700	797.153	801.680	811.450	732.320	740.703	702.747
790.391	925.923	842.317	840.697	847.777	757.220	764.967	714.767
778.260	975.550	875.717	866.970	872.040	767.107	782.090	707.867
766.491	1022.173	901.987	885.193	885.717	762.893	790.347	681.050
755.067	1065.097	922.347	895.950	885.293	742.670	781.777	633.020
743.973	1101.883	922.220	886.477	861.067	709.750	764.413	582.557
733.195	1130.330	903.477	864.477	832.550	686.727	756.677	560.697
722.721	1153.147	892.900	858.670	829.897	691.310	760.153	576.947
712.536	1167.530	900.647	871.363	845.930	712.080	767.083	608.133
702.631	1169.293	914.850	888.507	860.317	726.457	770.623	629.070
692.992	1164.553	922.043	896.063	864.343	724.913	762.803	629.277
683.610	1152.590	915.937	886.047	852.370	708.393	741.357	612.443
674.474	1125.147	893.877	857.687	820.603	680.123	709.477	587.693
665.575	1084.087	856.867	818.813	779.600	646.957	674.163	561.670
656.903	1033.490	813.497	780.973	740.577	609.397	636.603	535.947
648.451	976.547	772.307	741.720	699.253	569.900	596.273	504.903
640.209	919.277	729.090	694.573	653.873	529.157	554.600	467.150
632.171	863.803	679.867	645.863	608.273	488.047	511.573	426.943
624.328	809.770	630.833	600.457	556.980	450.863	471.020	386.993
616.674	754.487	581.880	552.693	505.687	411.830	430.720	350.903
609.202	696.880	533.467	505.253	460.210	369.913	387.887	320.043
601.906	643.023	488.447	462.897	417.217	334.177	346.877	287.073
594.778	592.360	445.183	420.743	378.300	302.927	311.280	255.147
587.814	541.967	402.710	381.770	344.310	270.427	281.937	231.023
581.009	495.393	363.650	347.350	315.490	240.617	254.937	207.883
574.356	457.863	330.233	314.413	285.540	218.417	230.157	187.653
567.850	425.087	299.563	282.867	254.507	200.413	210.087	172.497

561.487	393.097	273.713	253.617	231.407	182.653	192.023	155.923
555.262	362.337	250.183	231.263	210.117	165.607	174.023	142.600
549.171	333.470	227.210	213.440	187.627	150.033	157.117	130.750
543.210	307.250	207.697	195.897	167.807	135.373	141.787	115.993
537.373	283.263	190.303	177.733	154.050	120.613	126.020	103.607
531.658	264.617	175.733	164.127	143.387	109.773	113.590	98.680
526.061	248.097	159.537	148.840	133.127	102.157	104.847	94.823
520.577	229.787	145.667	134.410	119.180	95.007	98.510	87.733
515.204	207.920	136.237	125.537	105.133	90.703	90.590	80.923
509.939	188.547	126.613	117.423	98.673	82.490	82.553	74.897
504.778	175.380	112.413	107.807	93.497	75.887	79.150	69.783
499.717	162.403	101.200	97.440	86.970	71.780	74.660	65.863
494.755	152.103	94.003	91.460	83.890	67.067	67.683	62.413
489.888	140.117	88.980	87.163	79.043	60.800	66.407	59.303
485.114	127.707	82.103	78.057	70.080	56.140	61.653	55.277
480.429	114.347	74.063	71.547	65.893	56.263	59.657	52.490
475.832	103.307	69.560	70.330	62.840	53.437	59.800	51.833
471.320	95.180	66.517	68.877	60.140	50.897	54.760	52.190
466.891	92.500	64.697	65.150	59.723	54.243	51.720	51.173
462.542	86.427	63.617	60.457	56.000	53.963	52.233	52.177
458.271	78.317	59.900	57.677	56.163	53.653	50.747	51.287
454.077	70.133	54.993	56.760	58.510	52.820	49.343	47.713
449.956	65.623	55.630	57.157	57.337	51.520	51.590	46.903
445.908	65.570	57.623	54.887	56.483	51.927	51.003	48.720
441.930	65.627	57.010	57.037	54.703	50.873	53.740	46.500
438.021	65.737	57.557	54.927	53.953	52.253	54.297	49.020
434.178	66.100	54.280	50.303	57.883	54.480	53.227	49.523
430.400	62.550	56.513	51.467	55.670	54.670	51.833	48.943
426.686	58.973	54.803	55.847	53.977	52.323	53.187	49.453
423.033	62.330	53.743	56.953	53.703	52.533	52.767	50.770
419.441	61.003	57.557	55.933	56.477	52.583	54.620	49.613
415.908	61.247	57.933	54.307	56.677	52.580	55.590	47.800
412.432	65.207	55.843	52.870	54.860	52.083	53.950	48.393
409.012	63.763	55.500	56.390	55.170	51.247	53.327	50.553
405.647	63.953	56.520	56.927	56.970	49.807	52.243	51.593
402.335	61.760	56.670	56.383	56.703	51.043	49.943	49.820
NEOPRENE							
1010.012	131.010	124.608	135.440	135.860	144.307	120.807	129.073
990.415	170.820	157.048	180.463	173.680	182.743	150.450	166.800
971.555	212.293	193.703	214.327	215.443	226.510	190.857	210.533
953.392	256.773	240.608	245.510	257.380	266.460	227.960	261.270
935.888	302.403	286.983	284.880	302.193	304.827	260.357	308.780
919.006	350.247	330.177	337.620	354.320	347.993	296.583	356.523
902.716	405.703	380.668	391.200	414.960	398.623	343.053	415.623
886.985	465.393	434.993	435.360	475.790	456.780	391.017	480.460

871.787	523.620	489.845	478.203	533.167	514.153	432.720	540.890
857.093	580.793	542.492	535.790	594.447	569.647	473.930	601.750
842.880	641.077	593.593	602.243	659.390	630.003	518.253	670.663
829.125	700.290	644.453	659.593	716.807	686.943	559.807	740.440
815.804	754.980	693.207	707.640	769.780	736.500	598.363	806.013
802.900	811.043	743.173	759.090	825.940	789.220	643.457	869.497
790.391	864.673	795.863	808.387	883.320	839.400	691.370	931.280
778.260	907.443	843.222	848.783	932.657	880.910	732.483	986.277
766.491	947.677	888.253	885.147	972.147	920.377	770.250	1035.453
755.067	989.400	929.263	913.217	1006.953	955.727	804.960	1080.543
743.973	1022.587	958.663	931.453	1038.600	984.030	829.797	1114.697
733.195	1043.173	984.285	942.457	1065.370	1007.950	847.790	1141.780
722.721	1059.303	1007.357	953.163	1088.073	1022.313	865.127	1172.037
712.536	1070.420	1022.270	966.270	1102.080	1026.043	877.047	1194.557
702.631	1074.267	1028.990	970.317	1103.923	1026.553	879.810	1200.313
692.992	1070.077	1025.768	961.173	1100.443	1022.197	877.233	1199.133
683.610	1056.567	1012.198	944.327	1093.157	1005.653	868.090	1192.030
674.474	1031.730	985.122	923.697	1075.943	978.477	849.193	1169.517
665.575	996.257	947.888	898.087	1047.723	946.073	823.293	1133.863
656.903	955.123	908.762	861.837	1009.227	904.073	791.987	1090.637
648.451	909.347	866.278	812.203	963.770	855.400	752.243	1038.157
640.209	859.880	816.148	751.663	914.323	805.273	707.417	974.717
632.171	804.427	759.423	695.553	855.757	751.550	665.593	906.443
624.328	746.103	702.718	650.187	792.017	698.917	623.180	835.787
616.674	692.043	651.980	604.547	731.377	647.167	573.547	767.667
609.202	640.697	603.252	555.860	674.230	594.890	525.033	707.090
601.906	589.187	554.007	511.673	620.677	544.070	484.210	651.577
594.778	540.177	506.777	470.617	569.997	496.340	445.247	597.810
587.814	496.633	461.117	432.553	520.193	457.280	407.620	548.357
581.009	456.297	419.105	398.007	475.380	421.417	373.360	502.813
574.356	416.290	383.302	360.793	435.700	384.343	340.807	459.353
567.850	377.730	353.530	322.017	396.370	348.097	309.850	415.757
561.487	343.827	324.748	294.273	361.753	315.327	283.817	378.220
555.262	312.283	293.098	273.860	329.583	288.960	259.480	346.040
549.171	285.587	267.342	251.300	297.923	270.090	237.813	314.087
543.210	264.840	246.402	225.077	272.303	249.073	221.037	284.663
537.373	244.113	225.227	202.680	251.737	224.623	203.597	258.660
531.658	223.247	200.335	184.660	229.773	202.863	182.533	233.833
526.061	204.887	179.340	171.163	210.443	186.473	165.810	210.967
520.577	185.587	163.118	162.210	196.013	171.657	153.730	195.413
515.204	168.890	149.410	151.497	177.137	154.890	140.857	182.560
509.939	156.783	135.420	135.343	153.140	144.297	127.593	169.557
504.778	144.837	124.797	122.773	140.930	134.257	116.037	157.420
499.717	131.967	113.003	107.587	131.637	116.870	104.677	138.463
494.755	121.670	101.760	98.227	119.627	104.310	94.400	120.453
489.888	109.457	92.307	90.893	104.923	98.320	87.943	105.933

485.114	98.717	82.460	83.290	94.277	91.773	80.577	92.330
480.429	90.073	75.777	77.437	89.073	85.160	74.160	86.333
475.832	85.363	67.418	76.187	82.677	75.867	66.867	82.330
471.320	82.810	61.180	70.037	74.733	68.643	64.480	76.470
466.891	77.373	62.585	64.787	74.603	65.473	61.227	68.900
462.542	68.900	64.020	63.860	70.997	60.263	57.927	63.787
458.271	66.310	57.703	63.103	65.833	59.460	56.663	63.677
454.077	70.667	55.518	56.137	60.553	60.877	55.433	61.633
449.956	69.797	56.133	56.583	59.357	58.497	55.313	60.160
445.908	64.603	55.757	57.367	58.943	54.707	55.507	59.610
441.930	60.717	56.142	58.887	61.833	55.907	53.623	59.783
438.021	58.853	57.243	60.227	61.933	56.703	52.510	59.687
434.178	60.603	56.300	58.370	60.010	56.690	53.273	61.630
430.400	59.797	54.648	58.920	63.427	57.443	55.007	62.083
426.686	58.563	57.350	57.280	58.767	60.153	54.967	60.503
423.033	57.550	56.553	58.600	53.850	61.207	55.560	61.513
419.441	56.787	56.638	57.583	52.450	57.677	53.733	60.810
415.908	58.407	55.193	59.067	57.893	54.580	53.047	61.767
412.432	56.893	51.470	62.313	59.667	57.403	54.570	62.507
409.012	55.557	53.362	62.233	58.357	58.847	52.923	58.467
405.647	60.303	58.663	59.430	59.743	55.827	51.960	57.773
402.335	62.700	55.305	58.377	60.270	56.020	54.217	58.733
SATIN							
1010.012	235.073	190.023	193.523	210.257	232.457	221.510	224.530
990.415	306.983	240.970	244.393	264.393	298.440	278.567	280.997
971.555	382.867	297.397	299.090	329.400	365.583	343.137	346.190
953.392	457.253	362.067	357.773	407.367	433.887	416.750	407.230
935.888	545.557	432.273	423.737	486.640	505.120	492.473	471.060
919.006	646.440	507.937	492.610	564.943	587.467	567.287	551.397
902.716	746.567	592.337	566.680	647.427	677.853	651.783	634.383
886.985	844.710	674.353	641.487	728.080	758.833	734.840	708.417
871.787	945.430	750.857	711.703	809.550	835.107	812.033	780.687
857.093	1055.557	832.700	782.617	904.140	921.007	895.707	859.737
842.880	1170.100	923.050	854.277	995.797	1006.213	974.893	937.943
829.125	1270.407	1008.207	923.827	1071.327	1079.407	1042.103	1005.557
815.804	1360.893	1085.873	987.117	1151.870	1153.623	1107.450	1070.433
802.900	1458.767	1167.030	1042.037	1233.480	1227.840	1172.357	1129.507
790.391	1554.393	1246.597	1087.063	1291.880	1284.550	1226.343	1176.323
778.260	1640.040	1309.547	1117.420	1337.390	1325.223	1264.233	1220.360
766.491	1720.493	1358.480	1137.463	1376.473	1359.837	1286.610	1257.647
755.067	1789.113	1401.320	1136.333	1389.130	1371.350	1291.097	1277.370
743.973	1841.863	1437.823	1109.580	1381.703	1361.380	1287.230	1286.890
733.195	1886.320	1465.090	1092.083	1382.473	1365.797	1292.873	1301.317
722.721	1916.177	1479.973	1101.960	1400.780	1382.340	1309.447	1322.010
712.536	1913.990	1479.547	1124.807	1415.147	1388.000	1320.563	1334.750
702.631	1890.410	1470.747	1138.963	1412.803	1383.563	1319.630	1328.777

692.992	1870.013	1458.133	1132.997	1397.373	1366.067	1304.767	1306.413
683.610	1845.117	1432.210	1110.000	1366.850	1326.867	1268.930	1267.983
674.474	1794.790	1390.053	1076.407	1326.573	1277.890	1223.090	1213.577
665.575	1729.477	1339.600	1037.353	1278.567	1228.453	1173.493	1155.113
656.903	1656.620	1275.673	987.413	1216.940	1166.190	1110.710	1092.737
648.451	1569.690	1197.053	927.023	1144.433	1087.800	1038.700	1021.010
640.209	1473.387	1120.400	863.617	1071.107	1008.893	968.320	948.017
632.171	1378.710	1048.683	801.993	1003.857	936.617	898.937	873.633
624.328	1284.677	975.473	743.487	934.250	863.577	824.917	796.033
616.674	1194.303	900.797	687.047	864.013	795.170	753.853	724.493
609.202	1112.003	828.067	633.990	795.373	732.477	690.377	664.187
601.906	1024.020	764.833	577.470	722.397	666.470	629.233	608.837
594.778	930.507	701.957	517.853	653.580	604.973	571.957	553.197
587.814	847.187	634.193	466.767	593.100	552.993	519.313	500.543
581.009	777.920	575.400	422.100	536.260	500.433	466.577	451.017
574.356	715.863	526.587	382.637	483.143	449.343	416.977	407.490
567.850	656.200	478.773	347.337	436.620	408.360	377.367	372.160
561.487	606.510	435.773	312.000	399.037	375.140	346.197	337.847
555.262	563.863	400.000	280.977	363.407	344.500	318.783	304.493
549.171	521.527	364.493	254.290	328.877	312.380	293.043	280.223
543.210	478.173	329.340	231.430	297.367	281.080	267.880	255.820
537.373	433.753	298.083	214.013	269.213	253.540	241.453	229.313
531.658	391.467	270.700	195.143	246.047	229.887	217.917	209.913
526.061	355.527	247.267	175.030	227.183	210.320	198.577	190.777
520.577	331.190	223.680	158.280	209.460	194.023	183.577	170.950
515.204	306.557	200.713	140.840	188.080	177.280	169.927	154.267
509.939	273.327	183.330	124.573	167.847	159.337	151.110	141.723
504.778	244.730	170.183	115.167	153.777	142.633	132.863	130.660
499.717	219.017	154.827	108.040	143.460	130.253	119.990	118.717
494.755	195.327	137.407	98.337	131.270	119.957	108.650	104.447
489.888	178.397	120.593	89.583	112.773	109.303	97.553	95.540
485.114	162.150	110.830	83.313	100.797	100.107	90.793	87.860
480.429	148.347	102.997	78.017	91.930	86.773	83.683	79.670
475.832	134.067	93.983	71.743	90.187	79.747	76.413	75.150
471.320	120.950	88.407	68.310	85.443	80.587	72.177	70.517
466.891	109.727	85.240	63.677	82.877	77.417	71.600	66.613
462.542	100.713	79.223	62.433	77.777	72.383	70.570	66.267
458.271	91.783	76.977	64.633	74.557	69.520	68.653	68.037
454.077	85.043	70.647	62.260	72.247	66.023	66.493	65.977
449.956	81.133	76.260	59.593	70.247	68.583	66.210	63.557
445.908	79.410	74.093	60.763	71.073	70.357	65.390	61.493
441.930	80.353	71.953	62.843	69.747	66.047	68.717	66.450
438.021	77.863	68.763	60.520	66.007	65.363	65.233	67.823
434.178	74.453	67.733	61.340	66.553	64.787	65.213	68.067
430.400	76.707	66.630	60.383	71.103	66.580	65.170	64.450
426.686	78.740	70.367	61.197	69.617	67.000	65.593	64.547

423.033	76.787	66.517	59.750	67.277	67.910	65.687	66.717
419.441	76.667	66.380	60.523	70.543	66.780	65.827	68.187
415.908	78.420	65.873	63.240	70.900	66.250	63.003	64.380
412.432	75.163	67.257	60.023	68.843	65.160	61.073	63.223
409.012	74.147	67.707	57.470	70.497	68.110	64.070	62.640
405.647	77.197	67.713	58.913	70.137	67.067	65.937	67.123
402.335	78.550	70.307	61.177	68.773	64.530	64.103	67.690
VELVET							
1010.012	214.363	264.327	267.613	291.383	285.527	302.237	289.157
990.415	277.987	346.857	342.827	376.437	365.407	384.493	370.443
971.555	353.610	440.677	430.843	465.727	459.197	482.093	465.247
953.392	446.077	538.863	535.100	556.280	563.580	595.187	576.813
935.888	540.297	642.663	643.437	664.893	668.870	710.433	697.217
919.006	632.633	750.940	755.707	789.743	772.153	826.317	817.057
902.716	736.950	871.340	881.980	929.107	891.120	960.850	941.707
886.985	853.143	999.707	1012.113	1070.000	1020.593	1093.430	1066.740
871.787	973.530	1118.623	1137.340	1202.157	1144.720	1210.870	1180.813
857.093	1097.693	1232.957	1262.897	1338.743	1272.980	1338.403	1295.283
842.880	1230.180	1357.450	1396.870	1487.290	1396.320	1470.873	1409.803
829.125	1356.643	1477.833	1519.410	1625.010	1499.583	1594.163	1509.240
815.804	1465.900	1577.193	1619.567	1743.797	1593.197	1719.897	1610.287
802.900	1578.927	1669.390	1718.837	1861.267	1685.927	1846.193	1718.130
790.391	1696.547	1754.730	1813.587	1965.360	1770.350	1951.683	1809.310
778.260	1796.677	1821.133	1886.160	2038.247	1835.350	2030.417	1874.933
766.491	1886.740	1869.830	1934.623	2095.300	1887.833	2096.267	1916.480
755.067	1973.257	1893.770	1961.243	2139.217	1918.423	2140.173	1929.690
743.973	2043.513	1881.950	1962.533	2154.230	1917.817	2156.440	1917.850
733.195	2101.740	1852.147	1960.923	2158.743	1918.360	2179.053	1918.523
722.721	2164.770	1845.620	1991.510	2169.983	1932.423	2214.130	1947.400
712.536	2212.527	1863.547	2032.967	2175.923	1948.743	2233.367	1973.733
702.631	2228.920	1882.760	2052.650	2171.880	1963.150	2233.013	1977.983
692.992	2238.327	1887.413	2058.050	2155.363	1962.840	2215.340	1956.057
683.610	2240.477	1865.480	2043.643	2112.477	1924.690	2165.607	1903.467
674.474	2215.170	1804.523	1990.263	2049.237	1857.117	2086.090	1833.353
665.575	2168.130	1716.197	1916.390	1978.940	1782.007	1999.677	1754.733
656.903	2105.983	1624.900	1837.893	1890.690	1695.847	1910.397	1657.677
648.451	2021.387	1535.350	1744.410	1789.063	1595.727	1806.993	1552.300
640.209	1911.873	1439.590	1638.863	1687.433	1495.477	1694.067	1448.927
632.171	1793.057	1333.263	1536.210	1577.767	1392.347	1580.863	1336.763
624.328	1669.640	1227.757	1426.790	1461.397	1283.627	1462.167	1224.197
616.674	1535.373	1125.053	1309.337	1353.773	1186.637	1344.787	1123.730
609.202	1399.603	1023.690	1204.533	1254.577	1087.967	1230.733	1035.393
601.906	1274.980	934.617	1107.137	1151.573	988.633	1118.787	943.713
594.778	1155.980	851.897	1006.007	1042.850	895.993	1020.163	850.187
587.814	1046.050	771.880	913.400	942.727	810.587	929.520	772.123
581.009	951.867	699.200	833.917	855.010	734.697	839.027	707.417

574.356	867.360	634.827	757.623	774.287	668.050	756.677	646.933
567.850	793.243	577.370	689.090	703.333	610.963	682.600	582.873
561.487	730.520	521.250	633.867	642.497	556.483	617.640	527.687
555.262	670.430	468.500	585.490	586.040	509.100	559.353	481.933
549.171	610.910	425.977	538.803	533.110	471.410	506.033	437.787
543.210	556.833	384.587	492.147	488.643	436.283	458.500	402.103
537.373	508.473	340.857	448.477	449.620	400.897	411.380	368.473
531.658	464.500	307.487	407.233	407.280	365.467	374.693	329.497
526.061	430.813	283.107	366.590	366.647	332.970	345.120	295.047
520.577	401.907	255.170	331.063	334.783	311.027	307.687	276.097
515.204	366.630	230.627	296.123	306.530	277.467	274.440	258.647
509.939	332.773	212.043	266.810	279.220	243.487	251.653	232.417
504.778	302.827	193.477	242.900	250.223	216.887	228.290	206.123
499.717	273.253	175.277	219.867	219.830	191.210	204.530	184.477
494.755	243.127	160.823	200.973	191.417	174.350	181.550	164.747
489.888	209.150	151.540	183.193	165.580	158.633	155.707	140.863
485.114	179.197	136.330	159.760	147.520	140.640	140.690	126.540
480.429	164.273	118.873	143.137	130.430	124.490	133.327	117.980
475.832	155.603	114.590	128.567	114.700	117.553	120.697	110.250
471.320	144.840	107.897	117.677	110.647	109.497	108.547	103.960
466.891	134.717	95.130	112.347	103.437	103.583	99.970	90.173
462.542	127.860	88.087	102.837	96.393	98.873	94.280	88.380
458.271	119.103	86.277	93.060	93.560	93.273	92.243	85.340
454.077	107.493	85.383	93.673	87.007	88.947	89.093	81.693
449.956	98.053	83.160	92.780	81.793	85.500	85.170	78.353
445.908	92.040	84.397	87.003	85.057	80.457	85.323	78.920
441.930	91.923	80.423	83.267	81.693	78.067	84.797	78.933
438.021	89.593	79.633	80.233	83.403	82.840	82.567	79.037
434.178	84.387	77.193	81.547	84.060	84.900	84.077	78.640
430.400	85.313	76.487	79.440	80.597	81.987	85.540	77.750
426.686	82.507	75.013	80.693	81.763	84.263	81.543	79.880
423.033	79.997	78.323	79.733	83.117	83.710	77.593	77.703
419.441	79.567	78.193	82.207	80.527	82.783	79.033	76.920
415.908	83.793	77.167	82.033	81.687	81.947	82.877	76.990
412.432	86.170	80.677	79.353	79.530	81.843	86.907	74.580
409.012	88.400	82.220	80.900	78.553	81.000	88.243	77.763
405.647	85.223	81.110	79.800	80.680	84.063	84.290	78.750
402.335	84.940	76.253	82.190	82.490	82.613	85.860	81.670